# WIRELESS COMMUNICATION IN A COLLAPSED MINE TUNNEL

Godknows Musa

A dissertation submitted to the Faculty of Engineering and the Built Environment, University of the Witwatersrand, Johannesburg, in fulfilment of the requirements for the degree of Master of Science in Engineering

Johannesburg, September 2020

# Declaration

I, declare that this dissertation is my own, unaided work. It is being submitted for the Degree of Master of Science in Engineering at the University of the Witwatersrand, Johannesburg. It has not been submitted for any degree or examination at any other university.

Signed: 

Date: 21/09/2020

# Abstract

The mining industry in South Africa is one of the biggest contributors to the country's Gross Domestic Product (GDP) and employs almost half a million people. Most of the mines, where mostly gold, platinum and diamonds are mined, are underground mines. During the mining process, miners' health and safety is of paramount importance. However, there have been numerous accidents in underground mines due to structural failures and rock fall which sometimes lead to tunnel collapses and inevitably the tragic problem of the missing or trapped miner. Rescue efforts are impeded by the lack of a communications infrastructure because the available infrastructure either gets destroyed or loses connectivity after the accident has happened. A reliable communication infrastructure is therefore seen as the first step towards addressing the saddening issue of the missing/trapped miner. The realisation of such a good communications infrastructure comes with the major task of designing new robust systems which are able to survive and still be able to establish connectivity after an accident has occurred in the underground mine. The current research aims to model the communication channel of a collapsed underground mine tunnel and to perform an evaluation on the performance of a Wireless Sensor Network (WSN) in a collapsed mine tunnel. The channel modeling part in the research focuses mainly on the modeling of the path loss profile which is dependent on transmission power, centre frequency and antenna gain. The research also focuses on the performance of a WSN communication system in a collapsed mine because it is seen as the best communication system to be used in such a scenario due to the redundancy provided by it such as in a mesh network. In the end, an analysis is made on the suitable frequencies, transmission power and topologies for a communication system that will be effective to be used in a collapsed mine tunnel. The results from the path loss modeling show that the channel presented in a collapsed mine tunnel is a combination of the models obtained for a normal mine tunnel without any collapses and that of wave propagation through a rock medium. In the models obtained, a large attenuation is seen in the collapsed section of the whole tunnel as compared to the open air sections. Results from the performance evaluation show a decline in performance as the transmission frequency increases and as the transmission power is reduced. Overall results suggest that a suitable communication system in a collapsed mine tunnel is that which makes use of a centre frequency below 6MHz when considering a maximum transmission power of 1000mW, for scenarios with a maximum collapse width of 5m and a receiver sensitivity of -80dBm.

*Dedicated to my sister and brother-in-law,*

*Isabel and Elbert Chinhamora.*
*It is because of you that I have come this far.*

# Acknowledgements

I am indebted to:

| | |
|---|---|
| Dr. Asad Mahmood and Professor Frederick Cawood | my supervisors, for their academic support, encouragement, mentorship and guidance throughout the course of the research. |
| Sibanye-Stillwater | for financially sponsoring this work. |
| CeTAS - Centre for Telecommunication Access and Services at the School of Electrical and Information Engineering | for providing the personal computer used in the research. |
| Mr. I. Zaman | for providing the micro-controller units used for the wireless sensor network performance evaluation. |
| Altair | for giving a free student license for the tunnel propagation simulation software. |
| My family | for their moral support, financial support and encouragement throughout all these years. |

# Contents

# List of Figures

# List of Tables

# List of Acronyms

| | |
|---|---|
| **3D** | **3 D**imensional |
| **3G** | **T**hird **G**eneration |
| **AC** | **A**lternating **C**urrent |
| **ACK** | **ACK**nowledgement |
| **CAD** | **C**omputer **A**ided **D**esign |
| **CIM** | **C**ascade **I**mpedance **M**ethod |
| **CIR** | **C**hannel **I**mpulse **R**esponse |
| **CSIR** | **C**ouncil for **S**cientific and **I**ndustrial **R**esearch |
| **CTF** | **C**hannel **T**ransfer **F**unction |
| **DSSS** | **D**irect **S**equence **S**pread **S**pectrum |
| **EM** | **E**lectro **M**agnetic |
| **FDTD** | **F**inite **D**ifference **T**ime **D**omain |
| **FSPL** | **F**ree **S**pace **P**ath **L**oss |
| **GDP** | **G**ross **D**omestic **P**roduct |
| **GO** | **G**eometrical **O**ptical |
| **IFT** | **I**nverse **F**ourier **T**ransform |
| **ISM** | **I**ndustrial, **S**cientific and **M**edical |
| **LAN** | **L**ocal **A**rea **N**etwork |
| **LOS** | **L**ine **O**f **S**ight |
| **LQI** | **L**ink **Q**uality **I**ndicator |
| **LTE** | **L**ong **T**erm **E**volution |
| **MAC** | **M**edia **A**ccess **C**ontrol |
| **NLOS** | **N**one **L**ine **O**f **S**ight |
| **PC** | **P**ersonal **C**omputer |
| **PDP** | **P**ower **D**elay **P**rofile |
| **PER** | **P**acket **E**rror **R**ate |
| **PHY** | **PHY**sical |
| **PNA** | **P**rogrammable **N**etwork **A**nalyzer |
| **RF** | **R**adio **F**requency |
| **RFID** | **R**adio **F**requency **ID**entification |
| **RMS** | **R**oot **M**ean **S**quare |

| | |
|---|---|
| **RSSI** | **R**eceived **S**ignal **S**trength **I**ndicator |
| **SNR** | **S**ignal to **N**oise **R**atio |
| **SSM** | **S**tatistical **S**egmental **M**ethod |
| **TE** | **T**ransverse **E**lectric |
| **TLM** | **T**ransmission **L**ine **M**atrix |
| **TM** | **T**ransverse **M**agnetic |
| **TOA** | **T**ime **O**f **A**rrival |
| **TTA** | **T**hrough **T**he **A**ir |
| **TTE** | **T**through **T**he **E**arth |
| **TTW** | **T**hrough **T**he **W**ire |
| **UHF** | **U**ltra **H**igh **F**requency |
| **UWB** | **U**ltra **W**ide **B**andwidth |
| **VLF** | **V**ery **L**ow **F**requency |
| **VNA** | **V**ector **N**etwork **A**nalyzer |
| **WLAN** | **W**ireless **L**ocal **A**rea **N**etwork |
| **WSN** | **W**ireless **S**ensor **N**etwork |

# Chapter 1

# Introduction

Mining is a significant contributor to the GDP of most resource-rich countries and South Africa is one of the countries whose economy relies on mining. This has been the case from a historical point of view and up to today. This can be seen by the fact that today, the mining industry in South Africa contributes to almost half of the country's export revenue. More than half a million people are directly employed in this sector and almost the same number of people are employed indirectly [1], [2].

Many of the gold mines in South Africa, especially in the Gauteng region, are underground mines. The need to continue to go deeper, as the shallower gold ore becomes depleted close to the surface, means it becomes even more dangerous for human beings to work in such conditions, as the deeper you go the more humid and hotter it becomes [2], [3].

From a cost perspective, the amount of money that has to be invested in infrastructure such as ventilation and the increasing costs of energy and electricity, since almost half of the electricity costs incurred by an underground mine goes to ventilation, will incur cost burdens on the mining operations and hence the mining process might not be very economical [4], [5]. One of the recent calls in this industry has been to introduce robot machines and state-of-the-art technology to improve the mining process as this will cut costs such as ventilation as humans will no longer be required to work in these tough conditions and this will also create more opportunities and jobs for competence in the driving technology for automation [6], [7].

However, since the mining industry is a significant employer, the introduction of machines to replace these workers has been strongly opposed by the many trade unions who represent these workers [8]. With the continual need to keep digging deep, this calls for smart technology to be incorporated into the mining process for reasons such as efficiency but most importantly, miners' health and safety. However, in one way or another, this smart technology that will be introduced in the underground mining space will require some form of communication system to enable this technology to communicate to and from the underground and the surface of the mine, to the mine control room. The communication might be between machine-to-machine, machine-to-man or man-to-man.

In addition, the working conditions in these underground mines require stringent health and safety measures to be put in place in order to protect the health and lives of the vulnerable miners who work there. One of the facilitating architectures and requirements to this cause is the provision of a good communication system.

From a safety and rescue point of view, communication with the miner, either by giving them visual warnings and/or voice/video communication, is one of the vital steps in ensuring their health and safety. Therefore, in this regard, communications plays and will continue to play a major role in the mining industry especially in underground mines. In recent years, research has focused mostly on the design of communication systems to facilitate miners' health and safety, mostly funded and pushed for by various governments' mine, health and safety councils such as the Mine and Health Safety Council (MHSC) in South Africa and the National Institute for Occupational Safety and Health (NIOSH) in the United States of America.

## 1.1 Research problem

One of the greatest challenges in South African gold mines is the extraction of gold in narrow reefs at depths hostile to human survival (small narrow tunnels where communication is still expected to be established).

To reach the ore body, development tunnels or haulage tunnels have to be dug from the main shaft of the mine which miners will use as the access to the ore and for machinery to transport the mined ore. This makes these areas busy and hence the need for communication systems to be established in these areas.

Due to many reasons, the mine tunnels in underground mines sometimes experience rock falls i.e. debris of rocks falling either from loose earth or poor anchoring support. This has the effect of damaging the communications infrastructure installed, especially systems which make use of wires e.g. a WiFi communication system which makes use of a fibre or LAN network backbone.

This results in the loss of communication connectivity within the underground mine space where the rock fall would have occurred and in the process endangering miners' safety, because when the communication system is needed the most that is when it is failing. This results in undesired circumstances such as the loss of communication with the miners. In most cases, these miners will be trapped as a result of the rock fall and they will require the communications infrastructure as the first step towards their tracking and eventually their rescue.

Therefore, the major issue at hand is actually that of the missing or trapped miner. One such case study was proposed to be investigated by the Wits Mining Institute (WMI), from a communications point of view, after the Lily Mine accident in South Africa. Although the accident was a different scenario, in which the whole mine shaft collapsed as opposed to just a mine tunnel, the realisation of the importance of communications in the underground mining space and especially in collapsed mine scenarios was brought to attention [9].

### 1.1.1 Case study: Chilean mining incident (Chile)

33 miners were trapped 700 meters underground for more than 69 days after the tunnel they were mining underground collapsed blocking the path for them to go out. Rescue operations were impeded initially by the fact that the location of the miners was not known and there was no communication with the miners underground. Rescue efforts had to be carried out by drilling exploratory boreholes in trying to find the location of the trapped miners [10].

### 1.1.2 Case study: Lily mine incident (South Africa)

When a surface lamp room container, where miners must go through before going underground for mining, disappeared after a crown pillar collapsed, three miners were trapped underground in the container. Up until the compilation of this research (a period of about 3 years), rescue operations to locate the container and find the three trapped miners have been fruitless. No communication with the trapped miners has been possible [11].

## 1.2 Motivation for research

The motivation of this research comes from the fact that we would like to overcome the issue of the missing/trapped miner due to rock falls which result in blocked tunnels and the destruction of communications systems (loss of connectivity). Communications should be in place when a rock-fall happens and hence this research aims to find a way of keeping connectivity so that the communication problem of the trapped/missing miner can be addressed. The research does not aim to completely solve the problem but aid by addressing one of the important issues in this regard.

Figures 1.1 and 1.2 depicts the scenarios for a normal as well as a collapsed mine tunnel where a communication wireless communication system has been installed. Towards solving the issue of missing/trapped miners, it is imperative to have robust communications systems in the underground mine tunnel which will likely survive a rock fall so that it will still be possible to establish communication between the trapped/missing miners and rescuers above the ground.

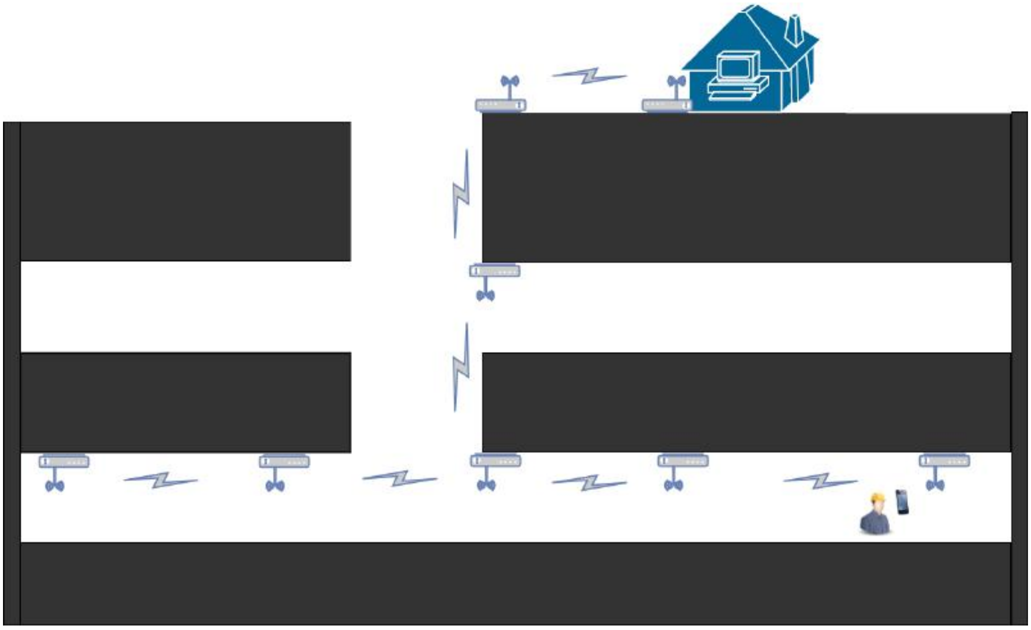

Figure 1.1: Normal mine tunnel with a wireless communication system installed

In this regard, the first step in designing such a robust communication system will be to understand the channel model presented by such an environment where the mine tunnel would have collapsed and second to know the performance of existing communication systems in the same environment (collapsed or blocked mine tunnel) with the aim of coming up with design improvements to enable resilience and self-healing capabilities.

## 1.3 Research questions

This research aims to answer three main questions with regards to the loss of connectivity in a mine tunnel after a rock fall or mine tunnel collapse as depicted in Figures 1.3 and 1.4:

1. *What is the pathloss profile of a partially/fully collapsed underground mine tunnel in context of a WSN system?*
2. *What is the system performance of a WSN communication system after a rock fall in an underground mine tunnel?*
3. *What is the optimal network architecture (with a closer look into a WSN topology) which will likely survive and be able to still establish connectivity after an underground mine tunnel collapses?*

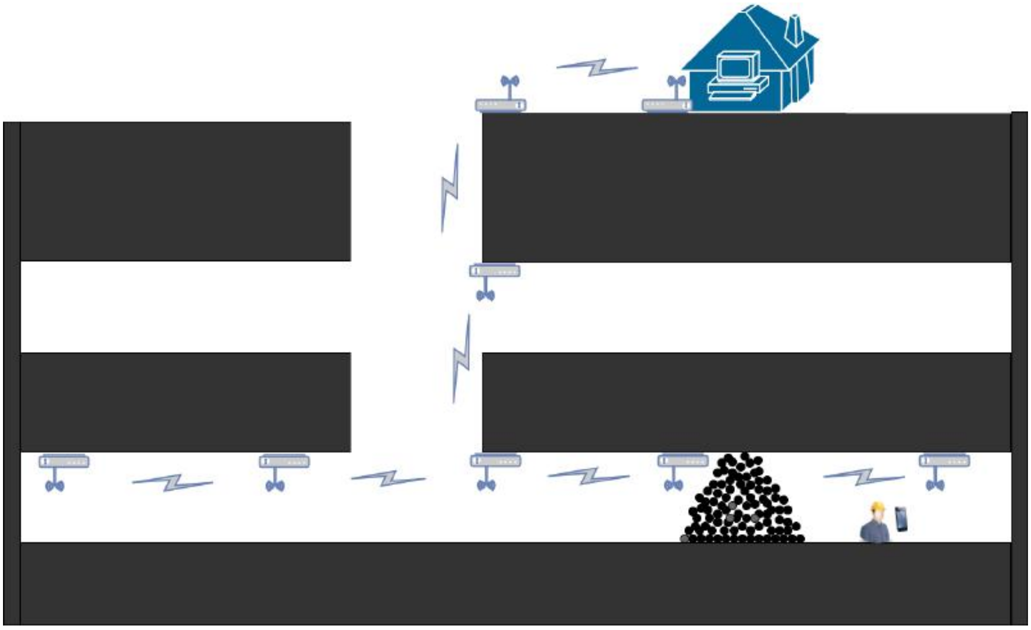

Figure 1.2: Collapsed mine tunnel with a wireless communication system installed

## 1.4 Objectives

The objectives of the proposed research are as follows:

- Identifying suitable analytical channel modeling techniques to model a partially and a fully collapsed mine tunnel in a suitable simulation tool.
- Finding how the path loss behaves with respect to the geometry of the collapsed tunnel and the different separation distances between the transmitters and receivers.
- Performing an evaluation of a WSN communication system in a non collapsed tunnel and see the change in behaviour in a partial collapsed scenario.
- From the channel models obtained and the performance evaluation carried out, to come up with recommendations for WSN network topology designs that will be able to establish a network connection in a collapsed underground mine tunnel.

## 1.5 Research scope

The research problem will only be limited to mine tunnels which do not have metal anchoring and support. The work will be focusing mainly on communication systems

Figure 1.3: A collapsed mine tunnel. Adapted from [12]

which are Wireless Sensor Networks (WSN) and partial considerations will be extended to other systems which make use of 3G, LTE, Wifi/ZigBee and other ISM frequencies and therefore typical considerations such as node separation distances and transmission power for these systems will be the major considerations in the outline of this work.

In the channel modeling exercise to be done, similar techniques associated/suitable particularly for WSN with respect to the underground mine tunnels will be considered along with associated parameters such as the distances between the transmitter and the receiver and the amount of power transmitted.

## 1.6 Dissertation outline

The dissertation is outlined as follows:

Chapter 2 (*Background*) is split into four mains sections. The first section gives a review of underground mine communication systems and discusses about the concept of wireless sensor networks. The second section gives an overview of the fundamentals of channel modeling. The third section reviews existing techniques and related work with respect to channel modeling for underground mine tunnels, with the aim of choosing suitable techniques to use to best answer the research questions. A comparison of the techniques is outlined. The last section provides the performance metrics of interest that

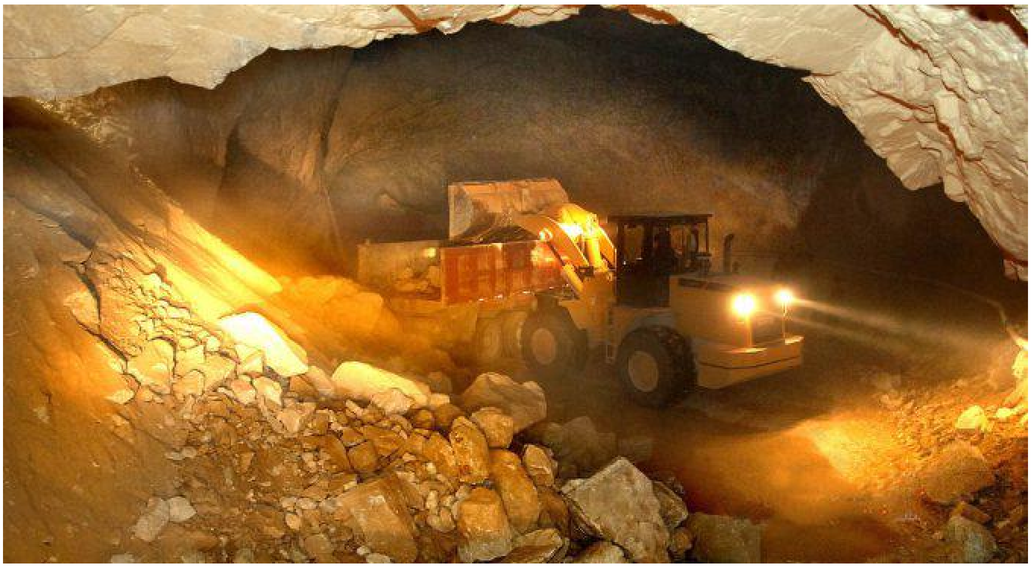

Figure 1.4: Removal of debris from a collapsed mine tunnel. Adapted from [13]

are particular to a wireless sensor network and accounts of related works are provided.

Chapter 3 (*Research methodology*) outlines the channel modeling and performance evaluation procedures adopted in the research.

Chapter 4 (*Channel modeling results*) presents the channel models (path loss profiles) obtained for different frequency bands namely 3G, LTE, Wifi/ZigBee and other ISM frequency bands. A discussion, with a closer look into the development of a communication system for collapsed scenarios in underground mine tunnels, is provided.

Chapter 5 (*Experimental results*) presents the results of a performance evaluation, with a closer look at the RSSI of a sample WSN communication system in a non-collapsed and a partially collapsed mine tunnel environment.

Chapter 6 (*Conclusions, future work and recommendations*) reviews if the research questions posed in Chapter 1 were answered and discusses areas of further improvement for this research.

## 1.7 Conclusion

This chapter has outlined the background for the problem that motivated this research. The answering of the research questions posed in *Section 1.3* will aid in the design of robust and resilient communication systems for underground mines which will be able to sustain common mine tunnel collapses and also be able to provide a communication path between the miners trapped underground and rescue personnel on the surface of the mine which will be a first step towards the solving of the missing/trapped miner problem where communication is very vital.

# Chapter 2

# Background

## 2.1 Chapter overview

In this chapter, there are four mains sections which are presented. In the first section, underground mine communication systems and wireless sensor networks are reviewed. The goal is to build a foundation for understanding of modeling techniques and work of related nature and the relevant communication systems to which they are applied in the underground mine communications space. The second section discusses the fundamentals of channel modeling in general. In the third section, channel modeling techniques for underground mine tunnels are presented. Different techniques have got their own advantages and disadvantages and are more appropriate in different situations. Related works with regards to the techniques which are found in journals and research papers are considered. The goal is to find techniques and appropriate models to use in the modeling of the different scenarios to be considered in *Chapter 3*.

In the last section, the key performance metrics to consider when performing an evaluation of a wireless communication system, specifically a WSN network, are discussed. This is further supplemented by taking a look at some of the work done in this space and also having an overall overview of the considerations taken in the topology design of a WSN network.

## 2.2 Underground mine communication systems

Underground mines are typically composed of rough terrain, dynamically changing environments populated with muddy waters, humid conditions and often very high temperatures [14]. These are difficult conditions to work in and often result in accidents, both natural and man-made, which can lead to loss of human life. This calls for efficient and reliable communication systems to be in place to help most importantly in the event of an

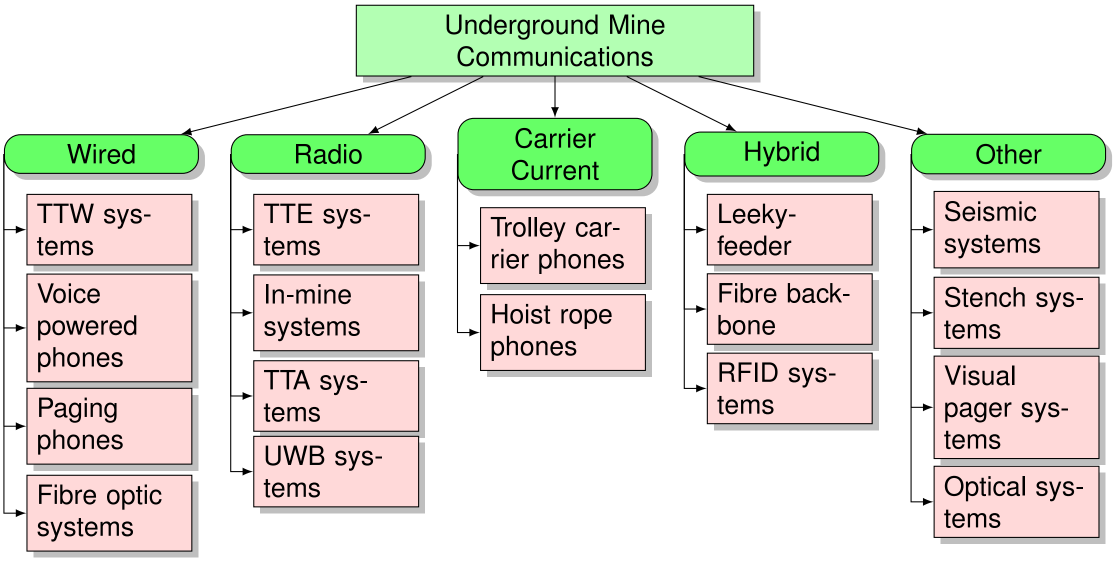


Figure 2.1: An overview of underground mine communication systems

emergency and from an economical point of view, to improve production. Communication systems in underground mines are mostly needed for mine asset management, mine operations monitoring, event management, remote vehicle operation and mine security.

If reliable communication is one of the vital requirements in solving the trapped or missing miner problem after an underground mine tunnel collapse, it is important to understand the communication systems currently available in this space.

An overview of the communication technologies that are and/or have been employed in the underground mining space is shown in Figure 2.1 and adapted from [14]. Underground mine communications are characterised into 3 main categories based on the medium of signal propagation. These are Through-The-Air (TTA), Through-The-Wire (TTW) and Through-The-Earth (TTA) communication systems. There are also other systems which make use of the combination of these categories to come up with hybrid solutions.

### 2.2.1 TTW

Wired communication is facilitated by making use of a conducting wire to carry modulated electrical signals from the transmitter unit to the receiver unit. There are two kinds of wired communication systems that are used; (i) party line system where each broadcast from one node is received by all the other nodes and, (ii) private line system where communication is only established between two nodes and the connection is provided by a packet switch [14]. Previously the switching used to be done manually by an operator at a call centre but has since been computerised [15].

Some of the early TTW systems which were used in underground mines, but have since been widely replaced, include magnetic phones (one of the earliest), voice-powered phones, paging phones, dial-and-page phones [14].

Most of the wired systems that have since been deployed widely in the underground mines include mainly LAN networks and WLAN networks which offer high data rates and improved networking capabilities.

One of the advantages of TTW systems is that they usually do not have to adhere to stringent power requirements as most of the energy is radiated within the wire itself and hence does not pose the danger of a fire which can be caused by the ignition of flammable gases (one of the strict requirements for TTA systems in underground coal mines) [16]. The other advantage of wired communication in the underground mines is that if there is a mine collapse and the wires do not get snapped, a fixed channel will always exist i.e. the parameters of the channel will not change because the signal will still have to travel via the same wire. The other advantage is that of high data rates.

The shortfall of wired communications in an underground mine is their inconvenience due to the need to always keep two-way communication, such as between man-to-machine, man-to-man and machine-machine. Imagine the need for someone always having to walk to where a magneto phone is located to make a call and the need to have wires always trailing a machine to keep a communication link. The other problem associated with TTW communication systems is the fact that they are prone to failures in the event of mine collapses and emergencies, where they are actually needed the most [14]. The cost of installing a wired communications system is enormous and due to the dynamic conditions of underground mines, this poses a huge financial burden on modern underground mines which have to be economically viable and hence reduce costs where possible.

### 2.2.2 TTA

Through-the-air wireless communication in underground mines is facilitated by making use of the open underground mine galleries as the medium of radio wave propagation. One of the biggest challenges encountered in the underground mine environment is the rough terrain of the mine galleries. Many communication systems employed in the underground mine environment were originally designed either for the ground open-space or indoor communication systems [15]. This therefore calls for proper channel models of the underground mines to be developed in order to design efficient TTA communication systems for the underground mines.

It is interesting to note that almost all or most of the communication systems which are being deployed in the underground mines right now, from asset management, security, voice and video communication; such as the Schauenburg mine access and environment monitoring system [17], Minetec tracking and positioning system [18] and Vibra-Tech seismic monitoring system [19], installed at the Wits Mock Mine at the University of the Witwatersrand, are all wireless systems which fall under TTA systems, and one of the challenges with this is the signal interference when all of these systems are 'cramped' up for example in a narrow underground mine tunnel.

One of the advantages of TTA systems in the underground mine space is their ease of deployment and scalability which happen to save huge costs of upgrading a network due to the dynamic nature of underground mine. The disadvantage is the requirement for TTA systems to be very robust due to the harsh environment in the underground mines and also the need to adhere to stringent transmit power regulations especially in underground coal mines.

### 2.2.3 TTE

Most TTE systems for the underground mines were developed through research pushed for by government legislation and funded by mine health and safety councils as a way of addressing the issue of communicating with trapped miners underground where the only communication infrastructure in place then, TTW systems, would have failed. Examples of early prototypes are the ones built out of the US MINERS act [20] and the CSIR SA prototypes for missing miner communications [21]. Almost all of the reviewed TTE systems are for the sole use of rescue operations (some form of solving the missing miner problem post or during accident).

TTE systems make use of very low frequency RF waves which can penetrate through rock. This usually enables an establishment of a communication link between the surface (where one unit is situated) and the subsurface of the mine (where more than one unit could be located) [22].

The advantage of these systems is their ability to penetrate through rock and the establishment of a communication link over great distances, such as from the surface of the mine all the way down to the different levels of an underground mine [23]. However, the disadvantage is the fact that most of these systems are limited to one-way communication only and is mainly because of the very low transmitting data rates. The other disadvantage is their bulky sizes which are not desirable in some very confined underground mine tunnels [20] and also the fact that they are too expensive.

#### Trapped/missing miner TTE solutions

As mentioned in *Section 2.2.3* most TTE systems were developed to come up with solutions to the trapped/missing miner problem and are based off of an architecture as

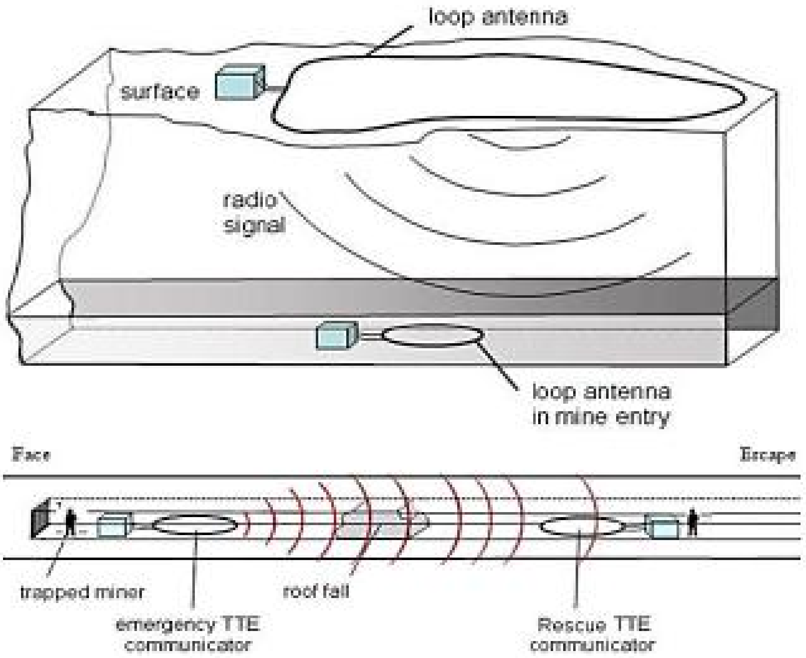


Figure 2.2: Architecture for a TTE mine rescue communication system. Adapted from [20]

shown in Figure 2.2. Some of the prominent systems developed and their attributes are summarised in Table 2.1 [20], [21], [24].

The limitation of most of the systems mentioned in Table 2.1 is their bulkiness and the provision of only text or paging capabilities and in the case of voice, it is only limited to one way communication and the speeds are very low which is something that is critical in an emergency situation and hence improvements need to be introduced. The maximum communication distance offered by many of these systems, as shown in Table 2.1 (a maximum voice communication distance of 240 metres), does not compare to the current depth of the deepest mine which is close to 4 kilometres. There is currently no network topology to support communication between many TTE units. The only communication is between two units and hence many units cannot be deployed in such a way as to increase the communication distance from the surface of the mine to the deepest place in the underground mine.

### 2.2.4 Wireless sensor networks

Wireless sensor networks consist of sensors incorporated into communication nodes. The nodes are made up of a micro-controller, battery unit, sensor unit, a communication

Table 2.1: TTE missing miner solutions

| Prototype | Technology | Frequency | Max Distance |
|---|---|---|---|
| Alertek, LLC | Analog large loop magnetic field | 3150 Hz | 177 m (voice) |
| E-SPectrum Tech | Compact electric field | 10 or 20 Hz | 177 m (text) |
| Lockheed Martin | Digital large loop magnetic field | 330 or 3200 Hz | 305 m (voice) |
| Stolar, Inc. | Small loop magnetic field | 2000 or 4000 Hz | 244 m (text) |
| Ultra Electronics | Digital large loop magnetic field | 4820 Hz | 183 m (text) |
| MineArc (RescueDog) | Electrode ground rods antenna | n/a | 1500 m (text) |
| Wadley (Wits Mines) | Helmet loop antenna | 100 & 350 kHz | 1800 m |
| Kutta - SWECS | PDA-type | n/a | 240 m (voice) |
| Vita Alert | Surface unit | VLF | 120m |
| CSIR Miningtek (SA) | Uniquely coded belt | 2.9 MHz | 30 m |

unit and an antenna which are all integrated together. Different routing protocols such as tree cluster and mesh network are utilised for the laying of the nodes in the network. However, for redundancy, a mesh network is usually implemented in most cases [25].

Here, the technology mostly implemented is ZigBee (which is derived from the IEEE 802.15.4) technology. Most of these systems which are deployed in the underground mining environment are not usually designed for this environment i.e. they do not take into consideration the channel model that is different in the underground mine compared to that at the surface. Most of the systems employed are surface systems which are just given a rugged body to withstand the harsh conditions of the underground mine tunnels.

The deployed systems have different applications ranging from sensing, security, monitoring, voice and messaging. Most of the WSNs deployed in the underground mines are mostly for sensing dangerous and hazardous gases such as carbon monoxide, methane, hydrogen sulphide and the sufficiency of oxygen for the miners [26]–[28]. Some WSNs provide for the sensing of the temperature and humidity within the mine environment. Personnel tracking is also one of the applications provided for by these systems where miners wear tags (such as RFID tags) and their position is mapped relative to the picking node [29]–[32]

The advantages offered by WSN systems include the low cost of implementation and ease of deployment. The motes used to make these networks can survive for up to 3 years on battery power. Due to the dynamic nature of the mining environment, it means the network, if it is built on a full-mesh or semi-mesh topology, can be extended easily without investing huge amounts of money. The low power that is used by these motes also means that most of them will not radiate a lot of EM power and therefore are suitable to be used in power restricted mining areas such as coal mines [16]. Unlike other wireless technologies such as Wifi and Ultra-Wide-Band which need a power (AC) infrastructure to be in place, a WSN can run off batteries.

In most architectures, due to the fact that a WSN should be as cost effective as possible, micro-controllers with less computational capabilities are employed in the sensor nodes and only a powerful computational controller or mini-PC is incorporated into the gateway node [33]. This is good in some applications that do not require the sensor nodes to process any data but only to relay the sensed data to the gateway router and where minimal delay can be tolerated. A trade-off therefore has to be considered in cases where delay cannot be tolerated and where a lot of computational power is required in the sensor nodes (a more powerful micro-controller will have to be adapted but will also mean more costs and more power consumption).

One other advantage associated with WSNs, especially in the underground mines, is their adaptiveness to scenarios such as roof falls where, for example, if one sensor node is destroyed the network can self-heal due to the routing and network topologies employed.

However, they also come with their own shortcomings. Among them is the lower bit-rates provided such as 250 kbps [33]. This means that the applications of WSNs are limited and in some cases a WSN will not provide real-time reporting which require video streaming which might be essential in emergency situations. Another disadvantage is that most of the developed systems based on WSNs are only limited to LoS (that is each node has to be in the line of sight of the neighbouring nodes which might be difficult in most mine galleries as they do not provide a perfect line-of-sight due to the terrain and rough walls).

## 2.3 Channel modeling

In RF communication which uses air as the medium of communication, a channel refers to the medium through which communication takes place between the transmitter and the receiver. The medium might consist of obstacles and obstructions in the path between the transmitter and the receiver. The channel is characterized by many parameters such as the distance between the transmitter and the receiver, the electrical and/or magnetic properties of the medium and any other obstacles within the channel medium [34]. For any efficient and reliable communication system design, the channel between the transmitter and the receiver must be first modeled [35].

### 2.3.1 Underground mine environment and structure

Due to the nature of the underground mine terrain (curved corners, imperfect terrain, humid corridors), the design of a wireless communication system calls for the modeling of the underground mine channel. The structure of the tunnels or air passages are determined by the type of mining that is employed (vertical shaft, narrow reef, room-and-pillar and etc.) [36].

For room-and-pillar mining, the mined area can be thought of as a basement parking area but rather with inconsistently shaped pillars and which are also randomly shaped. The walls of the 'room' are however not smoothly shaped unlike a dry wall made from mortar - the one which would be found in a proper room in a house or any building. For cut-and-fill mining, the mine area is a collection of tunnels, where the ore is actually being mined and the other tunnels are used for transport and/or ventilation. For long-wall mining, the mine area can be thought of as a tunnel due to the steel structure that supports the long wall face [36].

### 2.3.2 Channel modeling theory

What usually defines the channel (medium) is the channel impulse response (CIR). The received signal will be determined by the convolution of this channel impulse response with the transmitted signal as defined by equation (2.1) in the time domain [34].

$$y(t) = h(t, \tau) * n(t) \tag{2.1}$$

where: $h(t)$ = channel impulse response
$\tau$ = channel delay
$n(t)$ = noise within the channel
$y(t)$ = received signal.

In this work, it is important to understand what happens when a signal encounters a new medium or an obstacle. This is because in a collapsed mine environment, LoS scenarios will be limited due to the introduction of rock debris within the mine tunnel, therefore it is essential to know the effect on the signal when it reaches another surface. The other reason is that, naturally in a mine environment the signal will always be encountering a lot of different surfaces with different geometries [35], [37].

One or a combination of the following phenomena listed below will happen when a signal (wave) reaches a medium that is different to the one it was travelling in before [34]:

- **Reflection**: when the waves reaches a surface and depending on the angle of arrival of the wave, the wave will be partially or fully reflected.
- **Diffraction**: when a wave passes around an obstacle and gets spread out as if new 'smaller' waves are starting to emerge from the diffracting object,
- **Refraction**: when a wave meets a corner of a boundary and the angle at which it arrived at is changed,

- **Scattering**: when the wave reaches a surface and is forced to travel in many (non-uniform/criss-cross) form, say multiple reflections plus diffractions and refractions; all these as a result of one surface. This is the main phenomenon in underground mines because of the rough and uneven surfaces,
- **Absorption**: when a wave reaches another surface but some of the energy is absorbed by the material of the new surface and possibly some is reflected or refracted or diffracted.

### 2.3.3 Wave propagation

There are two main phenomena that a wave experiences when it propagates which are path loss in LoS situations and shadowing in NLoS situations (shadowing due to obstacles in the path of travel of the signal wave) . Path loss and shadowing happen at large distances and bring about large-scale propagation effects. However propagation effects due to multipath and on small-scale fading happen over short distances and bring about small-scale propagation effects [38].

#### Path Loss

When a wave travels naturally within the air it will experience a loss in its energy even if there are no obstacles within the path and this is referred to as Free space path loss (FSPL). This is directly proportional to the distance (generally square of the distance) that the wave travels and is represented by equation (2.2) [34]:

$$FSPL = \left(\frac{4\pi d}{\lambda}\right)^2 \tag{2.2}$$

where: $d =$ distance
$\lambda =$ wavelength of signal

It is noted that in some instances where there are structures which exhibit a wave-guide nature such as smooth walled tunnels, path loss is somewhat reduced because of the constructive interference as a result of reflections off the walls. However in mining tunnels with uneven walls, the reflections tend to be destructive and hence increase path loss [35]. A more general equation which describes path loss is given by (2.3) [34]:

$$P_r = P_t P_o \left(\frac{d_o}{d}\right)^\alpha \tag{2.3}$$

where: $P_r$ = the received power at distance $d$
$P_t$ = the transmitted power at distance $d$
$P_o$ = the received power at distance $d_o$
$\alpha$ = the path loss exponent.

Equation (2.3) can be represented in dB form as:

$$PL_{dB}(d) = \overline{PL_{dB}(d_o)} + 10\alpha \log \left( \frac{d}{d_o} \right) \tag{2.4}$$

where: $\overline{PL_{dB}(d_o)}$ = the mean path loss at $d_o$.

The pathloss is more useful in characterizing the signal propagation in LoS areas.

### Fading

Fading is divided into two main categories, small-scale and large-scale fading. Small-scale fading happens when considering rapid fluctuations of the received signal strength over very short distances and short times. Large-scale fading happens when considering large fluctuations which happen over large distances [39].

Some of the phenomena that bring about fading and some of the parameters used to characterize it are discussed in this section.

**Shadowing** This is loss of the transmitted signal strength due to signal absorption, scattering, diffraction and reflection. The effect of shadowing adds to the overall effect of path loss where the overall effects can be represented by (2.5) [34]:

$$PL_{dB}(d) = \overline{PL_{dB}(d_o)} + 10\alpha \log \left( \frac{d}{d_o} \right) + \chi \tag{2.5}$$

where: $\chi$ = a Gaussian normally distributed random variable (in dB and a result of shadowing) with standard deviation $\sigma$.

The effects of shadowing can be seen by the difference in the received signal power at places that are at a same distance $d$ from the transmitter and having a lognormal distribution (lognormal shadowing) [34].

**Multipath** When the signal is sent from the transmitter, it takes multiple routes due to reflections, this results in the copies of the signal travelling different distances which results in them reaching the receiver with different phases and strength. At the receiver, the different signals will have an overall increase or decrease in strength and phase [34].

One of the important representation of the received signal that is obtained as a result of the multipath effect is the power-delay profile of the signal. Due to the difference in length of the different travel routes, a single transmitted impulse will result in multiple copies of the same impulse being received at the receiver, usually with different signal strengths, and they will be received at different times, with a delay $\tau$ and this generates the power-delay-profile. If a signal is delayed up to a point where it becomes too weak, the delay time is called the maximum delay spread $\tau_{max}$. A highly dispersive channel is represented by a large $\tau_{max}$. The RMS value of the delay-spread is usually used instead of the maximum [38].

The phenomenon of impulse response of the channel is represented by a discrete number of impulses as given in (2.6):

$$H(t,\tau) = \sum_{i=1}^{N} c_i(t)\delta(\tau - \tau_i) \tag{2.6}$$

The chosen value of $N$ and delay values $\tau_i$ depend upon what is considered a *significant level*. The model shown in (2.6) represents the channel by a delay line with $N$ taps [34].

**Coherence bandwidth** In the frequency domain of the power delay profile, the channel characteristics' dependence on frequency can be observed. The range of frequencies (bandwidth) for which the channel will be the same is the coherence bandwidth which has an inverse proportional relationship with the delay spread. A smaller coherence bandwidth channel results in a frequency selective channel in the sense that if the signal bandwidth is much greater than $B_c$, the channel amplitude values at frequencies separated by more $B_c$ will be independent. However, within the coherence bandwidth, all the frequencies are considered to have the same gain and linear phase for all components [34], [38]. A 50% coherence bandwidth is represented by (2.7) with a frequency correlation above 0.9 where $\sigma_\tau$ represents the delay spread :

$$B_c = \frac{1}{5\sigma_\tau} \tag{2.7}$$

**Coherence time** Due to the time varying nature of the channel characteristics, such as movement of the objects within it and/or transmitter and receiver, there will be a maximum time for which these characteristics will be assumed to be constant and this is referred to as the coherence time. This is the simple definition of coherence time as the actual measurement requires the use of the autocorrelation function of the signal to get the exact coherence time [38].

**Doppler effect** The effect is caused by the motion of objects in the channel. In addition to the power delay profile for a channel, the Doppler power spectrum gives an overview of the statistical power distribution of the channel for a signal wave transmitted only at a particular frequency (not the whole range of frequencies). The maximum frequency deviation for a single transmitted frequency is the maximum Doppler spread [38]. The Doppler spread can be related to the coherence time by (2.8):

$$CoherenceTime \approx \frac{1}{DopplerSpread} \tag{2.8}$$

A large Doppler spread is attributed to either a fast moving transmitter or a receiver and/or moving intermediate objects, where the channel will change fast and the coherence time will be small and the Doppler spread will be large [34].

## 2.4 Underground mine channel modeling techniques

Most propagation modeling techniques have put their focus on the received signal strength and represented it as a function of time and space. Doing this when the transmitter and receiver are a large distance apart is *large-scale* modeling whereas for short distances it is *small-scale* modeling. The rate at which the signal changes due to variations in the channel will determine if the channel is *fast-fading* or *slow-fading* [38] . The parameters discussed earlier (delay spread, coherence bandwidth, Doppler spread and coherence time) are the determining factors for a fast, slow, flat or frequency-selective fading channel. For fast-fading, the channel has rapid fluctuations in the received signals' amplitude and phase over a short period of time or transmission distance whereas for slow-fading, the channels fluctuations are slow compared to the signals' variation [38], [40]. For flat fading, the channel's response has a flat gain and a linear phase over the bandwidth that is greater than the signal's bandwidth whereas for frequency-selective fading the channel has a constant gain and linear phase over the bandwidth that is less than the bandwidth of the signal [40].

### 2.4.1 Analytical modeling

In the analytical modeling approach, the process involves finding a set of mathematical equations that describe the channel. Usually some factors and parameters used in this process are estimated and some are approximated and all these factors determine the quality of the model that will be obtained. Great accuracy requires that the parameters be stated precisely but from a time and computational point of view, this greatly increases the time and computer resources needed for the process to be completed hence the need to estimate and approximate parameters. A trade-off usually has to be done between computational resources and time and the level of accuracy required [35].

Some of the analytical models utilised especially in the underground mine space will be discussed in this section. Their suitability and the environments in which they are best utilised will be highlighted in a bid to pick or come up with the appropriate modeling techniques to be utilised in the analytical modeling part of this research.

#### Waveguide model

With respect to a mine tunnel, the waveguide model treats the tunnel as an oversized waveguide and the walls of the tunnel are treated as a lossy and reflective material [35], [41], [42]. A wavelength less than the cross-sectional dimensions of the tunnel is usually used for propagation. Changes in the tunnel direction will result in attenuation by reflection and refraction at the intersection between the rock-air interface and changes in the tunnel dimensions will change the waveguide mode characteristics if the original dimensions were assumed to favour dominant mode propagation [41]. In the waveguide model there is the concept of modes which propagate from the transmitter in which some are considered as dominant modes and others as not. This is purely based on the angle of reflection off the tunnel walls (which are usually assumed to be smooth surfaces with no scatterers but is not usually the case in most of the real tunnel geometry in underground mines) [35].

The waveguide model discussed and presented here is from the works of Emslie *et al* [42] from which most waveguide models and other additions and modifications to the model have been derived. It provides the fundamental ground to the many waveguide models in existence today.

The dominant modes of a waveguide are the least attenuated of all the propagating modes. In the waveguide model, these least attenuated modes are the $E_{hor}$ (the mode with the electric field $E$ polarized predominantly in the horizontal direction) and $E_{ver}$ (the mode with the electric field $E$ polarized predominantly in the vertical direction) with respect to their dominant polarisation in the horizontal and vertical directions respectively [42]. The dominant field components of $E_{hor}$ are given by (2.9) and (2.10):

$$E_x = E_0 \cos(k_1 x) \cos(k_2 y) e^{(-ik_3 z)} \tag{2.9}$$

$$H_y = \frac{k_3}{\omega \mu_0} E_0 \cos(k_1 x) \cos(k_2 y) e^{(-ik_3 z)} \tag{2.10}$$

where: $E_0$ = electric field at the transmitter
$\omega$ = angular frequency of the signal
$\mu_0$ = permeability of free space
$x$ = horizontal distance in the tunnel
$y$ = vertical distance in the tunnel
$z$ = distance along the tunnel
$k_1, k_2, k_3$ = wave vector components along the x, y and z directions

In the case of perfectly conducting walls in the tunnel, the propagation modes of a hollow waveguide are pure transverse-electric (TE, i.e., $E_z = 0, H_z \neq 0$) and transverse magnetic (TM, i.e., $E_z \neq 0, H_z = 0$) modes. Depending on the frequency of signal propagation and the cross-sectional dimension of the concerned part of the mine tunnel, different modes of $TE_{m,n}$ or $TM_{m,n}$ (where $m$ and $n$ denote the index for the different modes) will propagate in the waveguide [35], [42].

For dielectric walls, a hybrid combination of these modes, where all the three Cartesian components of the electric and magnetic field being in these modes, exist. Because of the di-electric nature of the walls, any wave (the modes) which are radiated on the walls are partially refracted into the dielectric material and experience partial reflection back into the waveguide. The refracted part represents a power loss (as the waveguide model assumes perfect reflection and no refraction) [35], [42]. Maxwell's equation can be used to determine the cut-off frequency, propagation constant and propagation loss of each mode after getting the tunnel dimensions and tunnel material and also knowing the boundary conditions created by the interfaces between the interior of the tunnels and the wall materials [42]. These are some of the parameters which need to be properly defined when doing the simulation so as to get an accurate or close-enough channel model of the environment.

Along with these components, there are other less significant components in the $z$ direction and another $H$-field component in the $x$ direction. At high frequencies such as UHF, these components are considered negligible and can therefore be neglected. Out of this assumption, much of the propagation will be in the $z$-axis [42]. Due to the wavelenghts in the UHF band being smaller than most tunnel dimensions, the signal loss in the $E_{hor}$ and $E_{ver}$ are approximated [42] as represented in (2.11) and (2.12):

In equations (2.11) - (2.15) the parameters are defined as:

where: $\lambda$ = wavelength
$d_1$ = width of tunnel
$d_2$ = height of tunnel
$K_1$ = relative permittivity of the tunnel walls
$K_2$ = relative permittivity of the tunnel ceiling and floor
$h$ = root mean square roughness
$z$ = distance along the length of tunnel
$\theta$ = sidewalls' rms tilt angle about vertical axis
$x_0$ = traversal position of the antenna along the x axis
$y_0$ = traversal position of the antenna along the y axis

$$L_{E_{hor}} = 4.343\lambda^2 z\left(\frac{K_1}{{d_1}^3(K_1-1)^{\frac{1}{2}}} + \frac{1}{{d_2}^3(K_2-1)^{\frac{1}{2}}}\right) \tag{2.11}$$

$$L_{E_{ver}} = 4.343\lambda^2 z\left(\frac{1}{{d_1}^3(K_1-1)^{\frac{1}{2}}} + \frac{K_2}{{d_2}^3(K_2-1)^{\frac{1}{2}}}\right) \tag{2.12}$$

In [42], the scattering effect of the rough walls of the mine tunnel is considered as part of the additional loss to the $E_{hor}$ mode and is represented by equations (2.13) and (2.14):

$$L_{roughness} = 4.343\pi^2 h^2 \lambda\left(\frac{1}{{d_1}^4} + \frac{1}{{d_2}^4}\right)z \tag{2.13}$$

$$L_{tilt} = \frac{4.343\pi^2\theta^2 z}{\lambda} \tag{2.14}$$

In addition to the above losses for the dominant mode of propagation ($m$ = 1, $n$ = 1), there are additional losses which are: (i) refraction loss (proportional to $f^{-2}$), (ii) roughness loss (proportional to $f^{-1}$), (iii) tilt loss (proportional to $f$), there is also the antenna coupling loss. This happens as a result of the inefficient coupling of dipole antennas when considering the waveguide model. This loss is proportional to $f^{-2}$. This loss decreases with increasing frequency [35], [42].

This loss is represented as the half-wavelength dipole insertion loss for ($\lambda \leq$ the transversal dimensions of the tunnel) as:

$$L_{antenna} = \left[0.5233\frac{\lambda^2}{d_1 d_2}\cos^2\left(\frac{\pi x_0}{d_1}\right)\cos^2\left(\frac{\pi y_0}{d_2}\right)\right] \tag{2.15}$$

All the equations presented are when considering an omni-directional antenna. Many researchers have used this model as the basis of their works and have tried to make the model more accurate for different scenarios. Since the model only considers the dominant mode of propagation, it is only valid for the far-field region where the dominant mode (the one which is considered) is least attenuated [35]. It does not therefore model the behaviour of other modes or even the dominant mode in the near-field.

Breakpoints are employed into the tunnel geometry to distinguish between the near and far fields. Higher modes which are neglected in the Emslie model are actually dominant in the near field. However after the breakpoint and into the far field, the higher modes are attenuated greatly and that is the reason why the dominant mode is the only one considered in the far field [35]. The model will only give the path-loss of the environment under consideration and will not account of other parameters such as the power delay profile (PDP) and channel impulse response (CIR), which results in a partially defined channel model which does not completely characterise the channel.

In this regard, other works have proposed the concept of multi-mode waveguide modeling techniques in which many waveguide modes are considered. This enables the fast fluctuations of the channel to be characterized and also to get the power delay profile of the received signal at various locations within the tunnel such as the one implemented in [36].

**Optical and ray-tracing models**

In the optical and ray-tracing models, high frequencies are approximated by a discrete number of rays coming from the transmitter. When considering each ray, of importance to consider is its power which decreases with distance (usually using the free space model) [35], [43]. The distance travelled by the ray is determined from the 3D path taken by the ray. The challenge usually encountered is calculating this path as it is computationally expensive. The path tracing starts by the ray from the transmitter which travels in a straight line and then encounters a surface where the ray will experience different phenomena such as reflection, absorption, diffraction. The ray is traced until it reaches the receiver or some other criteria such as minimum energy is reached or a certain number of reflections have been reached [35]. The process is usually repeated until a certain number of defined rays have been transmitted from the transmitter to the receiver. In most cases, the ray-tracing method yields better results than other methods and gives something that is close to reality but the major disadvantage comes with computational cost which grows as the number of receivers and the number of surfaces are increased. The ray tracing technique is accurate when the area being considered is much larger than the wavelength of the wave under consideration [35], [42], [43], which is the case in most underground mine tunnels.

In [44], in addition to the attenuation modeling of smooth surfaces, surface roughness (due to scatterers) is included into the modeling which provides a modeling scenario close enough to reality. The roughness coefficients of the walls were calculated [44] as given in (2.16) and (2.17) for the walls and ceiling and floor of the tunnel respectively:

$$S_v^{\pm} = e^{-2(kH_v{}^{\pm}\sin\phi_v)^2} \tag{2.16}$$

$$S_h^{\pm} = e^{-2(kH_h{}^{\pm}\sin\phi_h)^2} \tag{2.17}$$

where: $H_v$ = root mean square of the deviation in height of the profile from the large-scale value on the vertical walls.
$H_h$ = root mean square of the deviation in height of the profile from the large-scale value on the ceiling and floor.
$S_v{}^{\pm}$ = roughness coefficient for the vertical wall of the tunnel
$S_h{}^{\pm}$ = roughness coefficient for the ceiling and floor of the tunnel
$k$ = wavenumber = $\frac{2\pi f_0}{c}$
$\sin\phi_h$ = ray incident angle on the ceiling and floor
$\sin\phi_v$ = ray incident angle on the vertical walls.

These are then considered into the overall attenuation equation to come up with equation (2.18) which represent the average field attenuation at the receiver from all the considered rays:

$$\overline{\alpha}(x,y,z) = \sum_{p=-\infty}^{\infty}\sum_{q=-\infty}^{\infty}\left(\frac{e^{-jkr_{p,q}}}{r_{p,q}}\right)\left(R_h^+S_h^+\right)^{\left|\frac{q+1}{2}\right|}\left(R_h^-S_h^-\right)^{\left|\frac{q}{2}\right|}\left(S_v^+R_v^+\right)^{\left|\frac{p+1}{2}\right|}\left(R_v^-S_v^-\right)^{\left|\frac{p}{2}\right|} \tag{2.18}$$

where: $\overline{\alpha}(x,y,z)$ = average field attenuation at the receiver from all the propagation paths.
$R_h{}^{\pm}$ = ceiling and floor reflection coefficient.
$R_v{}^{\pm}$ = walls reflection coefficient.
$r_{p,q}$ = index of path taken by a ray
$p$ = number of reflections from the walls.
$q$ = number of reflections from the ceiling and floor.

The attenuation, represented in equation (2.18), is then combined with the Friis equation to get the received power in the different sections of the mine tunnel by evaluating equation (2.19) :

$$P(x,y,z) = P_t\left(\frac{c}{4\pi f_0}\right)^2|\overline{\alpha}(x,y,z)|^2 \tag{2.19}$$

where: $c$ = the speed of light.
$P_t$ = transmitted power.

The optical model can provide great accuracy and can also be used in the near region of the transmitter. Simplification and approximations are usually done to the tunnel wall profile and roughness which can be hard to provide accurately.

In the Appendix of [42], the modes that are allowed to propagate in a rectangular tunnel with dielectric walls, ceiling and floors are approximated using a ray theory. In this theory, a ray which bounces from wall to wall and from ceiling to floor is considered. The ray makes reflecting angles $\phi_1$ with the walls and $\phi_2$ with the floor and roof. These dominant modes are defined in this ray model by the phase relations given by (2.20) where $d_1$ and $d_2$ are the width and height of the tunnel:

$$\sin \phi_1 = \frac{\lambda}{2d_1} \qquad \sin \phi_2 = \frac{\lambda}{2d_2} \tag{2.20}$$

Equation (2.20) is representative of the conditions that the phase shift undergone by the ray is 360 degrees after successive reflections from the two side walls or from the floor and roof. For higher frequencies, $\lambda$ is considered very small compared with $d_1$ and $d_2$ and (2.20) is approximated as:

$$\phi_1 = \frac{\lambda}{2d_1} \qquad \phi_2 = \frac{\lambda}{2d_2} \tag{2.21}$$

The number of reflections $N_1$ and $N_2$ experienced by the ray as a result of bouncing off the vertical and horizontal walls of the tunnels travelling a distance $z$ along the tunnel is given by (2.22):

$$N_1 = \frac{z\phi_1}{d_1} \qquad N_2 = \frac{z\phi_2}{d_2} \tag{2.22}$$

The attenuation factor for the ray intensity for this particular distance is then given by (2.23):

$$\frac{I}{I_0} = {R_1}^{N_1} {R_2}^{N_2} \tag{2.23}$$

where: $I_0$ = initial ray intensity
$I$ = attenuated ray intensity

$R_1$ and $R_2$ are the power reflection coefficients of the vertical and horizontal surfaces at the grazing angles $\phi_1$ and $\phi_2$ respectively.

Combining all the equations, the overall loss experienced by the ray is given by (2.24):

$$L = 5\lambda z\Big(\frac{1}{{d_1}^2}\log_{10}\frac{1}{R_1} + \frac{1}{{d_2}^2}\log_{10}\frac{1}{R_2}\Big) \tag{2.24}$$

The coefficients $R_1$ and $R_2$ for the $E_h$ mode of the vertical and horizontal walls, respectively are given by the Fresnel formulas (2.25-2.26):

$$R_{1Eh} = \left|\frac{K_1\sin\phi_1 - (\sin^2\phi_1 + K_1 - 1)^{\frac{1}{2}}}{K_1\sin\phi_1 + (\sin^2\phi_1 + K_1 - 1)^{\frac{1}{2}}}\right|^2 \tag{2.25}$$

$$R_{2Eh} = \left|\frac{\sin\phi_2 - (\sin^2\phi_2 + K_2 - 1)^{\frac{1}{2}}}{\sin\phi_2 + (\sin^2\phi_2 + K_2 - 1)^{\frac{1}{2}}}\right|^2 \tag{2.26}$$

and for the $E_v$ mode the reflectance are calculated as follows (2.27-2.28):

$$R_{1Ev} = \left|\frac{\sin\phi_1 - (\sin^2\phi_1 + K_1 - 1)^{\frac{1}{2}}}{\sin\phi_1 + (\sin^2\phi_1 + K_1 - 1)^{\frac{1}{2}}}\right|^2 \tag{2.27}$$

$$R_{2Ev} = \left|\frac{K_2\sin\phi_2 - (\sin^2\phi_2 + K_2 - 1)^{\frac{1}{2}}}{K_2\sin\phi_2 + (\sin^2\phi_2 + K_2 - 1)^{\frac{1}{2}}}\right|^2 \tag{2.28}$$

The losses due to surface roughness are represented by (2.29) just as considered in (2.13) in the waveguide modeling section (*Section* 2.4.1):

$$L_{roughness} = 4.343\pi^2 h^2 \lambda\Big(\frac{1}{{d_1}^4} + \frac{1}{{d_2}^4}\Big)z \tag{2.29}$$

**Hybrid models**

Hybrid models makes use of combining two or more analytical models to either simplify or gain more accuracy in the modeling process. This is useful in addressing the shortfalls of one technique and to be able to model regions not covered by one technique or where it is not very effective (e.g. the waveguide model is not effective in modeling the near-field and can therefore be complemented with the ray-optical model in a hybrid model to cover these regions).

The hybrid model presented here is formulated in [36] in which the waveguide part of the model makes use of a multi-mode model. The modes considered are represented by an eigenfunction solution to Maxwell's equations:

$$E^{eigen}_{m,n}(x,y) \approx \sin\left(\frac{m\pi}{2a}x + \psi_x\right)\cos\left(\frac{n\pi}{2b}y + \psi_y\right) \tag{2.30}$$

where $2a$ is the tunnel width, $2b$ is the tunnel height, $m$ and $n$ range from zero to infinity and represent the index of the modes and $x$ and $y$ are the distances along the width and height of the tunnel respectively. If $m$ and $n$ are even then $\psi_x$ = 0 and $\psi_y$ = $\frac{\pi}{2}$ but if $m$ and $n$ are odd, $\psi_x$ = $\frac{\pi}{2}$ and $\psi_y$ = 0. $\psi_x$ and $\psi_y$ are the phase shifts of the propagating waves along the $x$ and $y$ axis respectively.

Summing up all the modes yields the field at any point in the tunnel represented by (2.31):

$$E^{Rx}(x,y,z) = \sum_{m=1}^{\infty}\sum_{n=1}^{\infty} C_{mn}E^{eigen}_{m,n}(x,y)e^{-(\alpha_{mn}+j\beta_{mn})z} \tag{2.31}$$

where: $C_{m,n}$ = mode intensity
$\alpha_{mn}$ = attenuation coefficient
$\beta_{mn}$ = phase shift coefficient

represented by (2.32) and (2.33):

$$\alpha_{mn} = \frac{1}{a}\left(\frac{m\pi}{2ak}\right)^2 Re\left(\frac{\overline{k_v}}{\sqrt{\overline{k_v}-1}}\right) + \frac{1}{b}\left(\frac{n\pi}{2bk}\right)^2 Re\left(\frac{1}{\sqrt{\overline{k_v}-1}}\right) \tag{2.32}$$

$$\beta_{mn} = \sqrt{k^2 + \left(\frac{m\pi}{2a}\right)^2 + \left(\frac{n\pi}{2b}\right)^2} \tag{2.33}$$

where: $k$ = wavenumber = $\omega\sqrt{\mu_0\epsilon_0\epsilon_a}$
$\overline{k_v}$ = relative electrical parameter of the walls = $\epsilon_0\epsilon_v + \frac{\sigma_v}{j\omega}$

where: $\omega$ = angular frequency of signal
$\mu_0$ = permeability in free space
$\epsilon_0$ = permittivity in vacuum space
$\epsilon_v$ = relative permittivity of the walls.

To account for the higher order modes in the near-field neglected in the waveguide model, mode matching is done between the rays in the optical model and these higher order modes. The sum of the rays in the optical model is transformed into a sum of modes which can be adapted in the waveguide model. The derivations are performed in [36] and the result of the mode intensity after the transformation from the ray-optical rays is represented by (2.34):

$$C_{mn} = \left( \frac{E_o \pi}{ab\sqrt{1 - \left(\frac{m\pi}{2ak}\right)^2 - \left(\frac{n\pi}{2bk}\right)^2}} \right) \sin\left(\frac{m\pi}{2a}x_0 + \psi_x\right) \cos\left(\frac{n\pi}{2b}y_0 + \psi_y\right) \quad (2.34)$$

Using the Friis equation, $P_r = P_t G_t G_r \frac{\lambda^2}{\left(4\pi d\right)^2}$, and the mode intensity, the transmitted and received powers are related as given by (2.35):

$$P_r(x, y, z) = P_t G_t G_r \left( \frac{1}{E_0} \sum_{m,n} C_{m,n} E_{m,n}^{eigen}(x, y) e^{-(\alpha_{mn} + j\beta_{mn})z} \right)^2 \quad (2.35)$$

where: $G_t$ = transmit antenna gain
$G_r$ = receive antenna gain

For calculating the power delay profile for a wideband signal with bandwidth $B_w$, on a centre frequency of $f_c$ and with the assumption that the signal is real, the spectrum of the signal which is obtained from its Fourier Transform , can be seen as a sum of sinusoids in the frequency band $f \in \left[f_0 - \frac{B_w}{2} \quad f_0 + \frac{B_w}{2}\right]$ [36], with the assumption that the signal is real, the magnitude of Fourier Transform is an even function and depends on the frequency of the signal. The power delay profile is represented in (2.36) [36]:

$$w(t) = \int_{f_0 - \frac{B_w}{2}}^{f_0 + \frac{B_w}{2}} W(f) 2\cos(2\pi f t) \quad df \quad (2.36)$$

The different modes will have a propagation delay depending on the frequency and obtained using (2.37):

$$\tau_{mn} = \frac{z}{v_{mn}(f)} \quad (2.37)$$

where: $v_{mn}(f)$ = group velocity; which is given by (2.38):

$$v_{mn}(f) = c\sqrt{1 - \left( \frac{c\left(\frac{m\pi}{2a}\right)^2 + \left(\frac{n\pi}{2b}\right)^2}{2\pi f} \right)} \quad (2.38)$$

where: $c$ = speed of light

The above shows the dependence of the delay on the frequency for each mode and this means that the dispersion across the frequencies and different modes should be considered in the power delay profile calculations which yields (2.39) [36]:

$$P_{wB}(x,y,z,t) = P_t G_t G_r \left( \frac{1}{E_0} \sum_{m,n} \int_f \left[ C_{mn}(f) E_{m,n}{}^{eigen}(x,y,f) e^{-\alpha_{mn} z} A \right] \quad df \right)^2 \tag{2.39}$$

where:

$$A = S(f)\delta\Big(t - \frac{z}{v_{mn}(f)}\Big)\cos(2\pi f t - \beta_{mn} z) \tag{2.40}$$

where: $S(f)$ is the fourier transform.

$$\delta(x) = \begin{cases} 1, & \text{if } x \geq 0 \\ 0, & \text{otherwise} \end{cases}$$

**Full-wave models**

Finite-Difference-Time-Domain (FDTD) models are numerical techniques which solve the time-domain Maxwell's equations (Gauss law, Gauss law of magnetism, Maxwell's Faraday equation, Maxwell's corrected Ampere's law) [45]. Schemes that use linear wave equations and which are based on low order numerical methods are usually employed for RF wave propagation modeling. FDTD methods use a 3D grid model to approximate the real physical geometry (e.g. mine tunnel). The field evolution at each grid point is computed and the computational cost is proportional to the number of grid points. However the grid point must be very smaller than the wavelength of the wave under consideration, usually ten cells per wavelength for more accurate results [35], [45]. Because of this, and the fact that mine tunnel geometries are much larger than the wavelength usually under consideration, this will need large memory requirements and hence introduce computational complexities. Full wave models provide the most accurate results but however the 3D geometry should be as close to that of the mine as possible (which can be done by having a 3D scan of the mine tunnel). This however requires a lot of time and computer resources.

Transmission-Line-Matrix (TLM) method [45] models the medium as a homogeneous 3D space and then uses the physics of radio wave propagation through that medium. However, if the space is not homogeneous, the modeling can be done by joining reflection/transmission junctions that model how the wave is reflected, transmitted and how the speed changes when the wave moves across the different medium. A simplified version exists which considers only the waves that travel through the air and disregards the ones that travel through other mediums such as rock/earth. An addition to this simplification is the assumption/consideration that a single cell will not propagate any disturbances to other cells, but the disturbance's magnitude should be below a certain threshold [45].

The full wave models are the most accurate and provide the best CIR, channel fading. The only shortcoming is the requirement of a detailed 3D model of the area (tunnel) under consideration. This results in large computational and time costs.

**Knife-edge diffraction modeling**

Diffraction happens when Electromagnetic waves bend around corners to reach the place of interest which otherwise was not in the LoS - such areas are considered to be shadowed. The phenomenon is easily explained by Huygen's principle, which states that "as a plane wave propagates in a particular direction, each new point along the wavefront is a source of other secondary waves". EM field in the shadowed region is calculated by vectorially combining the elements from all these secondary sources because usually the EM waves reach the shadowed region after multiple diffractions and reflections [38]. In such scenarios, the knife edge diffraction assumes a single sharp edge (the edge being defined as having a thickness much smaller than the wavelength of the wave and separating the transmitter and the receiver).

The path loss in this model due to diffraction is obtained using the Fresnel Diffraction Parameter which calculates how deep the receiver is within the shadowed region. A negative value for this parameter means that the obstruction is below line of sight and a value below negative one (-1) means hardly any loss. A value of zero means that the transmitter and the receiver and the tip of the obstruction are all in line and the Electric field strength is reduced by half. For a value parameter of 5, the path loss rapidly increases to a value of 27dB [38]. The Fresnel Diffraction Parameter $v$ is defined as [38]:

$$v = h\sqrt{\frac{2(d_1 + d_2)}{\lambda \times d_1 d_2}} \tag{2.41}$$

where: $d_1$ = distance between the transmitter and the obstruction along the LoS
$d_2$ = distance between the receiver and the obstruction along the LoS
$h$ = the height of the obstruction with respect to the line of sight
$\lambda$ = wavelength

Knife-edge diffraction modeling can be useful in modeling some parts of a mine tunnel which are not in LoS and having an obstruction between them. However, this might be a simplification of the obstruction as usually the form of a real obstruction would be different than a simple knife edge.

**TTE modeling**

EM wave propagation in a dissipative medium such as rock is affected by two electrical properties namely conductivity and permittivity and their dependence on physical properties such as moisture content, non-homogeneity, temperature, pressure and frequency [41].

Therefore, the attenuation of a polarized wave propagating through rock (a lossy medium) is characterized by the rock's permeability, conductivity and permittivity which gives a fundamental wave equation which in turn gives the attenuation characteristics of the rock medium [41]. Analysing this wave equation and only considering the Electric field component in the positive $y$ direction can be expressed as (2.42) [41]:

$$\frac{\partial^2 E_y}{\partial x^2} - (j\omega\mu\sigma - \omega^2\mu\epsilon)E_y = 0 \tag{2.42}$$

where $\gamma^2 = j\omega\mu\sigma - \omega^2\mu\epsilon$ is the propagation constant (wave number) of the medium of propagation of interest, $\sigma$ is the conductivity of the rock, $\epsilon$ is the relative permittivity of the rock, $\omega$ is the angular frequency and $j$ is the unit complex number. The constant of propagation can be simplified to be $\gamma^2 = (\alpha + j\beta)^2$ where: $\alpha$ is the attenuation in nepers/m and $\beta$ is the phase shift in radians/m. Solving the wave equation for the attenuation and the phase shift gives (2.43) and (2.44) with frequency $\omega$ being the design parameter [41].

$$\alpha = \omega\left[\frac{\mu\epsilon\big\{(1+\frac{\sigma^2}{\omega^2\epsilon^2})^{\frac{1}{2}} - 1\big\}}{2}\right]^{\frac{1}{2}} \tag{2.43}$$

$$\beta = \omega\left[\frac{\mu\epsilon\big\{(1+\frac{\sigma^2}{\omega^2\epsilon^2})^{\frac{1}{2}} + 1\big\}}{2}\right]^{\frac{1}{2}} \tag{2.44}$$

$\mu$ is assumed to be the same as free-space permeability = $\mu_0$ = $4\pi \times 10^{-7}$H/m. From the same equations, the complex nature and the interdependence of the quantities involved can be observed [41].

The loss tangent of the medium is obtained from (2.45):

$$\gamma^2 = j\omega^2\epsilon\mu\big(\frac{\sigma}{\omega\epsilon} + j\big) \tag{2.45}$$

where $\big[\frac{\sigma}{\omega\epsilon} = p\big]$ is the loss tangent of the medium which expresses the electrical properties of the medium.

The relationship between the power of the transmitted wave at a transmitting antenna and the power received, after incorporating Friis equation may be conveniently expressed by (2.46) [41]:

$$\frac{P_r}{P_t} = G_t G_r (\frac{\lambda}{4\pi R}) e^{-2\alpha R} \tag{2.46}$$

where: $P_r, P_t$ = power at the receiver and transmitter
$G_t, G_r$ = gain of transmitter and receiver
$\lambda$ = wavelength of the transmitted signal
$R$ = separation distance between transmitter and receiver
$\alpha$ = attenuation constant of the medium as given by (2.43)

### 2.4.2 Comparison of analytical modeling techniques

A comparison (in terms of advantages and disadvantages) of the various analytical modeling techniques discussed in section 2.4.1 are given in Table 2.2 with respect to their suitability and applicability to different scenarios in the channel modeling of underground mine tunnels [35], [46].

### 2.4.3 Measurement-based modeling

Measurement based modeling of mine tunnels entails taking special equipment into the mine tunnel and analysing the channel characteristics using different techniques. Depending on the type of measurements taken, the results obtained come with different accuracy and complexity. There are two main types of measurement-based type modeling namely wideband and narrowband measurements. Narrowband measurements focuses on a specific (usually small) range of frequencies and as a result are far quicker and easier to obtain whereas wideband measurements take into account a wide spectrum of frequencies and require a lot of time to perform than narrowband [35], [47].

#### Narrowband measurements

Measurements for this are typically done at/around the carrier frequency and focus only within a small range of frequencies. In narrowband measurements, the focus is mainly on the signal's fading statistics and it's propagation loss due to the channel under investigation. The fading statistics are characterised into small and large scale fading. Small-scale fading are due to rapid fluctuations of the signal when small observation distances (wavelength size) are considered. Large-scale fading are for the fluctuations that occur to the

Table 2.2: Comparison of the different analytical modeling techniques

| Comparison of Analytical Modeling Techniques | | | | |
|---|---|---|---|---|
| | **Waveguide** | **Ray-Optical** | **Full-Wave** | **Hybrid** |
| **Pros** | • Easy to use and set up<br>• Requires few input parameters<br>• Provide fast estimation of attenuation<br>• Surface roughness and antenna effects considered | • Used to model high frequencies with more accuracy<br>• Models both near and far fields<br>• Surface roughness considered | • Provides most accurate results<br>• Applicable to most geometries including mines<br>• Surface roughness considered<br>• Completely characterises channel for wideband and narrowband, near and far fields | • Few input parameters<br>• Models near and far fields<br>• Wideband characteristics modeled<br>• Waveguide and Ray-Optical advantages |
| **Cons** | • Can not cater for high frequencies when wavelength is smaller than area considered<br>• Provides path loss only<br>• Can not predict near field behaviour | • Expensive computation with increase in number of modes and distance<br>• Less accurate for lower frequencies<br>• Provides path loss only<br>• Geometry dependant | • Complex to simulate and set up<br>• Complexity in computation with increase in size of geometry<br>• Can not cover wide array of geometries | • Expensive computation with increase in distance and modes<br>• Increase in bandwidth under consideration leads to more computational expenses |

signal at large distances (more than the signal wavelength) [35]. Statistical distributions such as Rayleigh, Rice, Nakagami, Log-normal are used for different types of wireless channels [35].

From the narrowband data, both the small-scale and large-scale components can be extracted by applying the right techniques [47]. Small scale fading is extracted by normalizing the received signal strength to it's mean value. From most experiments done in long straight tunnels, it was shown that the large-scle fading usually follows the log-normal distribution while the small-scale fading follows the Ricean distribution for LoS and Rayleigh distributions for NLoS [48], [49]. However, these distributions will not always hold true in different environments as they are terrain and environment dependent.

In most narrowband measurement studies done, it was observed that because of the mine tunnel's irregular and rough walls, multipath effects are sometimes destructive in nature and the pathloss exponents of ($n$ = 2) are common [50].

**Wideband measurements**

In wideband measurements, it is usually assumed that the channel acts as a linear filter from which the CIR of the channel can be characterized. From the CIR, other parameters associated with the CIR such as PDP (from which RMS delay spread, received power, time-of-arrival TOA) can be obtained. This information is useful in the design of wireless communication systems. The delay spread has been shown to depend on frequency as well. In some works 2.4 GHz was shown to have a larger delay spread than 5.8 GHz [46].

### 2.4.4 Related works for analytical and empirical modeling

Theoretical and experimental aspects of natural wave propagation of high-frequency waves in underground mines were performed in [51]. Narrowband and wideband measurements were taken to characterize the channels' longitudinal attenuation, coherence bandwidth, delay spread of the channel impulse response in various areas of the mine. The emphasis was mainly on field attenuation versus the distance between the transmitter and the receiver with the aim of finding an optimal frequency of operation for the analog transceiver. Frequencies used in the experiments where in the range of 150 to 900Mhz. The experiment was broken down into 2 parts; the first dealt with channel characterization in a straight tunnel and the second experiment was done in a room and pillar environment. In their literature review for theoretical modeling, Lienard *et al* [51] mentions that ray or modal approach (for the EM waves) can be used. Using the modal approach to get an analytical solution, the geometry of the problem is limited to circular or elliptical tunnels so that the air-ground boundary corresponds to a surface with coordinates to which the Helmotz equation is separable. They also note that if the gallery has an arbitrary shape, the ray-launching technique can be used by discretizing the walls of the mine gallery into planar facets [51]. Their modeling was limited to straight rectangular tunnels.

An approach called the “Cascade Impedance Method" (CIM) is used in [37] to predict the propagation in a complex and diffracting rough mine. The CIM basis is that in spite of reflections, diffractions and attenuation due to the roughness and the complexity of the channel in a mining tunnel, it is still a transmission channel and can be thought of as a transmission line and therefore a statistical approach can be used to predict the roughness of the surface of the mining tunnel by making an assumption that the behaviour is analogous to that of dielectric impedances with losses. In addition to the CIM, an SSM (Statistical method Segmental Method) technique is also applied to a non-canonical mining tunnel. The SSM technique divides the mining tunnel into many segments and each segment is further divided into sections and each section into cells in transversal and vertical directions. The tunnel is modeled as an impedance $[Z_0]$ and the magnetic field in free space is modeled as $[H_z^{(0)}(x,y,z)]$ and the magnetic field inside the 4 rough di-electric walls are modeled as $[H_1(x,y,z)]$, $[H_2(x,y,z)]$, $[H_3(x,y,z)]$, $[H_4(x,y,z)]$. Impedance cascading is then applied. The analytical modeling was done at 18 GHz. The mine gallery of interest was characterised by several attenuations caused by strong multipath, fading and significant diffraction [37].

Wideband measurements are carried out at a centre frequency of 2.4GHz in [52] and due to equipment restrictions, the frequency channel-sounding technique is utilised. The modeling was mainly concerned with extraction of parameters namely power-delay-profile, mean excess delay, rms delay spread, max excess delay, coherence bandwidth and path loss. Experiments were done at CANMET mine in Pittsburg, Pennsylvania with dimensions: length = 75m, width = 5m, height = 5m, with walls which are very rough and protected with a metallic grid. The floor is uneven and contains water plaques. The equipment utilised was an RF synthesizer (Tx) and a spectrum analyser (Rx) used for narrowband measurements. For the wideband measurements, a vector network analyser was used for transmission and reception of the RF signal. Omnidirectional antennas were utilised for the transmitter and receiver with a central frequency of 2.4GHz and a gain of 0dBi. A detailed measurement set-up is given on how the experiments were conducted. From measurements performed, the path loss exponent '$n$' was determined from narrowband measurements and from the wideband measurements, the magnitude of impulse response, excess delay, rms delay spread, max excess delay, coherence bandwidth, relative multipath total power and number of multipath components were obtained [52].

In [53], Vector Network Analysis measurements were done for the frequency interval of 850 MHz - 950 MHz with an MT8222-A-BTS Master in conjunction with 2000-1045 omnidirectional Anristu antennas. The path loss exponent was determined by considering the total received power at each distance and averaged locally over space using (2.47) to get the total received power at a specific distance $d$:

$$P_R(d) = \frac{1}{FL}\sum_{i=1}^{F}\sum_{j=1}^{L}|H(f_i,t_j;d)|^2 \tag{2.47}$$

where $F$ is the number of data points (in their case 551), $L$ is the number of local measurements at a specific distance $d$ (which denotes the distance between the transmitter and the receiver). $H(f,t)$ is the received power at that distance and $f$ is a representation of a single data point in space at that distance and $t$ denotes the number of measurements done at that local data point in space. The model for the path loss which was used is given in (2.48):

$$\log_{10} \frac{P_T}{P_R(d)} = \frac{A}{10} + n \log_{10}(d) \tag{2.48}$$

where $A$ = intercept and $n$ = path loss exponent.

Frequency dependent path-loss was also calculated. Noted was the fact that path loss usually increases as the frequency increases, and the relationship is often given by: $(PL(f) \propto f^K)$, where $K$ denotes the dependency and $PL(f)$ is spatially averaged to remove the small-scale effects. To get CIR, the Channel Transfer Function (CTF) was used and applying the IFT (Inverse Fourier Transform) to get the CIR. Measurements were done in an active coal mine in Brookwood, Alabama. The shaft covers a vast area with cross-cuts, escape ways, blockages and the ground in the mine was not flat. The walls were rough and covered with lime powder. Some walls and ceilings are supported by metal and wooden grids. The transmitter and receiver heights were chosen carefully to replicate a possible communication between devices [53]. The same procedure used in the measurements is the same as in [52] discussed above.

In [50], Rissafi *et al.* used a frequency range from 3-10 GHz in their experimental characterization of a UWB propagation channel in an underground mine. They used different antenna directivity to extract UWB propagation characteristics from a mine with rough surfaces. The mine had very rough surfaces that have a difference of 25cm between the maximum and minimum surface variations. The ground was not flat but sparse with puddles of water [50]. The dimensions of the mine were; a width of 2.5m to 3m and a height of 3m. The transmitter was fixed for all the measurements that were taken. The receiver was moved on a 49 point grid (7-by-7 points with a spacing of 5cm between each adjacent point), 5cm is equal to half of the wavelength of the lowest frequency component for uncorrelated small scale fading. However, for the large-scale path loss in LoS scenarios, the receiver was moved from 1-10m away from transmitter in intervals of 1m. The channel-sounding technique based on the scattering parameter $S_{21}$ was used. A network analyzer with two vertically polarized antennas; a double bridged directional horn antenna covering 1-18 GHz and an omni-directional one from 2-10 GHz, was used. The PNA used the frequency sweeping technique (7000 discrete frequencies over a 7 GHz bandwidth). At each distance point between the transmitter and the receiver, the complex channel transfer function (CTF) was measured 30 times. Log-normal, Nakagami and Rician distributions were fitted to the plotted data which was obtained [50].

Stating in their literature review, Sun *et al* [54] points out that full-wave models e.g. FDTD model, which models Maxwell's equations provides very accurate results in arbitrary geometries but may create unrealistic computational burden even for short tunnel paths. They developed a multi-mode model to analyse natural wave propagation in the near and far field regions in an underground mine tunnel. They implemented the Geometrical Optical (GO) model to do analysis on the field distribution of the excitation plane (the cross-section that has the transmitter antenna). The GO is better in terms of computation because the analysis of the rays is limited to a 2D model. Mode-matching is implemented to match the modes derived from a waveguide model to the field distribution derived by GO. The model's intensity is then calculated by numerical integration and the non-linear regression method. The path loss and RMS delay spread at any position in the tunnel are obtained by making use of the mode intensity and the waveguide model. The model developed is only applicable to underground mines which do not utilise the room and pillar mining method [54].

In his study, Hussain [47] obtained the channel characterization of the Wits Mock-Mine using different antenna parameters. He took an empirical modeling approach in which measurements were done within the mock mine at Wits. In his methodology, he mentions that to get the statistical behaviour of the radio channel, experiments had to be done at different positions in the mine. But since it was a measurement campaign, the system and equipment to be used had to be calibrated. The wideband measurements performed were to get the path-loss exponent, shadow fading statistics, the CTF, CIR, PDP, time dispersion parameters (mean excess delay, RMS delay spread and maximum delay spread) and the coherent bandwidth. Hussain points out that the path-loss exponent and shadow fading statistics can still be deduced from narrowband measurements at any location where the measurement is done.

The channel sounding method was used in taking the wideband measurements. Large-scale parameters were obtained from the transmission coefficient of the wideband measurements and the local average received power was measured at a track of $5\lambda - 40\lambda^2$ for the large-scale measurements. The small scale fading parameters were obtained from the CIR. For small-scale measurements, $P_\tau$ (multipath component power of the PDP) was obtained by spatial averaging of $|h(t,\tau)|^2$ (channel impulse response) over the local area. $P_\tau$ over the large-area was then obtained by summing up and averaging the measurements over the small-areas. He notes that the received power over a local area will not fluctuate significantly if the measurements are done with a bandwidth greater than the coherence bandwidth. The channel sounding technique utilised used the Vector network analyser for extracting large-scale and small-scale parameters from wideband measurements. Fast sweep time was utilised which is necessary to keep total sweep frequency measurements in a short interval for time-varying channels [47].

The channel sounder used operates in 2.4-2.5 GHz and 5.8-5.9 GHz frequency bands. The power for the VNA was kept constant at 0dBm (1mW) and a quasi-static channel was assumed. For the data acquisition, MATLAB scripts were used to analyse the large-scale and small-scale fading parameters. The linear least square regression method was used to evaluate the scatterers' received power over transmitted power as a function of the transmitter and receiver distances to evaluate the path loss exponent. Shadow fading was estimated by measuring the deviation of $\frac{P_R}{P_T}$ from the linear regression line. The Kolmogorov-Smirnov (KS) test was used to identify the line of best fit distribution for the shadow fading. From the frequency bands mentioned above, with a bandwidth of 100 MHz (time resolution of $10ns$), frequency steps of 0.182 units were used for the small-scale parameters. Using the Hamming window function, the time resolution was multiplied by a factor of 2. The 5.449 $\mu s$ temporal range (the inverse of frequency steps) was noted to be quite sufficient when comparing with the maximum excess delay and the propagation delays of the utilised cables. This minimised the phenomenon of aliasing [47].

Robins [46] used the hybrid analytical modeling technique to model the Wits Mock Mine approximating the tunnel to have a rectangular cross section with dimensions; (width = 3.026m, height = 2.690m, length = 66.24m). It was noted that approximating the tunnel as having a rectangular cross-section should have no significant effects on the results obtained [46]. The first set of simulations considered the ceiling/floor and walls to have the same electrical properties as the rock in [54]. The second set of simulations took into account the steel casing within the mock-mine tunnel for comparison with the first set of results. Distance increments were in steps of 0.01m considering a smallest wavelength of 0.05m (5 GHz frequency). The number of modes was initially set at 150 which was found to be excessive with a recommendation of around 50 modes thought to be enough and showing little difference in the results obtained [46]. The transmission power used in the simulation was assumed to be 1mW. Both wideband and narrowband simulations were performed.

## 2.5 Performance analysis of communication systems

From the problem statement, the performance analysis to be performed in this study is mainly concerned with the reliability of communication systems employed in the underground mines. This is with regards to their ability to be able to establish connectivity after a mine collapse. This means that the study is limited to analysis of the received power behaviour which is most relevant for monitoring connection/disconnection between nodes in different scenarios.

This part of the work is mainly concerned with identifying shortfalls that will be associated with common WSN systems employed in the underground mine tunnels in the event of common mine tunnel collapse scenarios.

Some of the metrics to consider in the performance analysis of communication systems are discussed in *Section 2.5.1*.

### 2.5.1 Performance metrics

[55] suggests and argues that there are five key performance metrics to be considered when a wireless communication system is evaluated and these are mainly coverage, capacity, co-existence, power consumption and security.

#### Coverage

This is the range over which the communication system can reliably connect devices. One thing to consider is the link budget which measures the ability of the wireless system to overcome things such as obstacles in the path of the signal and still be able to complete a link. This is affected and/or determined by three major factors which are the transmission power, the antenna gain and the receiver sensitivity. The fact that transmit power is limited and regulated especially in the unlicensed band, affects the amount of power that can be transmitted and the selection of antenna gain. In most cases the only variable left to vary is the receiver sensitivity. The sensitivity reflects the ability of the receiver to distinguish the signal from noise. One metric used is to compare the sensitivity with the thermal noise floor. However, in most cases the receiver sensitivity is limited by the hardware of the receiver. A good receiver sensitivity reflects the potential to operate when SNR measured on the log scale is negative[55].

#### Capacity

This is the amount of data that an access point can simultaneously handle at one time. Aggregate capacity could be considered which is different from the single-link throughput offered between one device and the gateway. Many single-link throughput capacities are modest but if there is a good multiple access scheme, the aggregate capacity could even be made higher. A raw PHY-layer data rate is usually not the same as the aggregate capacity because of things such as MAC overheads, poor multiple access techniques and the required margin to account for unpredictable traffic fluctuations. [55] notes the importance of balancing capacity and coverage in a cost effective wireless network performance since it is pointless to have a good coverage without the capacity to support the covered devices and also pointless to have a good aggregate capacity without the devices (not in range because of poor coverage).

#### Co-existence

This is the ability of a wireless system to coexist with other devices that have the ability to cause significant and dynamic interference. A robust network must be able to withstand interference from other transmitting networks, especially in the constantly changing propagation environment that is the hallmark of an underground mine. At every layer, interference mitigation techniques must be implemented e.g. Direct-Sequence-Spread-Spectrum (DSSS) at the PHY-layer to enable operation at negative SNR and ACKs at the MAC layer to ensure successful data transfer between the endpoint and gateway [55]. This is an important performance metric for a wireless communication system to be deployed in an environment such as a mine where the space is confined and there are many systems usually operating within the same ISM band.

#### Power consumption

This is the amount of power that the wireless system will require and is linked to the amount of time that a battery will last under the operation of the wireless system, especially for systems that run on batteries such as WSN systems. A good network design should allow for “low latency, highly responsive connections for continuously powered devices and an efficient connection for battery powered devices" [55]. Efficiency is determined by the underlying wireless protocol which boils down to the fact that minimum time and power must be spent when transmitting and receiving the communication signals. Such techniques utilised include “Fast Acquisition", “Adaptive-Modulation". The overall protocol design should aim that the endpoint is in a low power “deep sleep" mode for the majority of the time [55].

In the scenarios we intend to investigated in this research, the interest will be mainly on coverage because of the aspect of continuous connectivity after the tunnel blockage. The other metric to consider would be capacity for a WSN network where other nodes could fail and the connection to be established is by the nearest node to the one which has failed and hence should be still able to handle multiple calls more than it would have processed in a normal scenario (non-collapsed scenario).

### 2.5.2 Related works for performance evaluation

In [56], two parameters are used to check the quality of a network. These are the RSSI (radio signal strength indicator) and the LQI (link quality indicator). In the study performed, an omnidirectional propagation of radio waves from the transmitter was assumed (where the signals should propagate in all directions so as to be able to communicate with multiple nodes in a mesh topology layout). MRF24J40, CC2420 and ZENA WSN motes were used to carry out the experiments [56].

A dynamic wideband channel model is developed in [57] for harsh industrial areas. Furthermore, performance evaluations based on the IEEE 802.15.4 physical layer standards were conducted using the developed channel model. BER performance evaluations were performed in a simulated software package in which random bits were generated, an O-QPSK modulation and demodulation; and DSSS spreading and de-spreading techniques were utilised in conjunction with the developed channel model [57].

The performance of IEEE 802.15.4 was conducted in [58]. Six radios were used as the hardware for collecting the results. Each of the units consists of a radio module and a single board computer with local data storage. The measurements were done by placing these units in positions representative of a WSN layout in an industrial area setup. In the experiment conducted, RSSI, LQI and PER (Packet Error Rate) were measured. The measurements were done for both LoS and NLoS situations for the different combinations amongst the radio units [58].

Measurement campaign were done using two MEMSIC IRIS motes working at 2.4 GHz transmitting at a data rate of 250 kbps and an RF power of 3dBm with a receiver sensitivity of 101dBm. The motes implement the MAC and PHY layers defined in IEEE 802.15.4 protocol with a ZigBee Upper layer. RSSI, LQI and PER were analysed. Channels occupied by other systems such as Wifi were not considered and not used during the experiments and therefore issues of coexistence were omitted from the study [59].

### 2.5.3 Topology design of a WSN

In a wireless sensor network made up of many nodes, a node can communicate with other nodes within its wireless transmission range. However, nodes which are outside this transmission range but are able to detect the wireless signal are in the carrier sensing range [60]. Usually in a WSN, with the right topology, no infrastructure or centralized data management is needed. The network is dynamically formed and nodes manage themselves [60]. With this in mind, the challenge faced by WSN is the fact that a node has to be within the transmission range of another node. In the event of a mine tunnel collapse, and if a part of the network is lost, the remaining nodes in the network must make sure that communication can still be established. This can only be achieved if the transmission range of all the remaining nodes still overlap.

Some of the considerations in the design of a WSN and other ad hoc networks are that of connectivity, security, quality of service, energy consumption and routing optimization [60]. In addition to inheriting classical problems of other wireless networks, WSN networks and other ad hoc networks generate new challenges such as autonomy, lack of infrastructure, dynamicity and scalability [60].

However, the focus in this work will be to recommend the efficient placing of the nodes and the optimum frequency of operation in a WSN for greater coverage and maintained connectivity in the event of a mine tunnel collapse.

## 2.6 Conclusion

A review of existing and past underground mine communication systems has been outlined. Of importance in the review was the existence of other commercial products which have been developed to help solve the issue of communication after a mine tunnel collapse. However, most of the shortcomings of these solutions have to do with the fact that they are bulky in size and hence not ideal for miners to carry with in an underground mine environment.

The technology of wireless sensor networks was found to have some benefits when it comes to underground mine communications especially their low power consumption, self healing capabilities and low cost, which can be employed when developing a system that should still establish communication after a mine collapse.

Channel modeling fundamentals have been discussed which help in understanding the techniques employed when modeling underground mine tunnels.

This chapter has also outlined the most common channel modeling techniques employed in underground mine tunnels. A review of related research work in which some of the techniques have been used was considered. A comparison of the models in terms of their pros and cons has been given. This research work will subsequently make use of a combination of the Ray-tracing and TTE modeling techniques.

The last section of this chapter discussed the performance metrics of interest to look at when doing an evaluation of wireless networks which are coverage, capacity, coexistence, power consumption and security. One of the important metrics to mainly consider in the case of a WSN network is coverage. For the topology design of a WSN network, coverage also becomes an important consideration when designing for a network that should guarantee connectivity in the event such as a mine tunnel collapse.

# Chapter 3

# Research Methodology

## 3.1 Chapter overview

This chapter presents the methodology taken in the pursuit of the research to be able to answer the research questions. Mine tunnel collapse scenarios to be considered are presented and the appropriate modeling techniques are identified. The equipment and simulation software used in the research are also discussed.

## 3.2 Methodology

To the best of our knowledge, no other work has proposed the channel modeling of a collapsed underground mine tunnel, especially in the context of the topology design of a wireless sensor network.

This section presents the set of techniques and procedures undertaken to fully answer the research questions posed in *Section 1.3*. The work is divided into 3 major components; (i) The analytical channel modeling of the partially and fully collapsed mine tunnels; (ii) The use of standardised tools for channel modeling to compare the analytical channel models obtained in (i); and (iii) Performance evaluation of a WSN communication system in a collapsed mine scenario.

The steps followed for the execution of the research are outlined below:

1. From the literature review and similar or closely related works, the selection of appropriate channel modeling techniques and/or proposal of new techniques to be used in the simulations.

2. Choosing the appropriate techniques to conduct measurement based modeling and/or mine tunnel CAD simulation on the proposed scenarios in a bid to compare, contrast, validate and supplement the models obtained from analytical modeling.

3. Use the results obtained in steps 1 and 2 for the proposal of a WSN network topology/architecture and/or a hybrid network architecture suited to the channel models obtained in the study.

The methodology followed is shown in Figure 3.1.

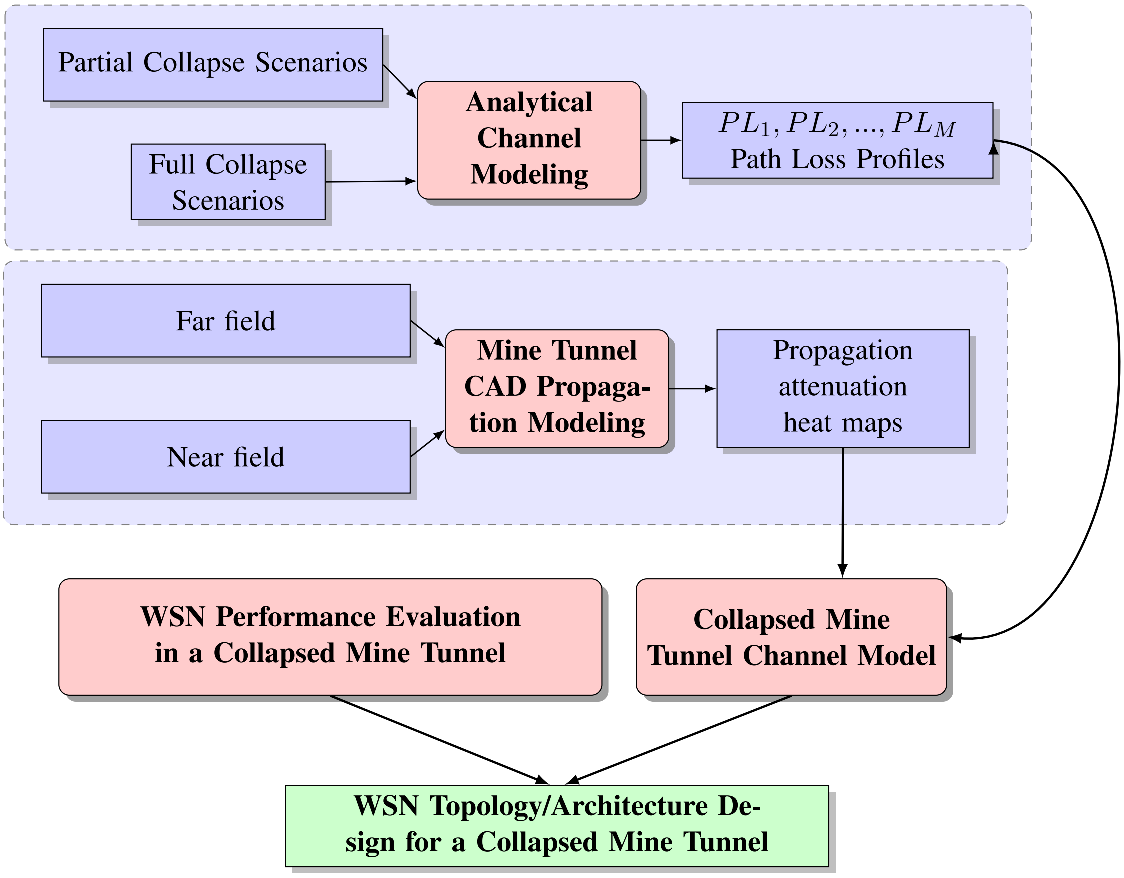


Figure 3.1: Research methodology

The different scenarios investigated and the tools and techniques used for each scenario are discussed in the next sections.

### 3.2.1 Channel modeling for WSN radios

When planning a WSN network, what is most important is coverage, which entails a focus on the amount of received power during the transmission to plan parameters such as the network budget. Unlike classical telecommunications, parameters such as coherence bandwidth, time of arrival, the power delay profile are not analysed in detail because of factors such as the complexity of each mote is kept to a minimum because of power and cost considerations, and generally the motes operate in small bandwidth or high symbol time regions, where the impact of such parameters are not significant. In the context of this work, low level parameters were not looked into. The focus was on the received power at the receiver from the transmitter.

### 3.2.2 Channel modeling: partial collapsed scenario

For simplification of a partially collapsed tunnel, Figure 3.2 with 3 sections numbered 1,2 and 3 was considered. There is a partial collapse (in the sense that the full height of the tunnel is not blocked) in the middle section. The other sections at the outer ends are still clear and an assumption was that no rock debris exists there.

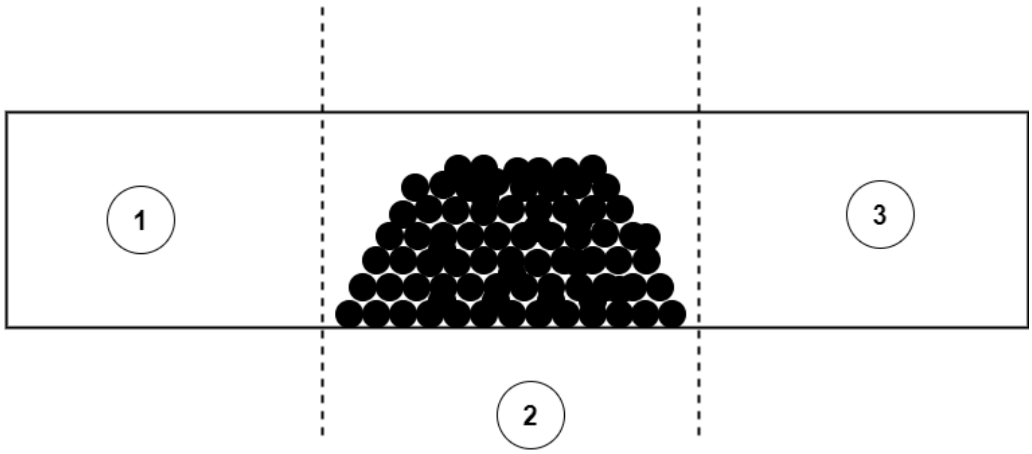


Figure 3.2: Tunnel partial-collapsed scenario

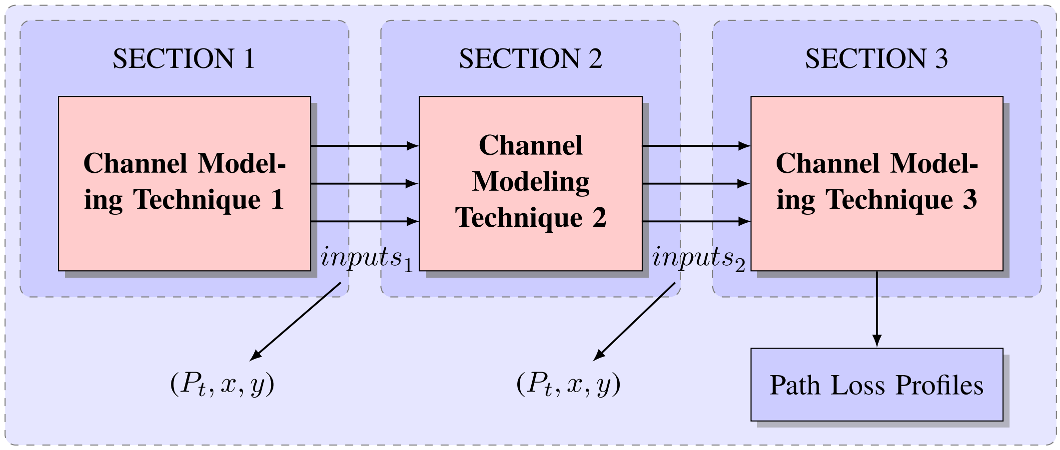


Figure 3.3: Tunnel split-section analytical modeling

Assuming that sections 1 and 2 are long enough, from literature presented as part of the background, there existed numerous works and techniques, as mentioned in the literature review sections of the background, which have modeled a normal/uncollapsed underground mine tunnel of similar geometry. These sections have been modeled as rectangular waveguides either with smooth surfaces or scatterers on the surface of the walls.

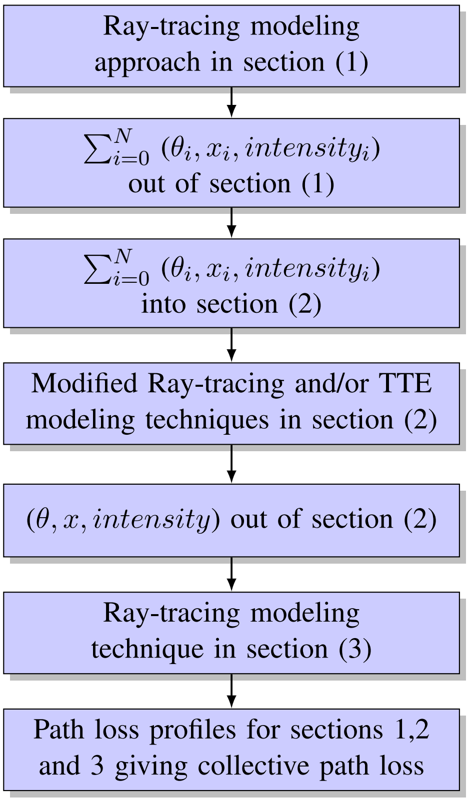


Figure 3.4: Partial collapse analytical modeling approach

The bulk of the research in our scenario was thus to try and model the middle 'collapsed' section and combine the result with that of the other two sections to come up with the overall channel model of the whole partial collapsed tunnel. An assumption was that the rock debris was perfectly stacked, such that there exists no air spaces between the debris and if signal propagation is to happen other than through the small air gap present, it had to be through-the-rock signal propagation.

The idea then was to model the three sections differently with their respective inputs (signal strengths and angles of arrival), e.g. section 2's input being the output of section 1 and the output from section 2 feeding into section 3 as outlined in Figure 3.3. In this sense each section was modeled differently with the appropriate techniques that best fitted in that particular section.

For modeling section 2, the parameter of interest was the smallest distance between the roof of the tunnel and the debris such that a person trapped in the tunnel could be able to fit through in the event of a mine tunnel collapse.

### 3.2.3 Techniques utilised - partial collapse

Because of the idea of using the output of one section to become the input to another section there arose a need of tracing the signal 'rays'. This called for a technique which

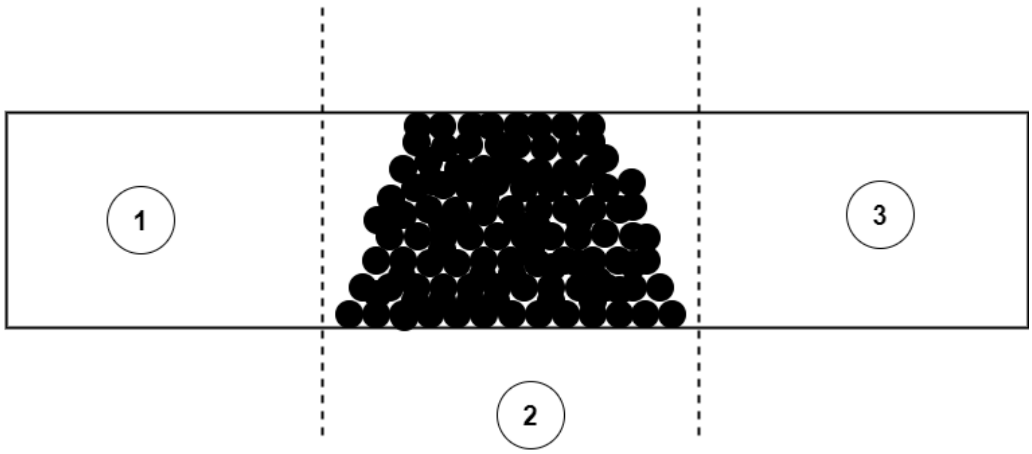


Figure 3.5: Full-collapsed scenario

utilises the concept of signal trajectory tracing. The ray-tracing [44] approach became an appropriate modeling technique with proper modifications to fit the scenario. However, only the path loss will be obtained for this part without including small scale fading effects. The procedure followed and the techniques utilised in this part of the modeling are illustrated in Figure 3.4.

### 3.2.4 Channel modeling - full collapsed scenario

Considering Figure 3.5, as opposed to the partial collapsed scenario, in a full collapsed scenario, section 2 is completely covered with rock/debris and hence a hybrid modeling technique in which section 2 had to be completely characterized using pure TTE methods in conjunction with TTA modeling techniques for sections 1 and 3 had to be used.

### 3.2.5 Techniques utilised - full collapse

Since the assumption was that there was no possibility of 'ray' propagation through the air over section 2, the ray tracing approach is not suitable for the full collapsed scenario in section 2 of Figure 3.5. The TTE model described in *Section 2.4.1* had to be adopted for this section. The ray-optical method was still adopted in sections 1 and 3. The imperative was then to use the signal strength from the output of section 1, which uses TTA modeling techniques, for use in section 2 which employs a TTE modeling technique. The procedure and techniques used in this situation are shown in Figure 3.6.

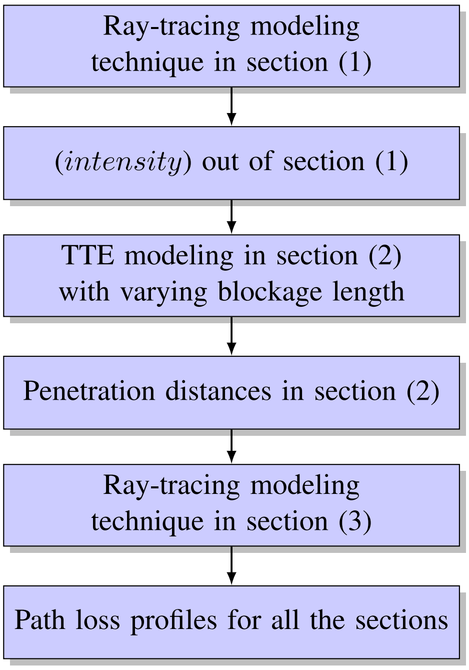


Figure 3.6: Full collapse analytical modeling approach

## 3.3 Mine tunnel CAD simulations

To compare, contrast, validate and supplement the models obtained in the analytical modeling, in which we divided the tunnel into sections of collapsed and non-collapsed sections, we used a software that is commercially used for channel modeling in different scenarios such as mine tunnels.

The result was the use of a 3D propagation modeling software suit, Altair Hyperworks' WinProp software suit for tunnels and underground [61]. A module in the software suit provides the ability to define arbitrary cross sections, curves and inhomogeneous mine tunnel terrains to provide for a realistic representation of a mine tunnel. The propagation modeling is done by using "highly accurate semi-empirical and ray-optical propagation models" [61]. The software suit has a graphical interface component (TuMan) where the 3D structure of the tunnel is defined, another graphical component (WallMan) where the electrical properties of the 3D structure of the mine tunnel are defined and PropMan where the propagation simulation is carried out by specifying the antenna properties and placements [61].

### 3.3.1 Procedure

The procedure followed the definition of the 3D geometry of the mine tunnel like the one used in the analytical modeling section. Thereafter, the specification of the electrical and magnetic properties of the tunnel walls, floor and ceiling was done. Lastly, the antenna parameters and placement in the tunnel were defined. The procedure is illustrated in Figure 3.7.

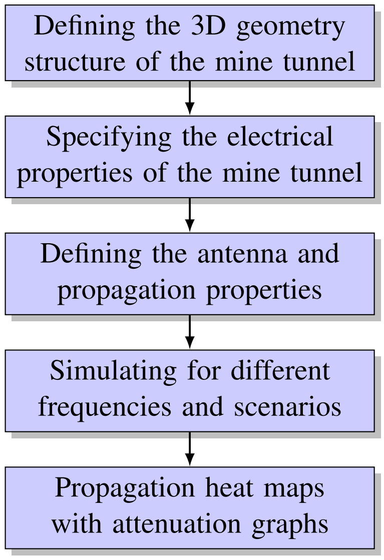


Figure 3.7: 3D CAD simulation procedure

## 3.4 Experimental setup

The evaluation was done with the use of microcontroller units that form a wireless sensor network. The frequencies considered were 434, 915 and 2400 MHz. The choice of frequencies was mainly due the available electronic devices for use in the research. The parameters varied in the performance evaluation were node separation distances for a normal tunnel situation without collapse and then for the scenario where the tunnel is collapsed to notice the change in the levels of signals obtained. The evaluation focused on obtaining the RSSI of the signal at the receiver units from the transmitter unit.

The figures of the experimental setup in the mock mine are shown in the results section of Chapter 5.

### 3.4.1 Procedure

Received power monitoring was done by porting the serial communication output of the values on the receiver microcontroller to a PC. These indicators were then used to translate the amount of coverage provided by each node in the WSN network. The procedure followed is illustrated in Figure 3.8.

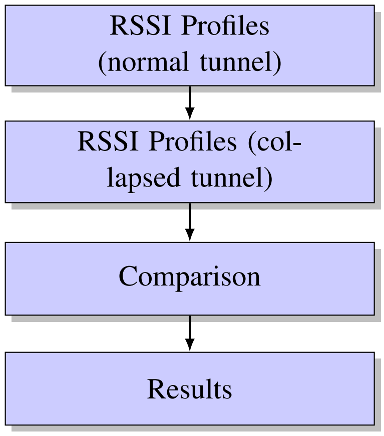


Figure 3.8: Performance evaluation procedure

## 3.5 Research equipment and simulation software

Analytical modeling simulations was implemented in MATLAB by creating models of the mathematical representations of the models and the definition of the underground mine tunnel scenarios to be simulated. The mine tunnel CAD simulation was done in Altair's WinProp software suit. For the performance evaluation, Zolertia Re-Mote [62] and Atmega328P micro-controller units were used. Network simulation and design was done in MATLAB for the network architecture design in the last part of the research.

## 3.6 Conclusion

In this chapter the methodology which was followed was presented. Different mine tunnel scenarios which were considered were introduced, namely a partial and a full collapsed scenario. The techniques and procedures followed in the different scenarios were discussed. The ray-optical modeling technique was chosen to be used for the non-collapsed section of the mine tunnel and the pure TTE method was chosen to be used in the collapsed section of the mine tunnel in the different scenarios. The procedure for the performance evaluation of a WSN in a non-collapsed and collapsed mine tunnel scenario was presented and had to be done using microcontroller based WSN motes at frequencies of 434, 915 and 2400 MHz with a focus on the RSSI of the received signal.

# Chapter 4

# Channel modeling results

## 4.1 Chapter overview

This chapter presents the results obtained from the channel modeling exercise. Techniques which were presented in *Chapter 3* in the methodology section were applied in the different scenarios, as shown in Figures 3.2 and 3.5. Analytical modeling was done using the ray-optical modeling technique which was found to be more suitable for the open air parts of the collapsed mine tunnel, a pure TTE modeling technique was applied for the collapsed section of the mine. In the first instance, the tunnel is modeled without any collapses in between, using the ray-optical method. This was done so as to compare with the results obtained by using the 3D propagation simulation software as the software itself has no capabilities of representing collapses in the tunnel geometries developed. The two sets of results were found to correlate especially for the set of higher frequencies which were considered. With this confirmation, the second part was to incorporate the TTE method into the collapsed scenarios. It was found to be difficult to verify the through-the-earth model as the 3D simulation software has no feature to incorporate a collapsed section in the geometry of the tunnel.

The set of frequencies chosen for simulation were based on a number of considerations such as frequencies in common use today, available electronic devices and lower frequencies which have better penetration distances. The maximum tunnel length under consideration in the analytical modeling was that of 90 meters due to the fact that nodes in a WSN network have a short range communication distance and also to match the length of the mock mine tunnel. However, for the 3D CAD simulation, a total of 30m could only be simulated due to restrictions on the student license acquired. A rectangular tunnel was considered.

## 4.2 Non collapsed scenarios

This section presents the results obtained for the case where the tunnel has no collapses. The analytical modeling parameters used in this scenario are given in Table 4.1. The electrical parameters used ($\sigma_r$ and $\epsilon$) are those of the rock material found in underground mines. The wavelength considered corresponds to the highest frequency of 5GHz used in the simulations. The number of modes was limited to 100 for computational reasons as there was no major difference in results obtained after 100 modes. Modeling was done for all the frequency bands mentioned in *Section 4.1*. The modeling exercise involved analysing the different path loss behaviours at different frequencies. The simulations were performed by modeling equation (2.18).

Table 4.1: No collapsed scenario analytical modeling parameters

| **Parameter** | **Values** | |
|---|---|---|
| Analytical tunnel dimensions | Height | 3.0m |
| | Width | 2.7m |
| | Length | 90m |
| Electrical properties | Tunnel $\sigma_r$ | 0.015 |
| | Tunnel $\epsilon_r$ | 5 |
| Antenna | Transmit power | 1 mW |
| | $G_t$ | 1 |
| | $G_r$ | 1 |
| Modes | Total | 100 |
| | Smallest $\lambda$ | 0.059m |
| 3D tunnel dimensions | Height | 3.0m |
| | Width | 2.7m |
| | Length | 30m |

Figures 4.1 and 4.2 show the path loss results obtained for the analytical modeling and the 3D CAD simulation respectively for 3G frequencies while Figures 4.3 and 4.4 show results for LTE frequencies, Figures 4.5 and 4.6 show results for Wifi/ZigBee frequencies and Figures 4.7 and 4.8 show the results for ISM frequencies.

From the set of results, it is evident that the path loss, i.e. the signal attenuation as a function of distance, increases as the frequency is increased. For example in Figure 4.1, the 850MHz path loss curve starts at -36dBm while the 900MHz one starts at -40dBm at 0 meters. This is true for all other sets of results presented. This behaviour is because of the inverse relationship between frequency and attenuation as represented by (2.2).

Heavy constructive and destructive interference observed in the near field of the transmitter comes as a result of the fact that rays of the signal bounces onto and off the walls and floors of the simulated mine tunnel. In that action and at certain distances, which corresponds to different multiples of the wavelength, rays of the signal propagate with different phase shifts and hence constructive and destructive interference takes place. This interference is less observed in the far field of the transmitter due to the fact that there are fewer signal rays propagating now in this region and their power has decreased substantially.

For the software simulation results, the transmitter is placed at the entrance of the tunnel (i.e. at starting distance of zero meters) at a height of 2 meters and the receiver is moved across the length of the tunnel at the same height of 2 meters to get the different RSSI values. Therefore, in Figures 4.2, 4.4, 4.6 and 4.8, the transmitter is located at the bottom of the Figures. These figures show the different power levels (represented by the different colours on the legend of the figures) along the length of the tunnel starting from where the transmitter is located moving across the other side of the tunnel.

From the software simulation results, the same can be said of the correlation between an increase in frequency and an increase in the signal attenuation with distance. In this particular case however, constructive and destructive interference could not be represented, even though it is happening, because the heat map represents a fitted linear curve of the optical ray tracing model applied in the simulation software. If the results were presented on a graph, they would have looked similar to the ones presented for this research's analytical modeling.

The two sets of results, i.e. the result from the analytical modeling and the result from the software simulation, show a good correlation for higher frequencies starting at 915MHz. For lower frequencies, a discrepancy is noticed between the two sets of results. A comparison of the results at 10m, 20m and 30m is provided in Table 4.2 where a huge discrepancy of more than 10dB is highlighted in red, a difference of 4dB-10dB is highlighted in yellow and a difference of less than or equal to 3dB is highlighted in green. The green highlights are what we are considering a good correlation in the rest of the discussion.This is because when the modal approach used in the ray-optical technique is applied to tunnels, it works well for higher frequencies especially the ones in the UHF range [43].

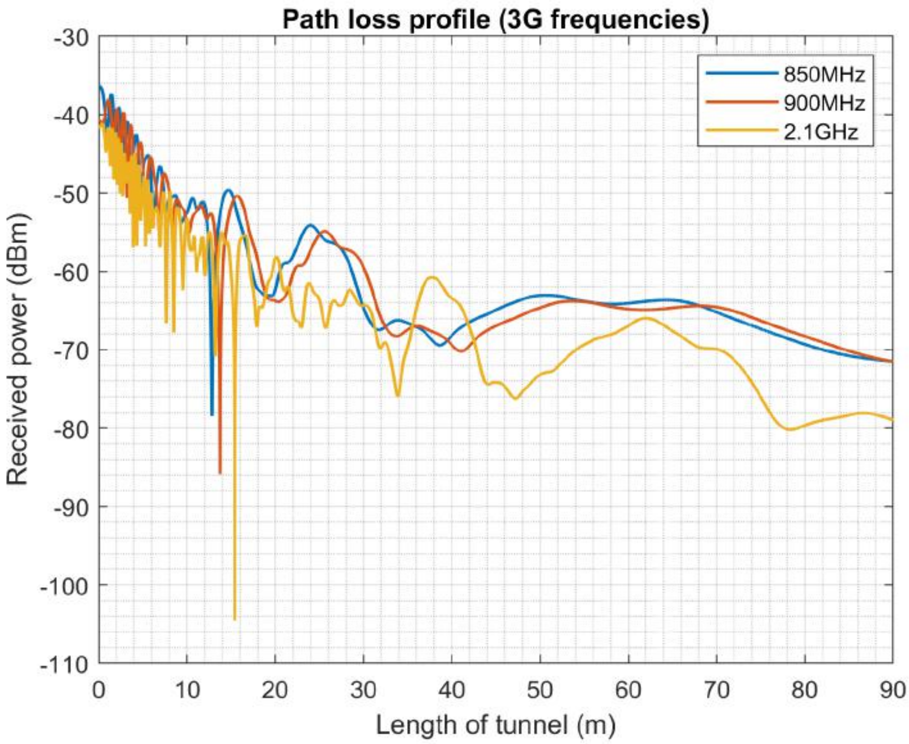


Figure 4.1: Ray-optical tracing analytical modeling path loss profiles for 3G frequencies for a non-collapsed tunnel.

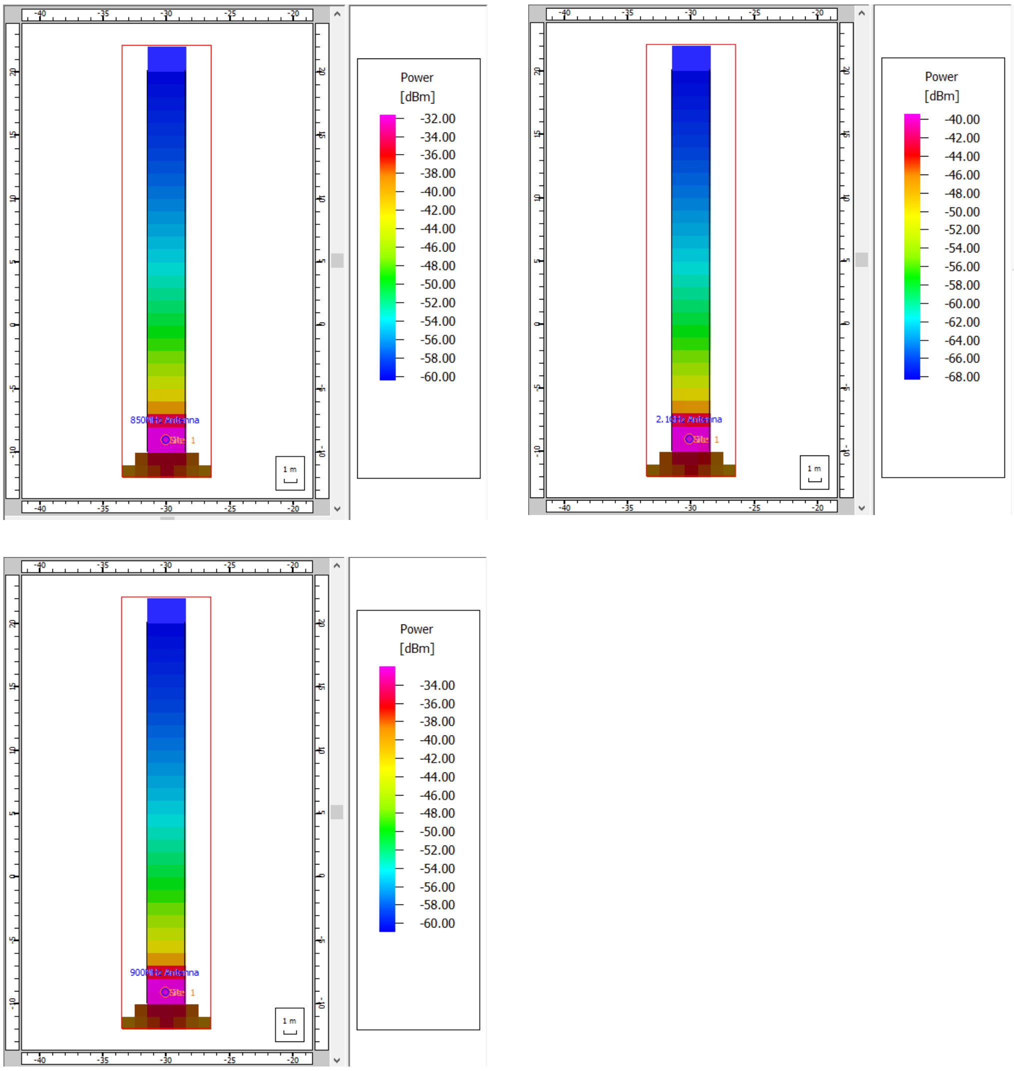


Figure 4.2: Tunnel 3D CAD propagation simulation received power heat maps for 3G frequencies for a non-collapsed tunnel. (From left) 850MHz, 900MHz and 2.1GHz. The heat map depicts the RSSI values (in dBm) in the virtual tunnel along the length (y-axis). The y-axis on the figures represent the length along the tunnel from the entrance to the exit. A total length of 30 meters is shown on the figures, from -10 m to 20 m on the scale. The x-axis represent the width of the tunnel i.e. the length of the opening of the tunnel. This is for all the heat maps presented in this chapter.

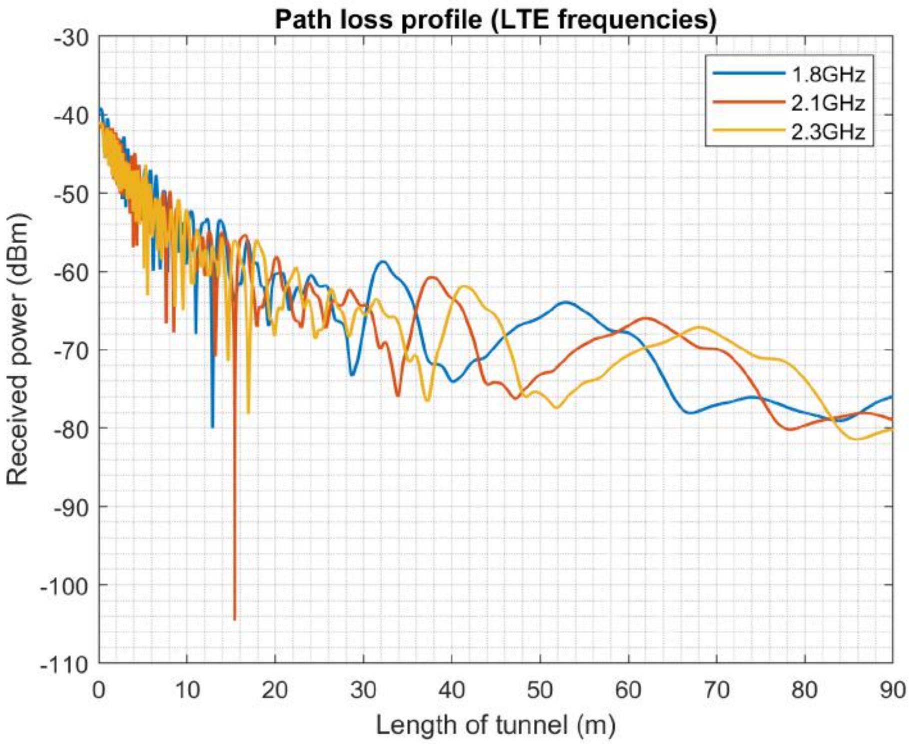


Figure 4.3: Ray-optical tracing analytical modeling path loss profiles for LTE frequencies

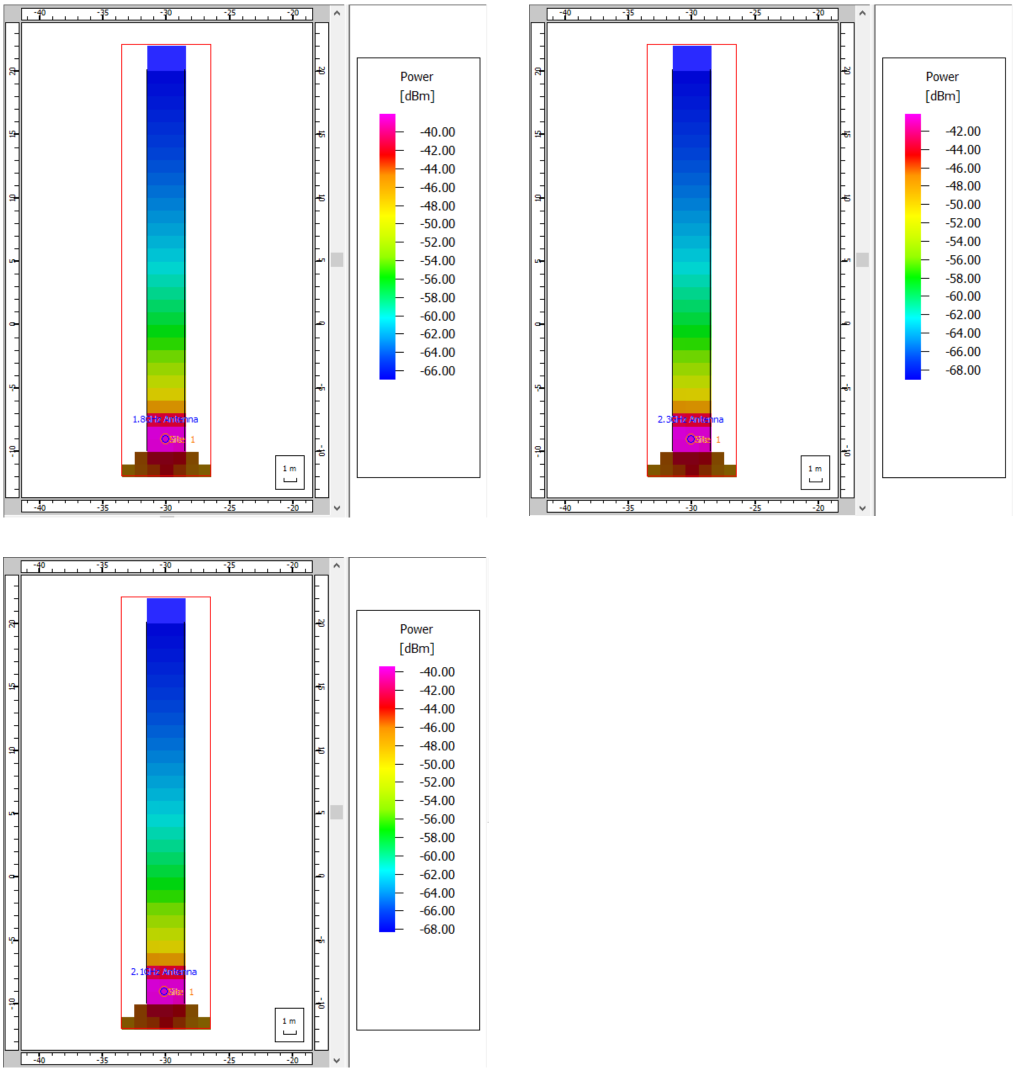


Figure 4.4: Tunnel 3D CAD propagation simulation received power heat maps for LTE frequencies for a non-collapsed tunnel. (From left) 1.8GHz, 2.1GHz and 2.3GHz.

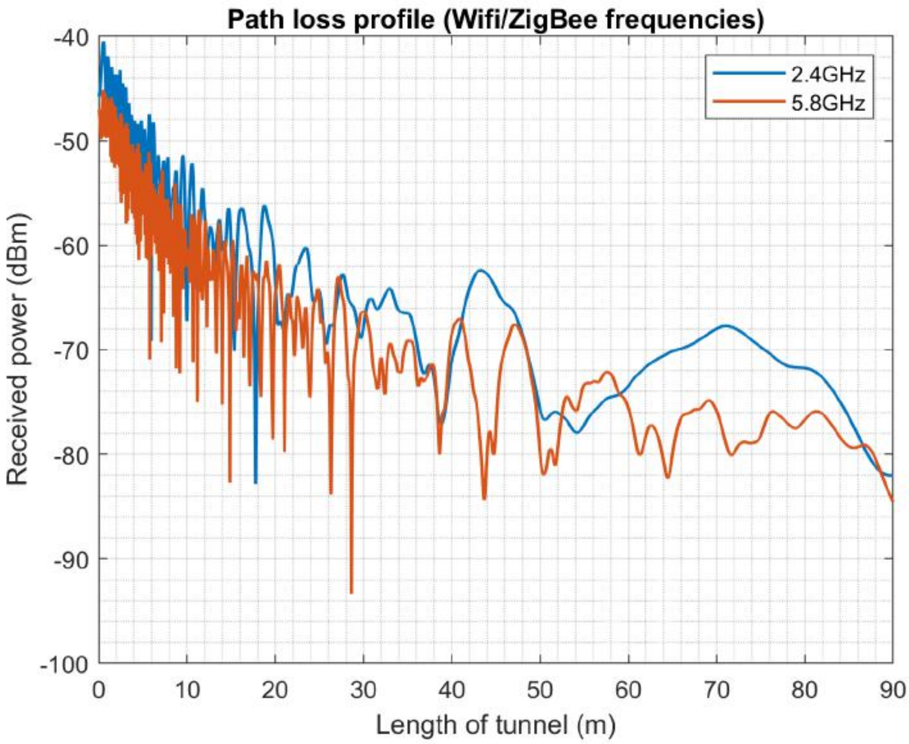


Figure 4.5: Ray-optical tracing analytical modeling path loss profiles for Wifi/ZigBee frequencies for a non-collapsed tunnel.

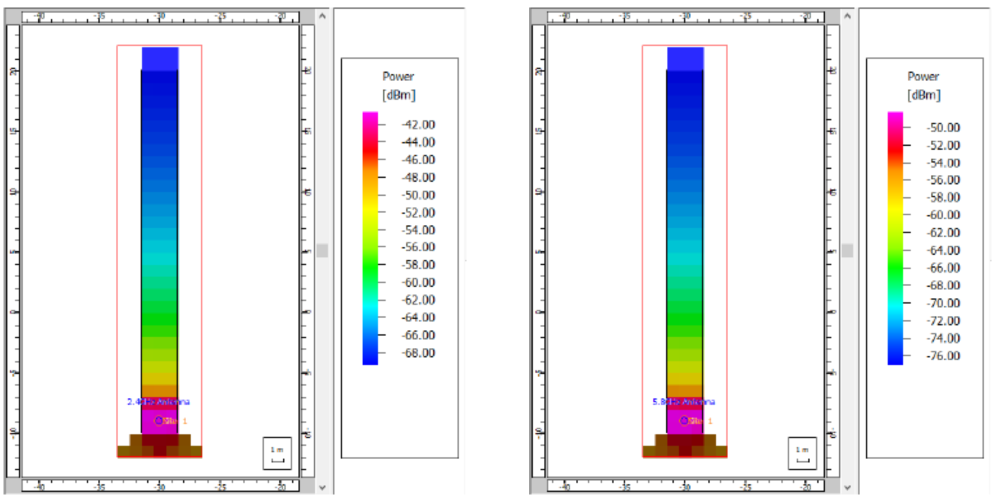


Figure 4.6: Tunnel 3D CAD propagation simulation received power heat maps for Wifi/ZigBee frequencies for a non-collapsed tunnel. (From left) 2.4GHz and 5.8GHz.

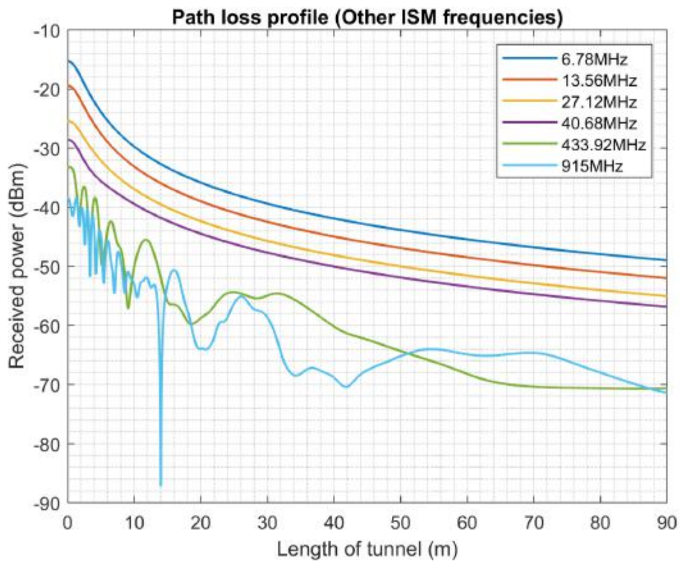


Figure 4.7: Ray-optical tracing analytical modeling path loss profiles for other ISM frequencies for a non-collapsed tunnel.

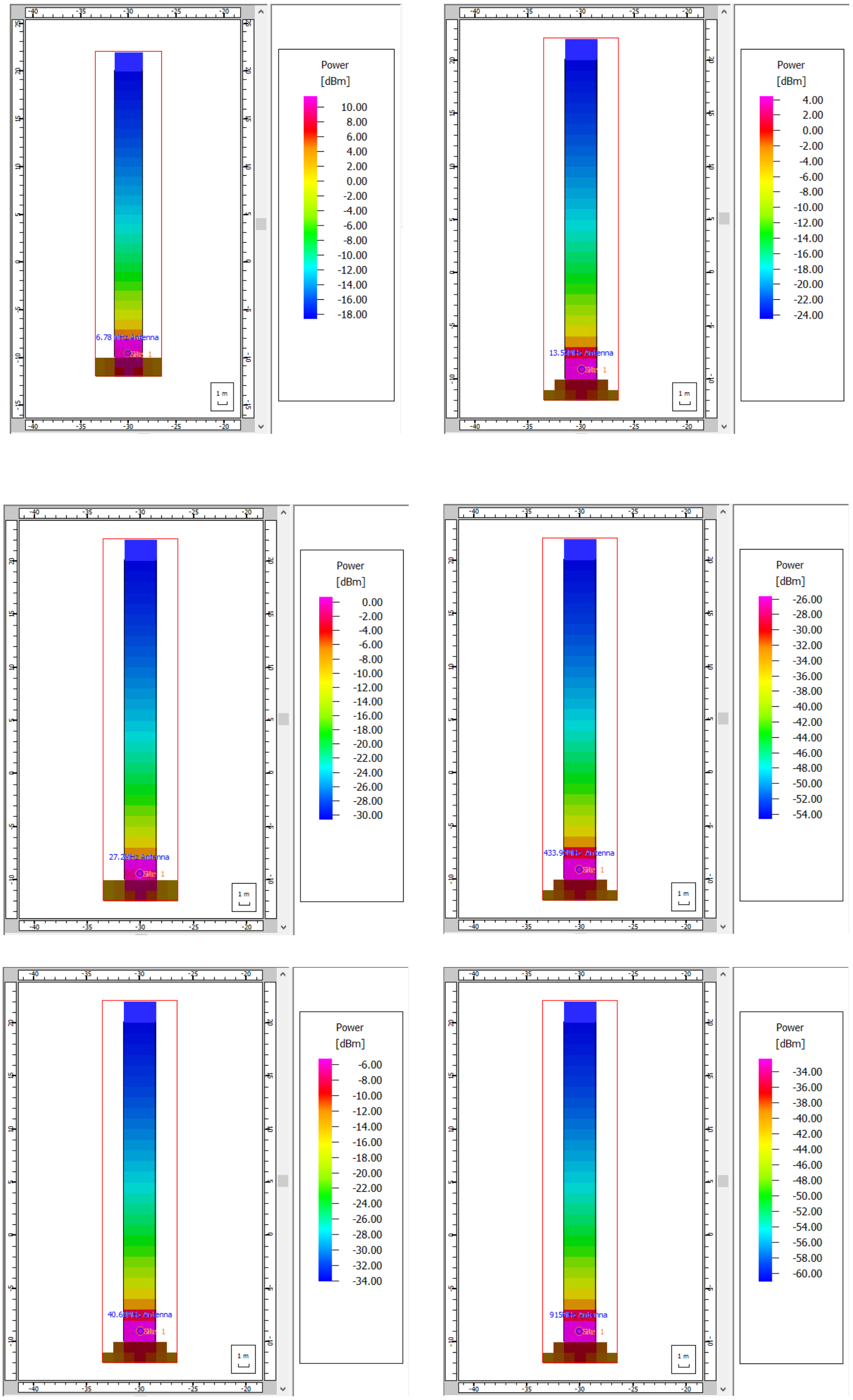


Figure 4.8: Analytical and simulation RSSI values comparison

Table 4.2: Analytical and simulation RSSI values comparison where **A** represents Analytical results and **Sim** represent Software Simulation results

| Frequency (MHz) | RSSI values at different distances (dBm) | | | | | |
|---|---|---|---|---|---|---|
| | **10m** | | **20m** | | **30m** | |
| | **A** | **Sim** | **A** | **Sim** | **A** | **Sim** |
| 6.78 | -30 | -5 | -36 | -15 | -40 | -18 |
| 13.56 | -34 | -14 | -39 | -21 | -40 | -24 |
| 27.12 | -37 | -16 | -43 | -27 | -42 | -30 |
| 40.68 | -40 | -22 | -42 | -30 | -46 | -34 |
| 434 | -48 | -42 | -58 | -50 | -56 | -54 |
| 850 | -52 | -50 | -60 | -58 | -63 | -60 |
| 900 | -53 | -51 | -64 | -58 | -58 | -61 |
| 915 | -52 | -49 | -64 | -57 | -60 | -60 |
| 1800 | -52 | -55 | -62 | -63 | -65 | -65 |
| 2100 | -54 | -56 | -58 | -65 | -64 | -68 |
| 2300 | -57 | -58 | -65 | -66 | -66 | -68 |
| 2400 | -57 | -58 | -60 | -66 | -68 | -70 |
| 5800 | -61 | -64 | -65 | -73 | -68 | -76 |

## 4.3 Fully collapsed scenarios

This section presents the results obtained for the case where the tunnel has a full collapse in the middle section as shown in Figure 3.5. The analytical modeling parameters used in this scenario are given in Table 4.3. The number of modes (rays) considered were limited to 100. This was because the results showed little difference after exceeding 100 modes. Modeling was done for all the frequency bands mentioned in *Section 4.1*.

Figure 4.9 shows the results of the TTE modeling, as modeled by (2.46), for a maximum rock length of 20m without considering it as part of a collapse in a tunnel. Attenuation is seen to increase with frequency as was observed in the ray-tracing analytical modeling results and of interest is the fact that this becomes almost the same for higher frequencies just after 433.92 MHz. This is because for higher frequencies and considering (2.43) and (2.46), the attenuation constant $\alpha$ becomes almost close to a constant. Unlike the constructive and destructive interference nature observed for the TTA section in earlier set of results, for the TTE section, propagation does not happen in air but rather in rock and there is no bouncing back and fourth of the propagating signal.

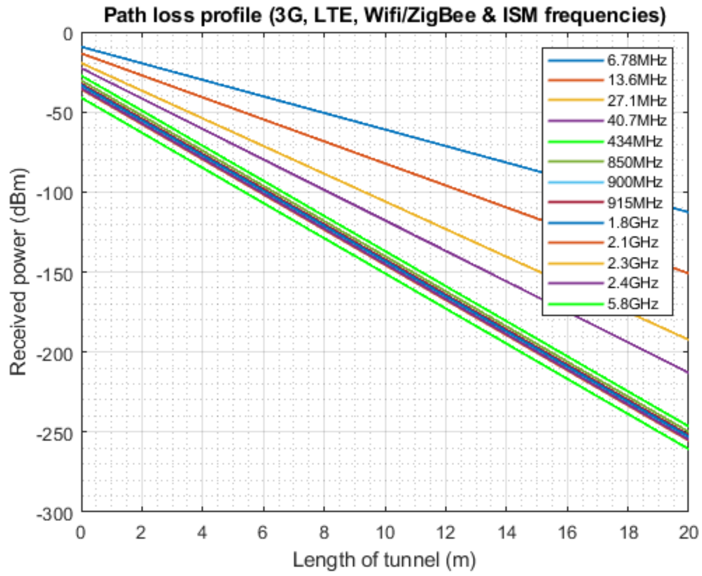


Figure 4.9: TTE modeling path loss profiles for a full collapsed section of the mine tunnel for 3G, LTE, Wifi/ZigBee and other ISM frequency bands.

Table 4.3: Full collapsed scenario simulation parameters

| **Parameter** | **Values** | |
|---|---|---|
| Tunnel dimensions | Height | 3.0m |
| | Width | 2.7m |
| | Length | 90m |
| Section 1 dimensions | Height | 3.0m |
| | Width | 2.7m |
| | Length | 30m |
| Section 2 (Collapsed) dimensions | Height | 3.0m |
| | Width | 2.7m |
| | Length | 10m |
| Section 3 dimensions | Height | 3.0m |
| | Width | 2.7m |
| | Length | 50m |
| Electrical properties | Tunnel $\sigma_r$ | 0.015 |
| | Tunnel $\epsilon_r$ | 5 |
| Antenna | Transmit power | 1 mW |
| | $G_t$ | 1 |
| | $G_r$ | 1 |
| Modes | Total | 100 |
| | Smallest $\lambda$ | 0.059m |

For this part of the exercise, considering the scenario shown in Figure 3.5, a method to combine the results was followed which calculated the amount of transmitted power from one medium to the other (between air and rock interfaces). The factor of the transmitted power is calculated by considering the electromagnetic theory on reflection of waves at normal incidence to the medium which they are propagating into. This entailed calculating the reflection coefficient from the intrinsic impedance of the medium of propagation which is given by (4.1) [63].

$$\eta_i = \frac{j\omega\mu}{\gamma_i} \tag{4.1}$$

where: $\eta_i$ = the intrinsic impedance of the medium of wave propagation
$\omega$ = angular frequency of the wave
$\mu$ = permeability of the material
$\gamma_i$ = complex propagation constant
$j$ = unit complex number.

The reflection coefficient at the boundary of the interface between layer $i$ and the next layer ($i$ + 1) is given by (4.2) [63]:

$$\Gamma_{i,(i+1)} = \frac{\eta_{(i+1)} - \eta_i}{\eta_{(i+1)} + \eta_i} = -\Gamma_{(i+1),i} \tag{4.2}$$

Equation (4.2) was then used to determine the transmitted power (by subtracting the reflected power from the transmitted power) from Section 1 to Section 2 (air to rock) and from Section 2 to Section 3 (rock to air) of Figure 3.5. This can be observed in Figures 4.10, 4.11, 4.12 and 4.13 where there are drops in the transmitted power between the two interfaces at 30m and 40m. A steep attenuation is observed in the region which is collapsed (Section 2 of the tunnel) than in the sections which are not collapsed. The greatest reflection losses are experienced at the rock-to-air interface because of the higher permeability of rock compared to that of air and as represented in equation (4.2) a higher reflection coefficient is then obtained at the rock-to-air interface than at the air-to-rock interface.

As noted previously with regards to the TTE path loss for higher frequencies, the attenuation almost becomes constant. This is observed in Figures 4.10, 4.11, 4.12 where the attenuation in section 2 is almost the same for all the frequencies considered after 850MHz.

Two cases were also considered as shown in Figures 4.14 and 4.15. These were the cases where the transmitting node is considered buried under the collapsed section and is trying to establish communication with other nodes in the TTA (air section) of the tunnel. Figure 4.14 illustrates the case where the collapsed distance is 1 meter while Figure (4.15) illustrates the case where the collapsed section under which the node is buried is 10 meters wide. It is evident that the more distance the signal has to travel in the TTA section, the more attenuation it is subjected to. This helps in understanding that in the collapsed section, the more debris that covers any of the transmitting or receiving communication devices, the more difficult it will be to establish communication especially when a mine tunnel collapses. This is useful in designing a resilient and a robust communication system to be used in such a scenario.

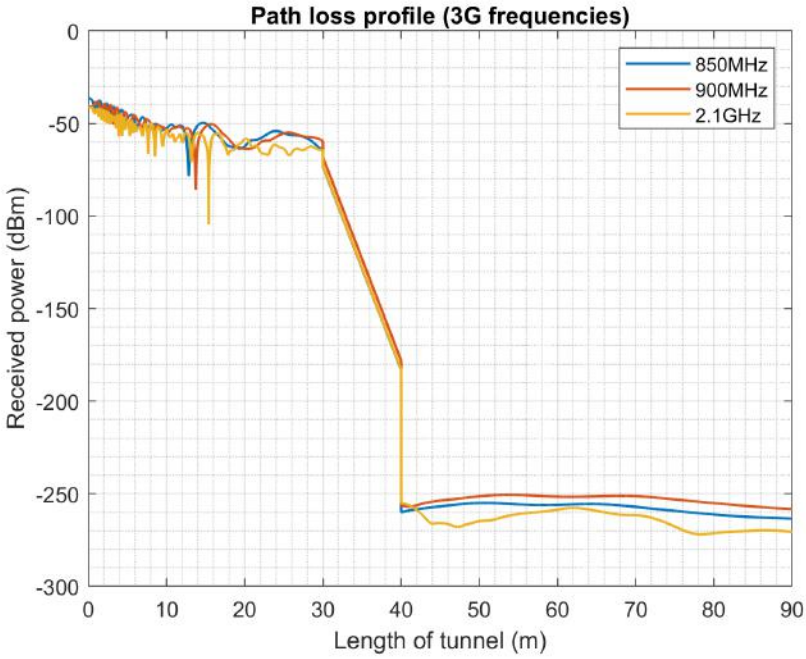


Figure 4.10: Combined optical ray-tracing and TTE modeling path loss profiles for a full-collapsed middle section tunnel for 3G frequencies.

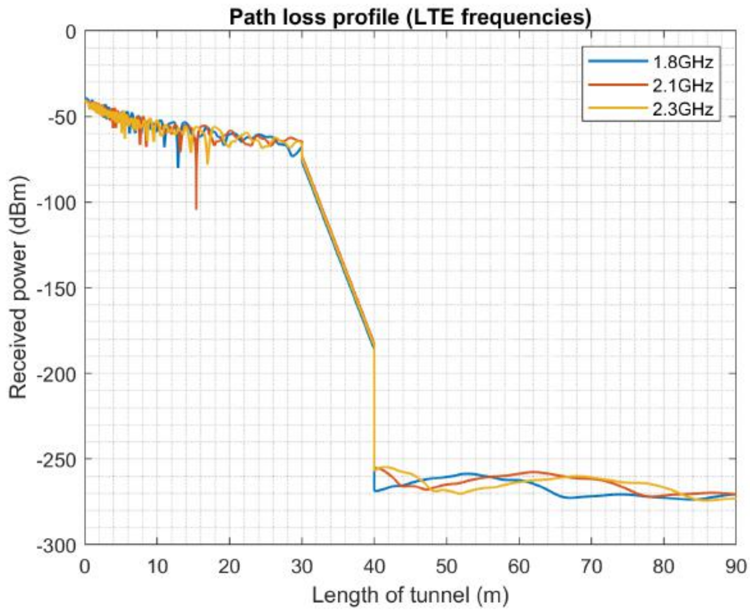


Figure 4.11: Combined optical ray-tracing and TTE modeling path loss profiles for a full-collapsed middle section tunnel for LTE frequencies.

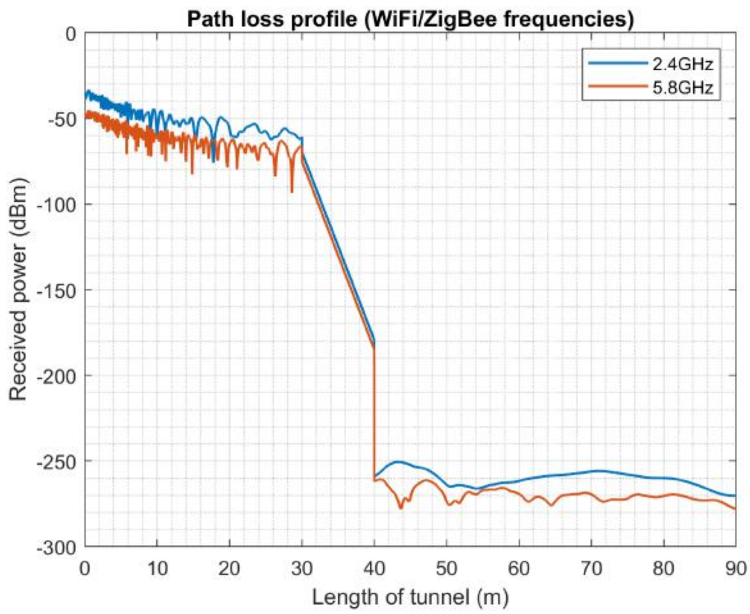


Figure 4.12: Combined optical ray-tracing and TTE modeling path loss profiles for a full-collapsed middle section tunnel for Wifi/ZigBee frequencies.

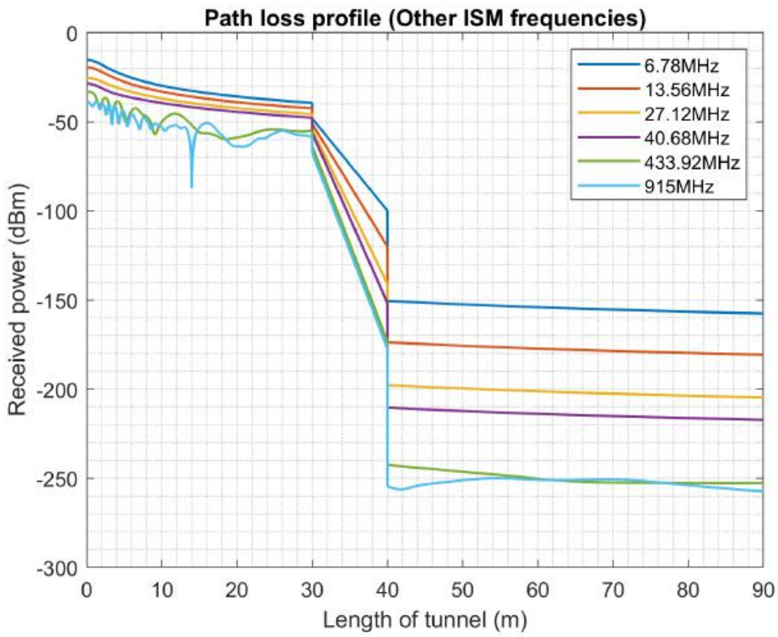


Figure 4.13: Combined optical ray-tracing and TTE modeling path loss profiles for a full-collapsed middle section tunnel for other ISM frequencies.

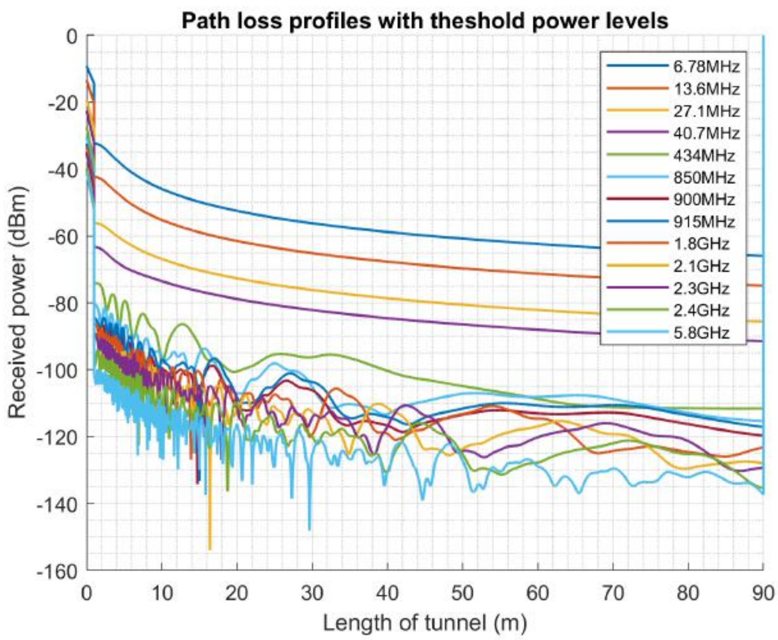


Figure 4.14: Combined TTE and ray-tracing path loss profiles for all considered frequencies considering a transmitting node buried under a 1m wide collapse.

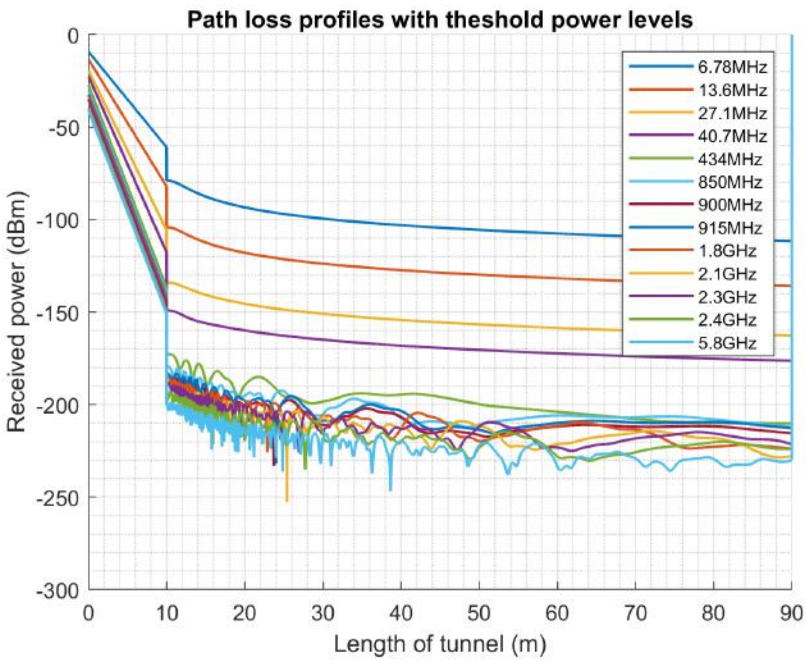


Figure 4.15: Combined TTE and ray-tracing path loss profiles for all considered frequencies considering a transmitting node buried under a 10m wide collapse.

## 4.4 Partially collapsed scenarios

This section presents the results obtained for the case where the tunnel has a partial collapse in the middle section as shown in Figure 3.2. The parameters used for modeling are given in Table 4.4 for the frequencies discussed in the chapter overview. For this case it was imperative to choose the worst case partial collapsed scenario of the middle section which was thought to be the case when there exists a distance to the roof of the mine tunnel where a miner cannot crawl through and make it to the other side of section 3 from section 1 through the middle collapsed section. This minimum distance was considered to be 30 cm.

The approach adopted was to model the two tunnels separately with the two separate heights (that of 3m and 30 cm) and see the difference in the two path loss profiles and from there infer the possible behaviour of the transmitted signal in the middle collapsed section. The assumption here was that at some point in time all the rays from the transmitter (after some reflections) have to pass through this gap and that a small inconsiderable fraction is transmitted through the rock section.

In Figures 4.16, 4.17, 4.18 and 4.19, the image to the left represents the scenario where the tunnel has a height of 3m and the one to the right with a height of 0.3m. The major observation is that there is a reduction in the signal attenuation in the near field but a greater attenuation in the far field, in the case of the reduced tunnel height (the case with 0.3m height) compared to the 3m case. In the reduced tunnel height case, the rays do not have to travel a long distance as compared to the 3 meter height case, hence the attenuation is far much lesser. This means that in the case where a mine tunnel collapse happens and it is not a full collapsed case, there is better and more chances of still establishing a communication link between communicating devices.

Table 4.4: Partial collapsed scenario simulation parameters

| **Parameter** | **Values** | |
|---|---|---|
| Tunnel dimensions | Height | 3.0m |
| | Width | 2.7m |
| | Length | 90m |
| Section 1 dimensions | Height | 3.0m |
| | Width | 2.7m |
| | Length | 30m |
| Section 2 (partially collapsed) dimensions | Air height | 0.3m |
| | Air width | 2.7m |
| | Air length | 10m |
| Section 3 dimensions | Height | 3.0m |
| | Width | 2.7m |
| | Length | 50m |
| Electrical properties | Tunnel $\sigma_r$ | 0.015 |
| | Tunnel $\epsilon_r$ | 5 |
| Antenna | Transmit power | 1 mW |
| | $G_t$ | 1 |
| | $G_r$ | 1 |
| Modes | Total | 100 |
| | Smallest $\lambda$ | 0.059m |

This is due to the fact that the signal has less reflections in the small tunnel compared to a bigger tunnel. Assuming signal propagation only through the air channel in section 2 of the partially collapsed tunnel, the result above then suggests that signal attenuation in this section should be worse than the case when the section has its full normal height.

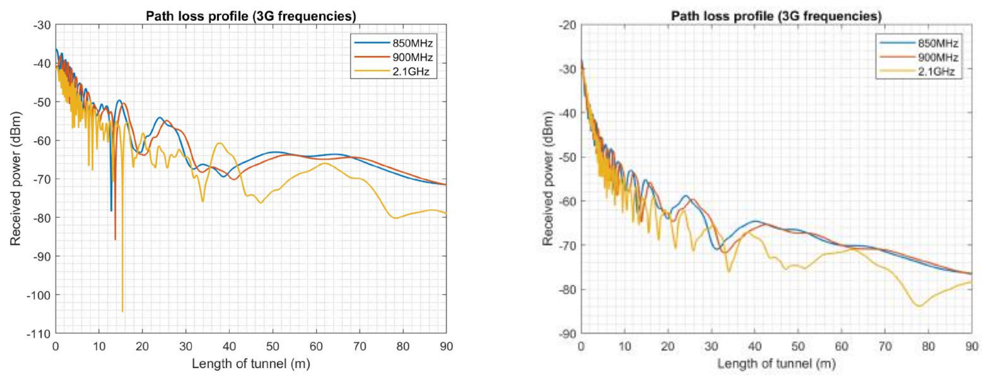


Figure 4.16: Ray-optical tracing analytical modeling path loss profiles for 3G frequencies for a non-collapsed tunnel with a height of (left) 3m and (right) 0.3m.

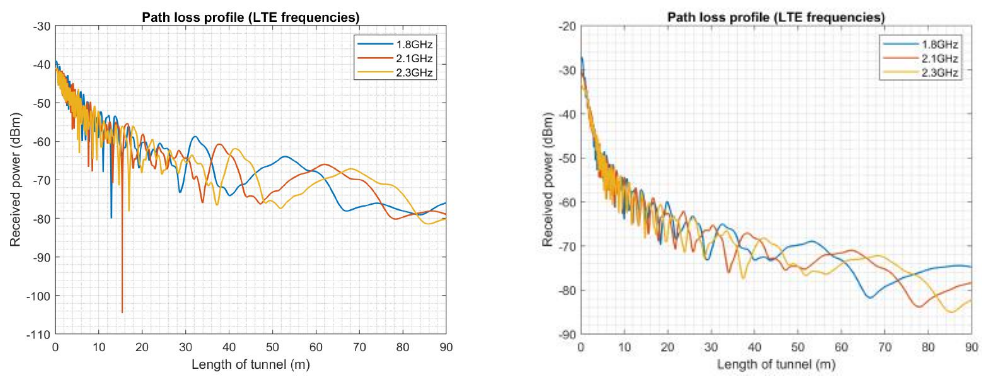


Figure 4.17: Ray-optical tracing analytical modeling path loss profiles for LTE frequencies for a non-collapsed tunnel with a height of (left) 3m and (right) 0.3m.

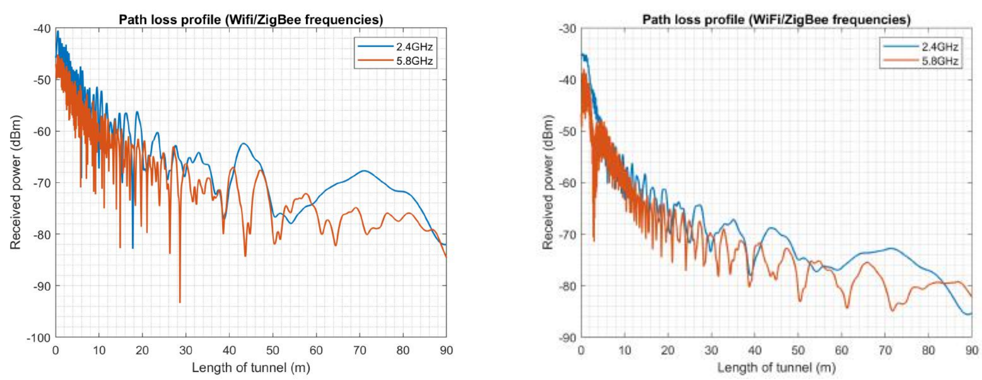


Figure 4.18: Ray-optical tracing analytical modeling path loss profiles for Wifi/ZigBee frequencies for a non-collapsed tunnel with a height of (left) 3m and (right) 0.3m.

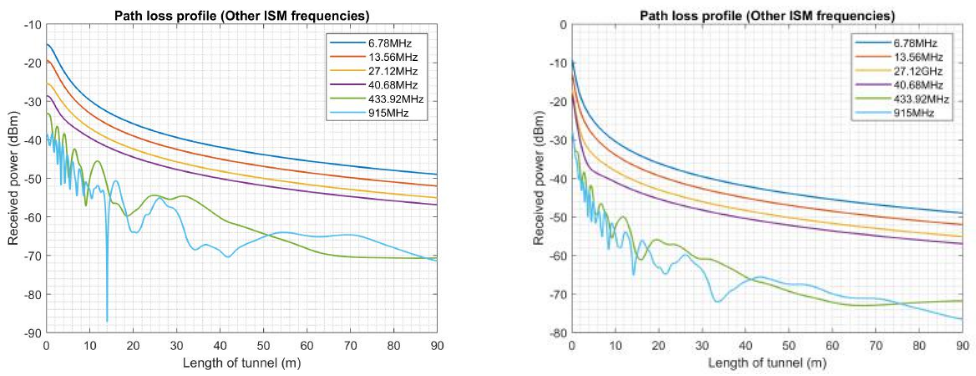


Figure 4.19: Ray-optical tracing analytical modeling path loss profiles for other ISM frequencies for a non-collapsed tunnel with a height of (left) 2.69m and (right) 0.3m.

## 4.5 Conceptual communication system in an underground mine based on results

This section aims to interpret the results obtained with an application that is relevant to a WSN communication system in an underground mining tunnel especially in the context of one that has collapsed. The major consideration of such a system is the area that it can manage to cover in the event of an accident that results in a collapsed tunnel scenario.

### 4.5.1 Coverage based on frequency and transmission power

Several coverage tests were performed on the channel models obtained. To get the total coverage area for a given frequency, a threshold of -80 dBm was considered on the given path loss profiles and a distance of 0.5 meters after the collapsed section of the tunnel was taken as the minimum reception distance. The 0.5 meter threshold is the consideration that there has to be a node at least 0.5 meters away from the collapsed section of the tunnel which will be able to get reception of the signals coming from the collapsed section of the tunnel. An RSSI of -80 dBm is considered good enough for WSN applications [64]. The variables under consideration were:

1. The transmission power
2. The centre frequency
3. Length of the collapsed section of the mine tunnel
4. Distance from where the transmitter is located in the TTA section to the collapsed section

A total of 1524 cases were considered as illustrated in Table 4.5:

where: $D =$ Distance from where the transmitter is located in the TTA section to the collapsed section

$C =$ Length of the collapsed section of the mine tunnel

$G =$ The total gain at the transmitter and receiver $G_r G_t$

The scenarios considered represent all the frequencies considered in the channel modeling exercise and all the frequencies on the log scale from 1 MHz to 10 GHz. All results obtained are shown in Appendix A.1 - A.4. The large set of results presented in Appendix A.1 - A.4. were to consider a wide variety of frequencies across a different and large set of varying dimensions in a way to consider possible mine tunnel collapsed scenarios. The observation from the results is that higher frequencies and a combination of lower antenna gain and large collapsed sections have a overall resulting effect of greater attenuation on the signal. Higher antenna gain and transmission power means a lot of power is available to the propagating signal which will make the signal travel far.

From the large set of results, with a special consideration to only the frequencies considered in the results of the channel modeling, a total of 5 cases were able to satisfy the condition imposed of a threshold of -80 dBm and 0.5 meters after the collapsed section. These results are shown in Figures 4.20, 4.21, 4.22, 4.23 and 4.24. This illustrates the need for more transmission power, higher antenna gain on a communication system that can be used in a collapsed mine tunnel.

The simulations were modeled using (2.18) and a combination of TTE modeling. From these results it is evident that an increase in antenna gain, a shorter collapsed section length and increasing the transmission power all yield better results. However, the frequencies which satisfied the conditions, imposed for the minimum required coverage, were all lower frequencies below 6.8 MHz, frequencies which require bulky antennas and are therefore not suitable for a portable WSN system. Also the transmission power in these success scenarios are too high for a low power communication system such as a WSN which is usually powered by batteries.

Table 4.5: Frequencies and scenarios considered for coverage measurements

| Freq (Hz) | Transmission power and scenarios | | | | | | | | | | | |
|---|---|---|---|---|---|---|---|---|---|---|---|---|
| | 1 mW | | | 10 mW | | | 100 mW | | | 1000 mW | | |
| | D(m) | C(m) | G(m) | D(m) | C(m) | G(m) | D(m) | C(m) | G(m) | D(m) | C(m) | G(m) |
| $\times 10^6$ | $\times 10$ | $\times 10$ | $\times 1$ | $\times 10$ | $\times 10$ | $\times 1$ | $\times 10$ | $\times 10$ | $\times 1$ | $\times 10$ | $\times 10$ | $\times 1$ |
| 1-9 | 1;2;3 | 0.5;1 | 1;4 | 1;2;3 | 0.5;1 | 1;4 | 1;2;3 | 0.5;1 | 1;4 | 1;2;3 | 0.5;1 | 1;4 |
| 6.8 | 1;2;3 | 0.5;1 | 1;4 | 1;2;3 | 0.5;1 | 1;4 | 1;2;3 | 0.5;1 | 1;4 | 1;2;3 | 0.5;1 | 1;4 |
| 10 | 1;2;3 | 0.5;1 | 1;4 | 1;2;3 | 0.5;1 | 1;4 | 1;2;3 | 0.5;1 | 1;4 | 1;2;3 | 0.5;1 | 1;4 |
| 14 | 1;2;3 | 0.5;1 | 1;4 | 1;2;3 | 0.5;1 | 1;4 | 1;2;3 | 0.5;1 | 1;4 | 1;2;3 | 0.5;1 | 1;4 |
| 20 | 1;2;3 | 0.5;1 | 1;4 | 1;2;3 | 0.5;1 | 1;4 | 1;2;3 | 0.5;1 | 1;4 | 1;2;3 | 0.5;1 | 1;4 |
| 27 | 1;2;3 | 0.5;1 | 1;4 | 1;2;3 | 0.5;1 | 1;4 | 1;2;3 | 0.5;1 | 1;4 | 1;2;3 | 0.5;1 | 1;4 |
| 30 | 1;2;3 | 0.5;1 | 1;4 | 1;2;3 | 0.5;1 | 1;4 | 1;2;3 | 0.5;1 | 1;4 | 1;2;3 | 0.5;1 | 1;4 |
| 40 | 1;2;3 | 0.5;1 | 1;4 | 1;2;3 | 0.5;1 | 1;4 | 1;2;3 | 0.5;1 | 1;4 | 1;2;3 | 0.5;1 | 1;4 |
| 41 | 1;2;3 | 0.5;1 | 1;4 | 1;2;3 | 0.5;1 | 1;4 | 1;2;3 | 0.5;1 | 1;4 | 1;2;3 | 0.5;1 | 1;4 |
| 50 | 1;2;3 | 0.5;1 | 1;4 | 1;2;3 | 0.5;1 | 1;4 | 1;2;3 | 0.5;1 | 1;4 | 1;2;3 | 0.5;1 | 1;4 |
| 60 | 1;2;3 | 0.5;1 | 1;4 | 1;2;3 | 0.5;1 | 1;4 | 1;2;3 | 0.5;1 | 1;4 | 1;2;3 | 0.5;1 | 1;4 |
| 70 | 1;2;3 | 0.5;1 | 1;4 | 1;2;3 | 0.5;1 | 1;4 | 1;2;3 | 0.5;1 | 1;4 | 1;2;3 | 0.5;1 | 1;4 |
| 80 | 1;2;3 | 0.5;1 | 1;4 | 1;2;3 | 0.5;1 | 1;4 | 1;2;3 | 0.5;1 | 1;4 | 1;2;3 | 0.5;1 | 1;4 |
| 90 | 1;2;3 | 0.5;1 | 1;4 | 1;2;3 | 0.5;1 | 1;4 | 1;2;3 | 0.5;1 | 1;4 | 1;2;3 | 0.5;1 | 1;4 |
| 100 | 1;2;3 | 0.5;1 | 1;4 | 1;2;3 | 0.5;1 | 1;4 | 1;2;3 | 0.5;1 | 1;4 | 1;2;3 | 0.5;1 | 1;4 |
| 434 | 1;2;3 | 0.5;1 | 1;4 | 1;2;3 | 0.5;1 | 1;4 | 1;2;3 | 0.5;1 | 1;4 | 1;2;3 | 0.5;1 | 1;4 |
| 500 | 1;2;3 | 0.5;1 | 1;4 | 1;2;3 | 0.5;1 | 1;4 | 1;2;3 | 0.5;1 | 1;4 | 1;2;3 | 0.5;1 | 1;4 |
| 600 | 1;2;3 | 0.5;1 | 1;4 | 1;2;3 | 0.5;1 | 1;4 | 1;2;3 | 0.5;1 | 1;4 | 1;2;3 | 0.5;1 | 1;4 |
| 700 | 1;2;3 | 0.5;1 | 1;4 | 1;2;3 | 0.5;1 | 1;4 | 1;2;3 | 0.5;1 | 1;4 | 1;2;3 | 0.5;1 | 1;4 |
| 800 | 1;2;3 | 0.5;1 | 1;4 | 1;2;3 | 0.5;1 | 1;4 | 1;2;3 | 0.5;1 | 1;4 | 1;2;3 | 0.5;1 | 1;4 |
| 850 | 1;2;3 | 0.5;1 | 1;4 | 1;2;3 | 0.5;1 | 1;4 | 1;2;3 | 0.5;1 | 1;4 | 1;2;3 | 0.5;1 | 1;4 |
| 900 | 1;2;3 | 0.5;1 | 1;4 | 1;2;3 | 0.5;1 | 1;4 | 1;2;3 | 0.5;1 | 1;4 | 1;2;3 | 0.5;1 | 1;4 |
| 915 | 1;2;3 | 0.5;1 | 1;4 | 1;2;3 | 0.5;1 | 1;4 | 1;2;3 | 0.5;1 | 1;4 | 1;2;3 | 0.5;1 | 1;4 |
| 1000 | 1;2;3 | 0.5;1 | 1;4 | 1;2;3 | 0.5;1 | 1;4 | 1;2;3 | 0.5;1 | 1;4 | 1;2;3 | 0.5;1 | 1;4 |
| 1800 | 1;2;3 | 0.5;1 | 1;4 | 1;2;3 | 0.5;1 | 1;4 | 1;2;3 | 0.5;1 | 1;4 | 1;2;3 | 0.5;1 | 1;4 |
| 2000 | 1;2;3 | 0.5;1 | 1;4 | 1;2;3 | 0.5;1 | 1;4 | 1;2;3 | 0.5;1 | 1;4 | 1;2;3 | 0.5;1 | 1;4 |
| 2100 | 1;2;3 | 0.5;1 | 1;4 | 1;2;3 | 0.5;1 | 1;4 | 1;2;3 | 0.5;1 | 1;4 | 1;2;3 | 0.5;1 | 1;4 |
| 2200 | 1;2;3 | 0.5;1 | 1;4 | 1;2;3 | 0.5;1 | 1;4 | 1;2;3 | 0.5;1 | 1;4 | 1;2;3 | 0.5;1 | 1;4 |
| 2300 | 1;2;3 | 0.5;1 | 1;4 | 1;2;3 | 0.5;1 | 1;4 | 1;2;3 | 0.5;1 | 1;4 | 1;2;3 | 0.5;1 | 1;4 |
| 2400 | 1;2;3 | 0.5;1 | 1;4 | 1;2;3 | 0.5;1 | 1;4 | 1;2;3 | 0.5;1 | 1;4 | 1;2;3 | 0.5;1 | 1;4 |
| 5000 | 1;2;3 | 0.5;1 | 1;4 | 1;2;3 | 0.5;1 | 1;4 | 1;2;3 | 0.5;1 | 1;4 | 1;2;3 | 0.5;1 | 1;4 |
| 5800 | 1;2;3 | 0.5;1 | 1;4 | 1;2;3 | 0.5;1 | 1;4 | 1;2;3 | 0.5;1 | 1;4 | 1;2;3 | 0.5;1 | 1;4 |
| 10000 | 1;2;3 | 0.5;1 | 1;4 | 1;2;3 | 0.5;1 | 1;4 | 1;2;3 | 0.5;1 | 1;4 | 1;2;3 | 0.5;1 | 1;4 |

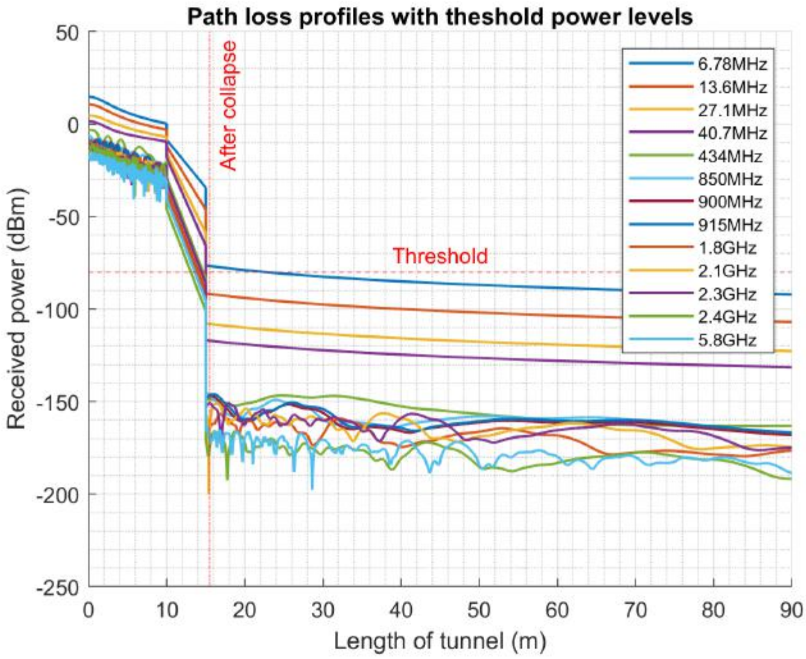


Figure 4.20: P = 1000mW, G = 1, D = 10m, C = 5m.

### 4.5.2 Sample placement of nodes

From the coverage tests done, a maximum of 30 meters radial coverage was obtained at a frequency of 6.78 MHz. Using this result, a sample chain-like node deployment was simulated in MATLAB to test full coverage for a sample mine tunnel which is 90 meters long. A chain-like deployment entails having the nodes alternate their location on either sides of the tunnel walls after a certain amount of distance (in this case 30 meters). This deployment is illustrated in Figure 4.25 and shows a full coverage of the entire tunnel with the provision of a 5 meter collapse anywhere within the tunnel.

The same was done by placing the nodes in the middle of the width of the tunnel separated by a distance of 30 meters per each node. This is illustrated in Figure 4.26 and the results show a full coverage of the entire tunnel with the provision for a 5 meter collapse. It was further investigated to find out if the deployment strategy had any effect on the coverage of the tunnel by a fixed number of nodes. Random placement positions along the width of the tunnel were generated and the coverage simulated and the results showed no difference in the coverage as long as the horizontal distances were maintained (in this case the 30 meter separation). The coverage was simulated by considering the radius and hence the circumference that each node covers in the tunnel (and hence network). The random cases considered are shown in Figures A.9 - A.18 in Appendix A.5 and one of the cases is shown here in Figure 4.27.

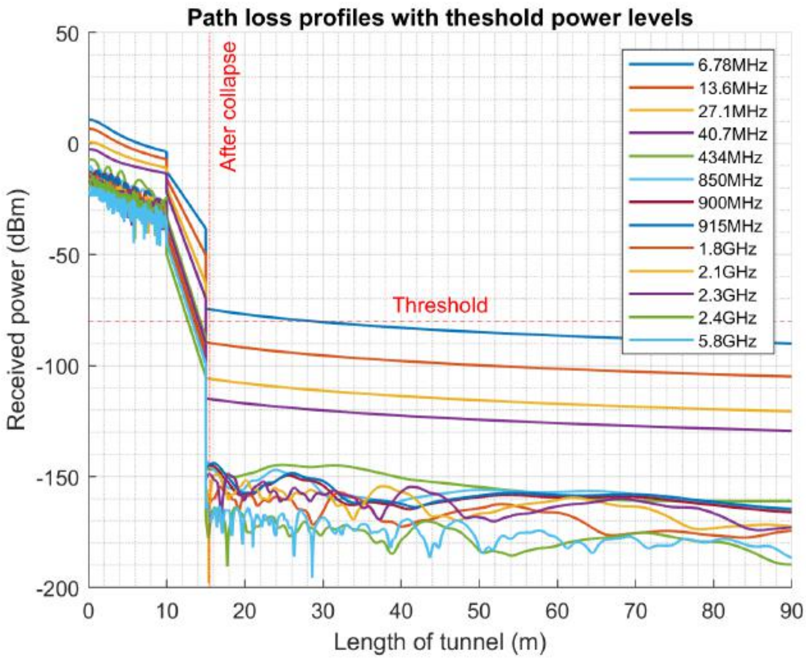


Figure 4.21: P = 1000mW, G = 4, D = 10m, C = 5m.

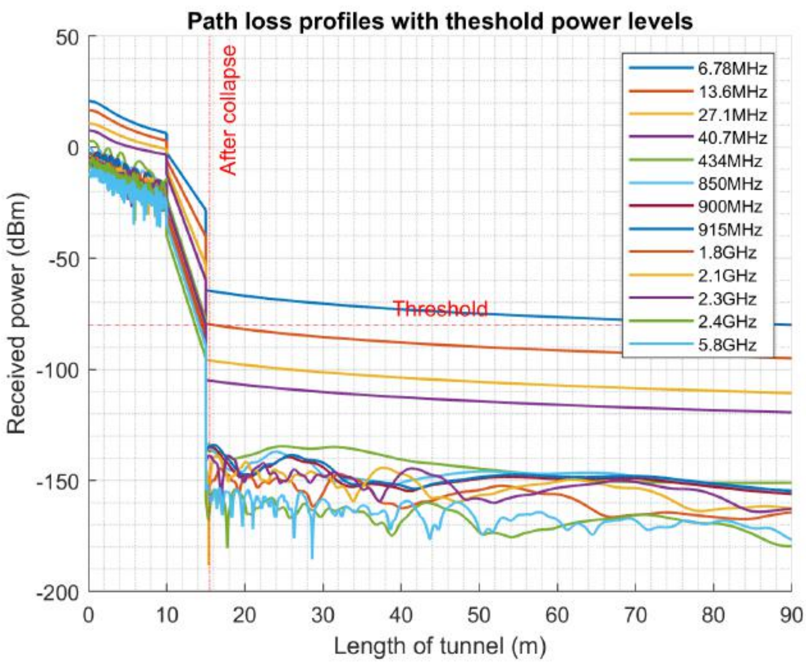


Figure 4.22: P = 1000mW, G = 4, D = 10m, C = 5m.

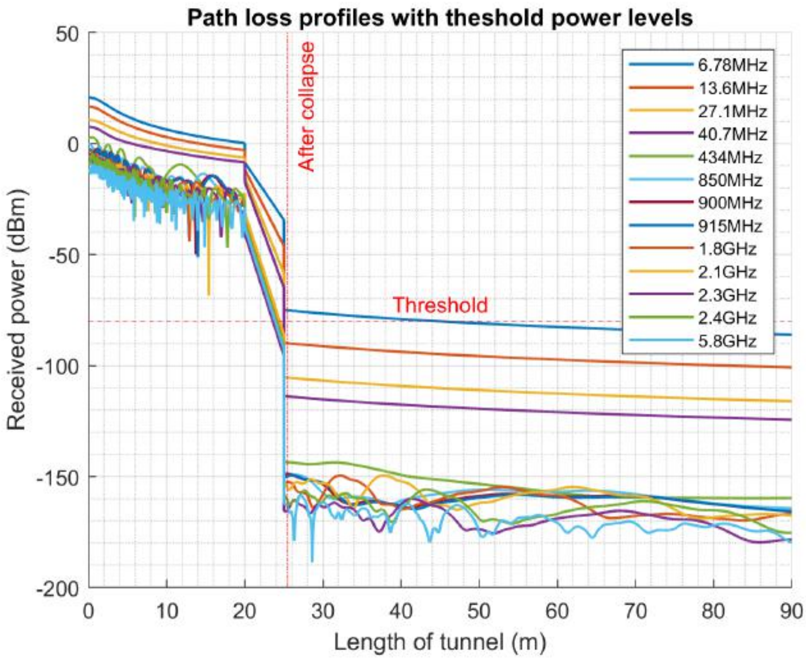


Figure 4.23: P = 1000mW, G = 4, D = 20m, C = 5m.

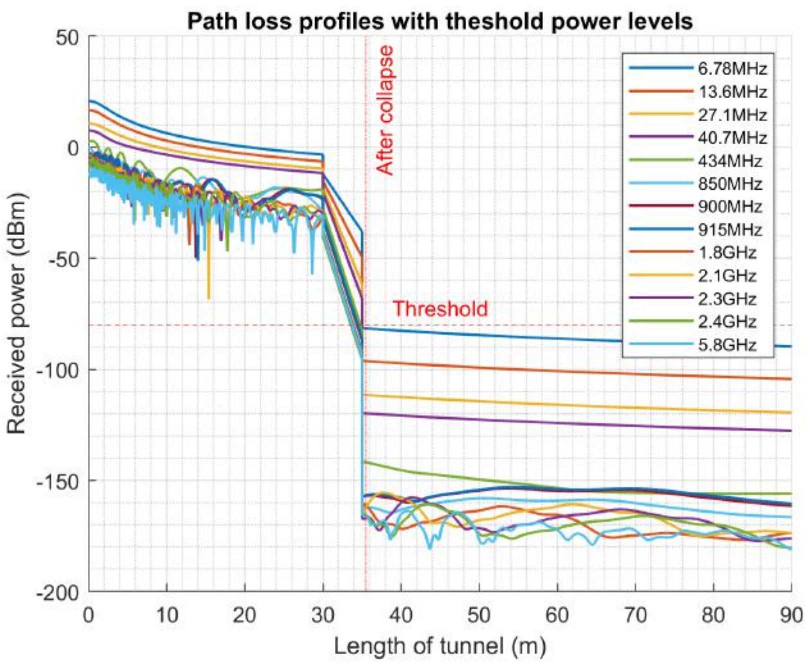


Figure 4.24: P = 1000mW, G = 4, D = 30m, C = 5m.

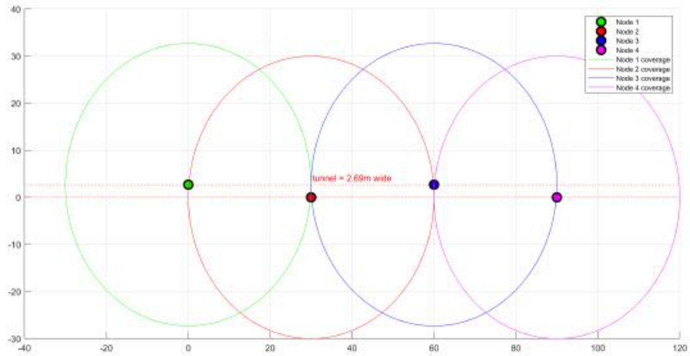


Figure 4.25: Sample deployment of 4 nodes in a 90 meter tunnel using the chain-line approach.

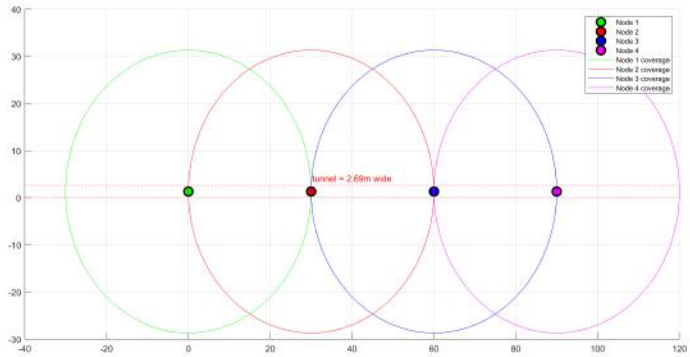


Figure 4.26: Sample deployment of 4 nodes in a 90 meter tunnel placing them in the middle of the tunnel width.

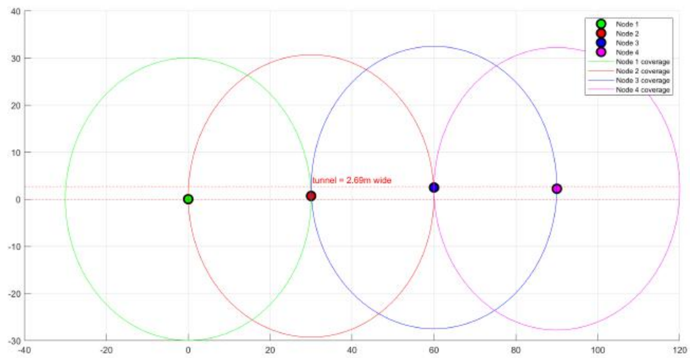


Figure 4.27: Sample deployment of 4 nodes in a 90 meter tunnel placing them randomly along the tunnel width.

### 4.5.3 Discussion

From the analysis presented in this chapter, the results shown for the software simulation show a linear like pattern as compared to the analytical simulation results presented in the graphs. The results presented in the graphs were analysed at a distance of 0.1 m in the model equation used. In this case, for the lower frequencies considered, a smooth or linear variation is observed as opposed to the random variations for the higher frequency cases. This observation is because for lower frequencies, the wavelength is much larger than the width of the tunnel whereas for higher frequencies the wavelength is much smaller than the width of the tunnel and there is more of constructive and destructive interference. These random variations are not observed however in the software simulation heat maps because the results are a linear curve fitting on the model used in the simulation. There is also an observation that the results do not start at 0dBm at 0m. This is because of internal power losses which are needed to drive the signal through the communication system and the antenna before it can be radiated to the outside surroundings.

From the testing of the channel models for coverage, it is clear that the major challenge is the propagation of higher frequency waves in the collapsed section of the mine tunnel (TTE section). For pure through-the-air (TTA) communication in a normal mine tunnel, the higher frequencies perform well, in most instances managing to cover the entire length of the mine tunnel (in this case 90 meters) as seen in Figure 4.5 where 5.8 Ghz covers the entire tunnel at a transmission power of 1 mW considering the extreme threshold RSSI of -80 dBm (it is important to note that an RSSI value of -80dBm is considered the worst case scenario reception value for WSN in order to have a good LQI [64]). The results suggest that to have decent coverage a very low frequency is required (in this case less than 6.8 MHz) at a higher transmit power with a decent gain at the transmitter and receiver. These frequencies are not suitable for a ***portable*** WSN communication system since the transmitter and the receiver in those instances will have to be big considering the fact that the size of an antenna has to be $\frac{\lambda}{2}$. In this case, that equates to a smallest antenna size of $\frac{2c}{f} = \frac{2*c}{6.8MHz}$ = 88 meters. However, higher frequencies can be used to establish a portable WSN system but then special attention would have to be given to its design such that communication does not break down in collapse scenarios. A lot of work has shown that WSN communication system work well in underground mine tunnel under normal conditions but in collapsed mine tunnel scenarios, which is the focus of this research, if a node in the WSN network is damaged during a mine tunnel collapse and for example is buried under rubble, for it to re-establish communication with other nodes, it will require a lot of transmission power, with regards to the minimum collapse dimensions considered in this work. Looking at Figures A.1.1, where no communication is possible at all, on the lowest frequency of 6,78 MHz under consideration, with the minimum threshold of -80dBm for communication, and Figure A.8.1, with the same dimensions but where communication is possible with the imposed RSSI threshold, an increase of a factor of 1000 (1mW vs 1000mW) in power and an increase of a factor of 4 in antenna gain is required.

## 4.6 Conclusion

In this chapter, results from modeling of the scenarios illustrated in Figures 3.2 and 3.5 were presented. For an additional case where the tunnel is non-collapsed (normal tunnel), ray-optical analytical modeling was performed and the results compared and validated with that from the simulation of the same tunnel in a 3D propagation software suit. Comparison of the ray-optical modeling results with those from the simulation using the software suit were in most parts in agreement for higher frequencies. For the partial collapsed scenario where a smaller air passage propagation height is considered, it was noticed that the attenuation is greater than in the case of a normal tunnel with a much bigger tunnel height. However, in the case of a full collapse, there are additional reflection losses on the interfaces where the air meets the rock and there is a steep attenuation in the rock medium as compared to the air medium. The testing of channel models obtained for coverage with a consideration to frequency, transmission power, distance of transmitter from the TTA section to the collapsed section of the tunnel and the length of the collapsed section of the tunnel have also been presented in this chapter. It was found out that the ideal range of frequencies which satisfy the -80dBm threshold for reliable communication, when taking into consideration a minimum collapsed section with a width of 5 meters, were those below 6.78 MHz. The other requirement still was the need to increase the transmit power and the gains at the receiver and transmitter. However these set of frequencies and requirements were deemed not suitable for a ***portable*** WSN communication system but rather a pure TTE communication system which makes use of low frequencies.

# Chapter 5

# Experimental results

## 5.1 Chapter overview

This chapter presents the results obtained when a performance evaluation on a WSN communication system was done in a mock mine at Wits University. The measurements in the evaluation were performed using Zolertia Re-Mote WSN nodes (one transmitter and one receiver) which are built for WSN prototyping especially in the research space [62]. The nodes have a dual frequency capability using an external mounted 915MHz antenna and a surface mounted 2.4GHz antenna. Measurements were taken for a scenario which represented a non-collapsed mine tunnel and scenarios which represented a collapsed mine tunnel. The two sets of results were then compared to see the difference in performance in the two cases. The measurements were taken in steps of 1 meter over a total distance of 60 meters. Some of the results are compared with those obtained from the analytical modeling section and a correlation is observed for the frequencies which were considered in the measurement exercise.

## 5.2 Test equipment and environment setup

The test environment was a mock mine at the Digital mining Laboratory at the University of the Witwatersrand in the basement of the Chamber of Mines building. The mock mine has same dimensions to those used in the analytical modeling section. Figure 5.1 shows the test set up with the nodes used for the measurements and the laptop computer used for results capturing. Measurements were performed over a distance of 60 meters in steps of 1 meter as illustrated in Figure 5.2. The transmitting and receiving nodes were mounted at a height of 1.5m using a tripod stand and in the middle of the tunnel (1.35m). A total set of 3 results were taken for each case scenario considered and the average considered for plotting.

Figures 5.3, 5.4, 5.5 and 5.6 show the collapsed scenario which was built by using bags of quartz granite which resembles the rock found in gold mines.


Figure 5.1: Transmitter node, receiver node and data logging computer used for performance measurements.


Figure 5.2: Marking of 1 meter steps on the floor of the mock mine tunnel.


Figure 5.3: Collapsed scenario with the transmitting node buried underneath the rubble (dimensions depicted are approximately 1m in dimensions).

Figure 5.4: Collapsed scenario showing where the transmitting node is buried.

Figure 5.5: Collapsed scenario showing the transmitting node at the bottom of the rubble before burial.

Figure 5.6: Collapsed scenario showing a closer look at the transmitting node at the bottom of the rubble before burial.

## 5.3 Behaviour in a non-collapsed scenario

The performance here was mostly focused on finding out the behaviour of received power (RSSI) in a mine tunnel environment for WSN motes designed primarily for indoor or outdoor environments.

Two frequencies using the Zolertia nodes were used in the testing due to the fact that the Zolertia Re-Mote nodes have dual frequency band capabilities (915MHz and 2.4GHz). The 434MHz frequency was also used through an RF69 antenna module integrated to a Atmega328P micro-controller unit. For the 2.4GHz band, the nodes make use of a transmission power of 3dBm and for the 915MHz band the nodes transmit at 14dBm. This is a limitation programmed on the nodes. For the 434MHz band, the Atmega units can only make use of a maximum transmission power of 7dBm without the use of automatic transmission control (which will not allow one to set a pre-set transmission power but rather the node will have dynamic transmission power). The averaged results of three sets are presented in Figure 5.7. As seen in the analytical modelling section and *Chapter 4*, the results here show an increase in attenuation as the frequency increases and constructive and destructive interference behaviour, as a result of the tunnel environment, which backs up the results obtained from the simulations done in *Chapter 4*.

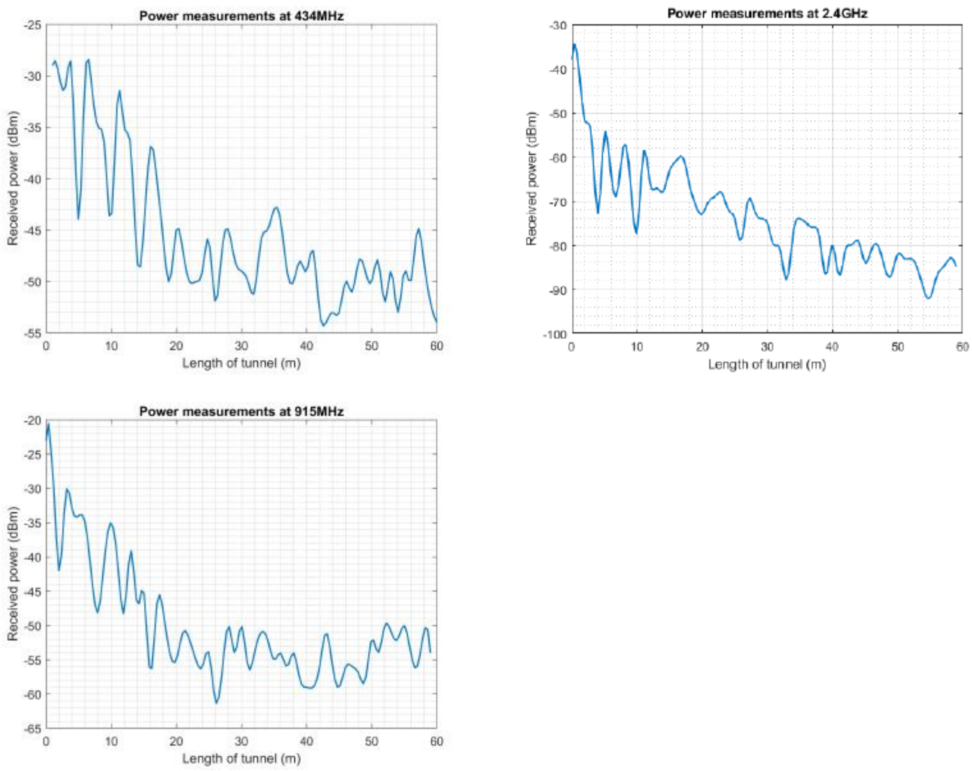


Figure 5.7: Received power for the non-collapsed scenario performance measurement at 434MHz, 915Mhz and 2.4GHz.

## 5.4 Behaviour in a full collapsed scenario

Figure 5.8 shows the averaged results of three sets obtained for the case where the transmitting node was buried as illustrated in Figure 5.3. Measurements were performed for 434MHz (at 7dBm transmit power), 915MHz (at 14dBm transmit power) and 2.4GHz (at 3dBm transmit power). Again results here show the same behaviour in terms of an increase in frequency strongly correlating to an increase in signal attenuation.

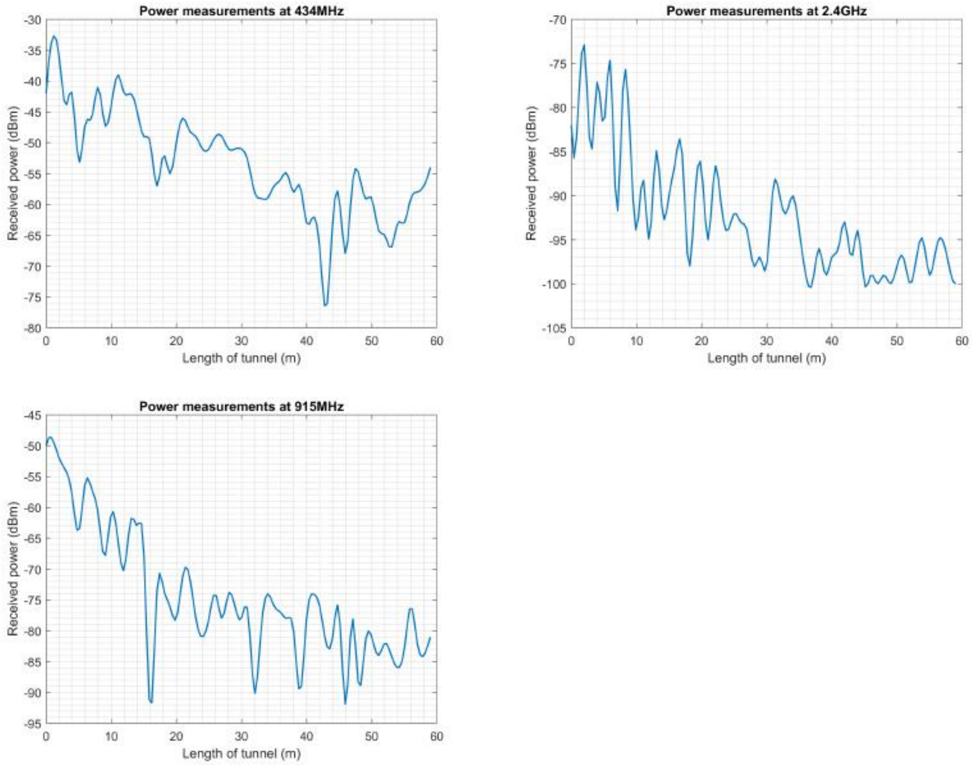


Figure 5.8: Received power for the collapsed scenario performance measurement at 434MHz, 915Mhz and 2.4GHz.

## 5.5 Comparison of results

Figures 5.9, 5.10 and 5.11 show the comparison of the received power for the measurements taken in collapsed and non-collapsed scenarios. For the 434MHz case (Figure 5.9) there is a loss of 12dBm because of the collapsed section under which the transmitting node is buried which translates to a TTE attenuation (including medium transmission losses) of 12dB/m. For the 915MHz case (Figure 5.10) there is drop of 30dBm due to the introduction of the 1m wide and 1m deep collapsed debris over the transmitter. This represents an overall attenuation (including medium transmission losses) of 30dB/m over this TTE section. For the 2.4GHz scenario (Figure 5.11) there is a drop of 40dBm representing an overall attenuation of 40dB/m in that case.

Figures 5.12, 5.13 and 5.14 show the compared results between the simulation where a node is buried under a 1m wide collapse section and the measured results under the same circumstances for 434MHz, 915MHz and 2.4GHz. The results show some strong correlation for the higher frequencies (i.e 2.4GHz) than the lower frequencies (i.e. 434

MHz). This could be due to the fact that the materials used in the construction of the collapsed scenario do not really represent the type of materials considered in the simulation exercise, material properties which correspond to materials found in real underground mines. The other fact is the possibility that the constructed collapsed scenario made use of stacked bags of broken debris which might still allow the existence of some air pockets and passages in the constructed collapse section which will exhibit some form of TTA loss profiles rather than pure TTE profiles.

A comparison was also done to compare the results obtained in this measurement exercise to those obtained in the analytical modeling section for the non collapse scenarios. The transmit power in the analytical modeling was adjusted to match that of 7dBm for the 434MHz case, 14dBm for the 915MHz case and to 3dBm to match the 2.4GHz case. Figure 5.15 shows the comparison of the simulated path loss and the measured path loss in a non collapsed scenario at 434MHz while Figure 5.16 shows the same comparison at 915MHz. Figure 5.17 shows the comparison for 2.4GHz. In this case there is a similarity in the profile but a drop of about 5dBm in the measured profile.

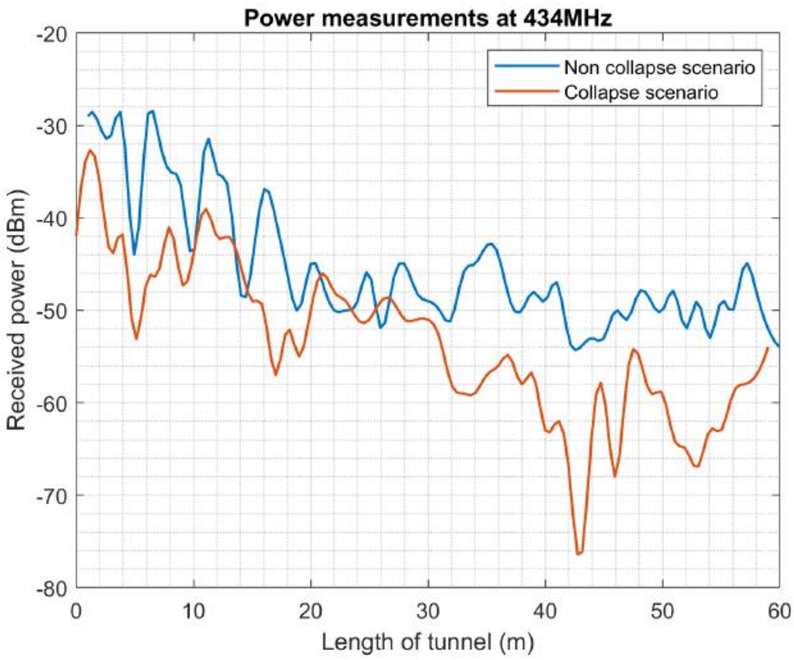


Figure 5.9: Comparison of results obtained for the collapsed and non-collapsed scenarios at 434MHz.

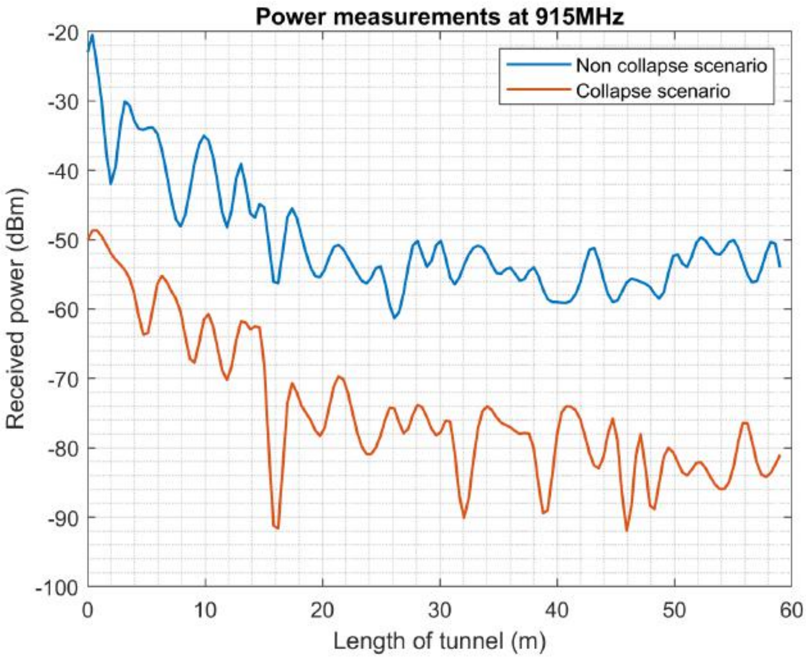


Figure 5.10: Comparison of results obtained for the collapsed and non-collapsed scenarios at 915MHz.

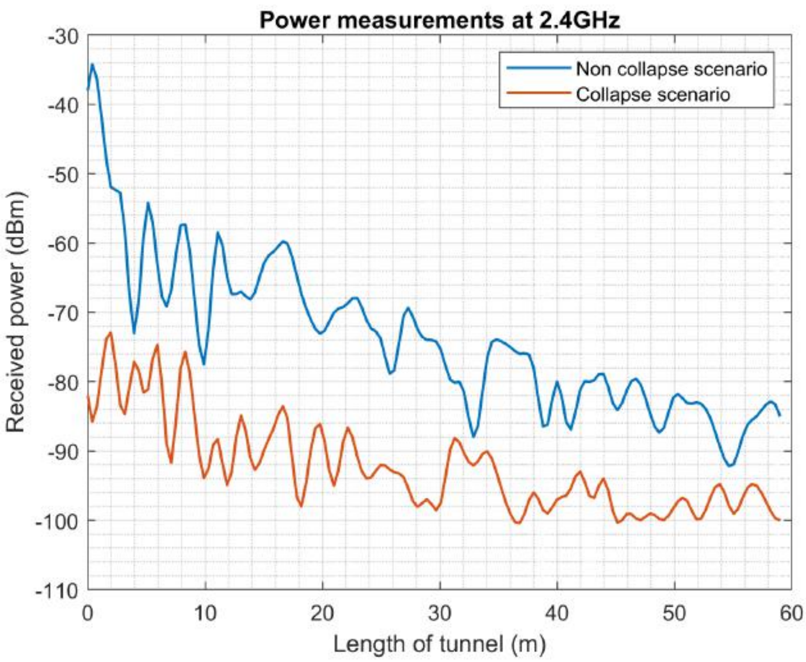


Figure 5.11: Comparison of results obtained for the collapsed and non-collapsed scenarios at 2.4GHz.

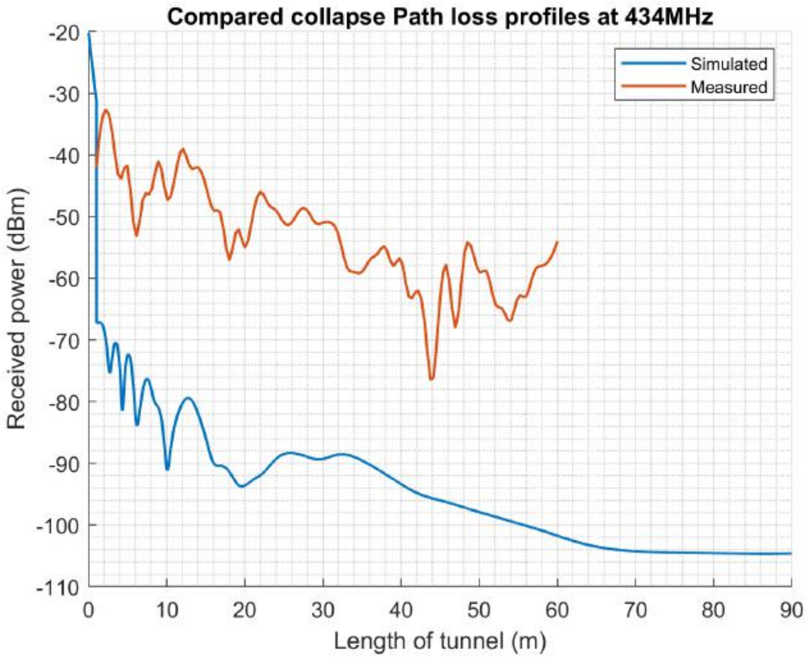


Figure 5.12: Comparison of simulated and measured path loss profiles at 434MHz at a transmission power of 7dBm in a 1m wide collapsed scenario.

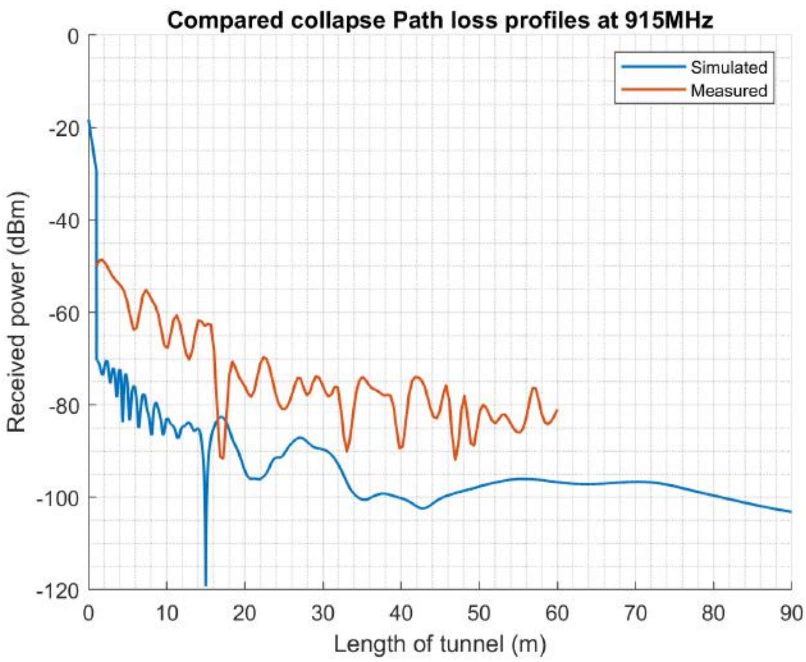


Figure 5.13: Comparison of simulated and measured path loss profiles at 915MHz at a transmission power of 14dBm in a 1m wide collapsed scenario.

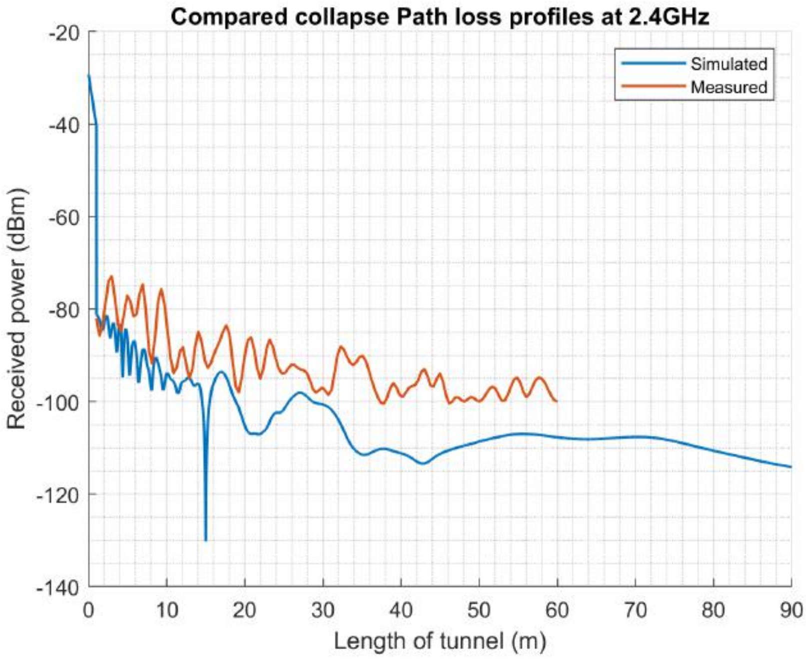


Figure 5.14: Comparison of simulated and measured path loss profiles at 2.4GHz at a transmission power of 3dBm in a 1m wide collapsed scenario.

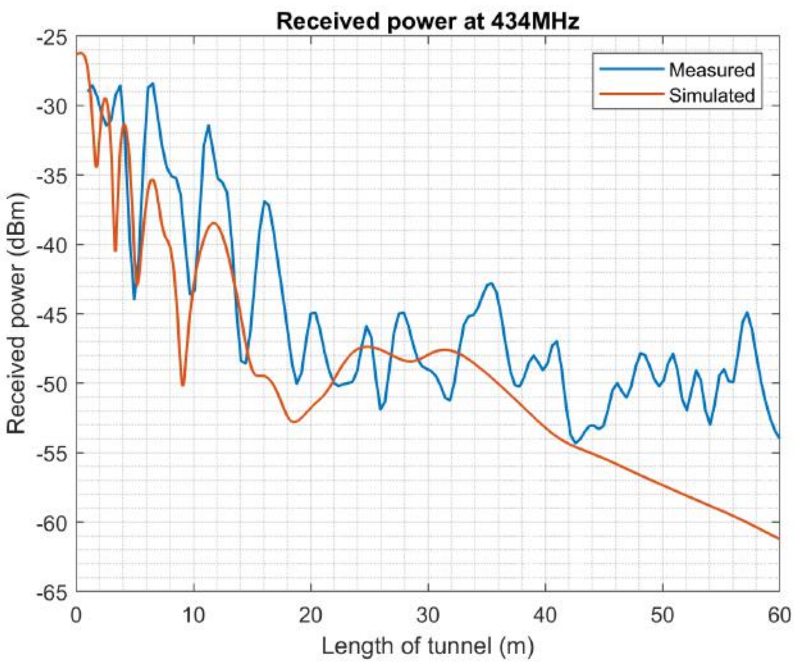


Figure 5.15: Comparison of simulated and measured path loss profiles at 434MHz at a transmission power of 7dBm.

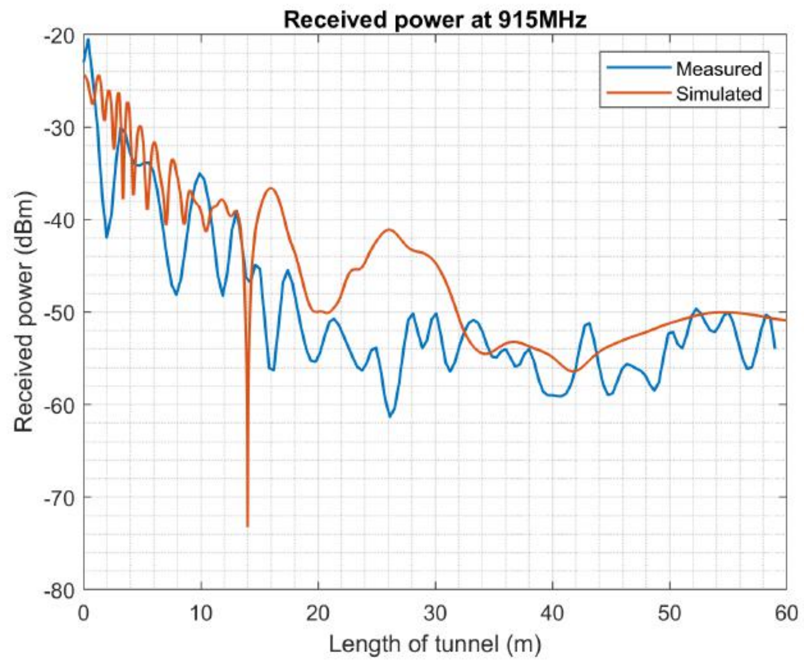


Figure 5.16: Comparison of simulated and measured path loss profiles at 915MHz at a transmission power of 14dBm.

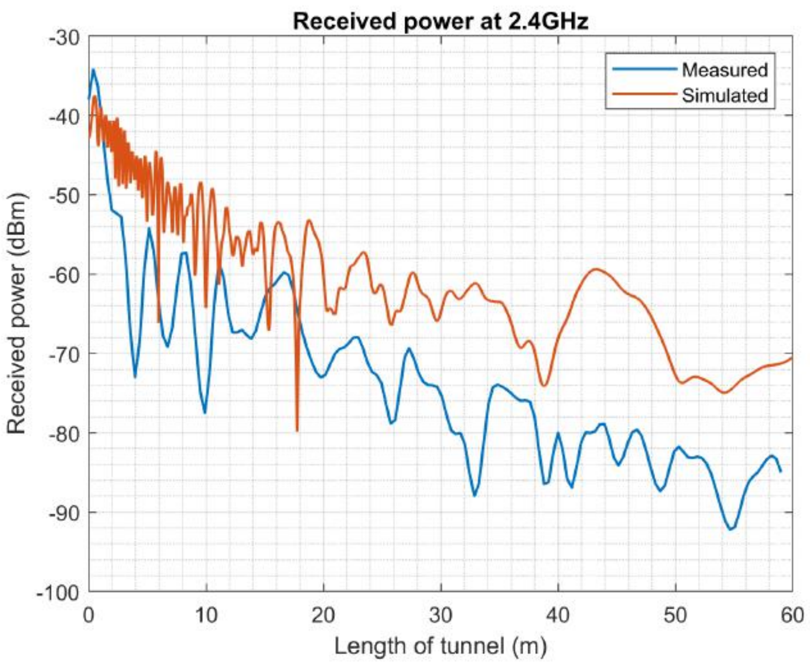


Figure 5.17: Comparison of simulated and measured path loss profiles at at 2.4GHz at a transmission power of 3dBm.

## 5.6 Conclusion

The results and discussion of the performance measurement of a WSN system in a non-collapsed and collapsed mine tunnel environment were presented in this chapter. A description of the testing environment and equipment test up at the Wits mock mine was given. The results presented showed a drastic decrease in the received power in the collapsed tunnel environment scenarios with an attenuation of 12dB/m, 30dB/m and 40dB/m for 434MHz, 915MHz and 2.4GHz respectively in the TTE section of the collapse. The measured results in the non collapsed scenarios showed some correlation but as well as some discrepancies with the results from the analytical modeling from *Chapter 6* for the three frequencies considered.

# Chapter 6

# Conclusions

## 6.1 Chapter overview

This chapter concludes this dissertation by giving a summary of the preceding *chapters* and reviewing how the research questions posed in *Chapter 1* have been answered. Future work and improvements to the current research are also proposed.

## 6.2 Summary of dissertation

The aim of this research work was to answer three fundamental questions posed in *Chapter 1* which were:

1. *What is the channel model of a partially/fully collapsed underground mine tunnel in context of a WSN system,*
2. *What is the system performance of a WSN communication system after a rock fall in an underground mine tunnel,*
3. *What is the optimal network architecture (with a closer look into a WSN topology) which will likely survive and be able to still establish connectivity after an underground mine tunnel collapses.*

*Chapter 1* gave a background of the motivation which led to the research questions being posed thereafter. The major reason was the need to have reliable communication systems in underground mines after a disaster occurs, which should help in the localization of miners as a first step towards their rescue. In *Chapter 2*, a literature review of underground mine communication systems and the concepts of wireless sensor networks were discussed. In addition, fundamentals of channel modeling were introduced as a foundation towards finding an answer to question 1. An overview and a review of existing techniques employed in the channel modeling of underground mine tunnels was also provided. The techniques were compared in a bid to adopt the best techniques to be used in the channel modeling exercise. From the techniques, a combination of pure TTE methods and the ray-optical tracing method were chosen to be used in the channel modeling exercise due to their applicability to the scenarios which were proposed to be investigated. The performance metrics of interest to consider when doing a performance evaluation of a wireless sensor network communication system were also discussed. From the discussion, coverage was considered as the metric of interest in line with the aims and objectives of this research. The steps followed in the conduction of the research were presented in *Chapter 3* as well as the software and hardware that were employed. The models for the techniques adopted in the research were written and simulated in MATLAB and measurements were done using Zolertia Re-Mote and ATmega WSN nodes. The channel modeling results were presented in *Chapter 4*. Some of the results simulated in MATLAB were validated through the use of a commercial software suit. However, there were other results in the simulations that did not match those obtained from the commercial software suit. This was mainly due to the fact that the frequencies in these scenarios were out of the range of frequencies which can be simulated using the ray tracing method in tunnels. The results showed an increasing attenuation of the received signal strength with an increase in the frequency. In the special case of the collapsed tunnel scenario, a huge attenuation at the rock and air interfaces was observed due to transmission losses from one medium to the other. There was also a considerable attenuation in the collapsed section of the tunnel compared to the open air sections. A section in this chapter presented a conceptual communication system based on the results and channel models obtained. The results showed that for a threshold of -80 dBm as the least expected RSSI in a WSN system, frequencies below 6.78 MHz should be employed in a collapsed mine tunnel with a collapsed section with a width of at most 5 meters. It was also observed that higher transmission power and a considerable gain is required. Sample deployment strategies based on the results obtained were presented. From these, it was shown that as long as the nodes are deployed at the fixed minimum reception distances along the length of the tunnel, the position along the width of the tunnel has no significant effect on the coverage of such a deployment. In *Chapter 5*, the results for the WSN performance evaluation in a mock mine were presented. The results obtained in the non collapsed scenarios correlated with those obtained in *Chapter 4*. A huge drop in performance (i.e the strength of the received signal) was observed in the collapsed scenarios with a drop of 12dBm, 30 dBm and 40 dBm for 434MHz, 915 MHz and 2.4 GHz respectively over a collapse width and height of 1 meter.

## 6.3 Assessment of research questions and their answers

The research questions posed in *Chapter 1* set objectives and goals for this research and a review of the questions and their main findings is important in the conclusion of this research. The main findings were:

### 6.3.1 Research question 1

*What is the channel model of a partially/fully collapsed underground mine tunnel in context of a WSN system ?*

The channel model in a such a scenario is a combination of the models obtained for a normal mine tunnel without any collapses using pure TTA methods and that of wave propagation through a rock medium making use of pure TTE methods. In the model, there are sharp drops in the transmitted power at the rock and air interfaces which are as a result of the transmission losses form one medium to another.

### 6.3.2 Research question 2

*What is the system performance of a WSN communication system after a rock fall in an underground mine tunnel ?*

The performance of a WSN in a collapsed mine tunnel is severely hampered by the introduction of rock debris as the new propagation medium. The losses in rock propagation are huge as compared to air propagation. For a system which is solely designed to be used as a TTA system like most commercial WSN solutions, the performance is dismal. The propagation through rock requires very low frequencies and a considerable amount of transmission power.

### 6.3.3 Research question 3

*What is the optimal network architecture (with a closer look into a WSN topology) which will likely survive and be able to still establish connectivity after an underground mine tunnel collapses ?*

A WSN system by design makes use of high frequencies and low power for transmission due to the fact that the transmitting and receiving nodes are, in general, small and compact in size. From the results of this research, it was shown that lower frequencies and high power transmission are required for communication in a collapsed mine tunnel. A communication system that makes use of lower frequencies and high transmission power as the commercial solutions highlighted in Table 2.1 are thus suited to a collapsed mine tunnel scenario. The communication in these systems can further be improved by incorporating some of WSN design topologies having self healing capabilities which will help in cases such as when some of the nodes are damaged. The positioning of the nodes of any such other system which makes use of the suitable frequencies requires that the nodes be positioned at the minimum coverage distance along the length of the tunnel and at any point along the width of the tunnel.

## 6.4 Future work and recommendations

Because of stringent safety and compliance requirements when it comes to the use of electronic and telecommunications equipment in mines, this research was conducted in a mock mine at the University of the Witwatersrand. It is therefore recommended, if it becomes possible and easy to extend the work, to an active and real underground mine. The collapse scenarios created were limited due to the nature of the mock mine used. In future it is recommended to have a bigger test site where many collapse scenarios can be created. The ideal frequencies for communication in a collapsed mine tunnel were found to be very low and unsuitable for a portable WSN communication system which made the bases for the hypothesis before this research work started. After observing this result, it will be imperative then to take a look at suitable hardware corresponding to the frequencies suited to be used in collapsed mine scenarios, for it to be used for rescue purposes in underground mines.

# Appendix A

# Coverage Path Loss Tests and Sample WSN Deployments

The figures presented here show the coverage tests and sample WSN deployments as outlined in *Chapter 4*. The acronyms in the captions of the figures are given as:

where: $P$ = Transmission power (1 mw, 10 mw, 100 mW and 1000 mW) representing a log scale.

$D$ = Distance from where the transmitter is located in the TTA section to the collapsed section (10m, 20m and 30m).

$C$ = Length of the collapsed section of the mine tunnel (5m and 10m).

## A.1 1 mW Transmission power

### A.1.1 Gain = 1

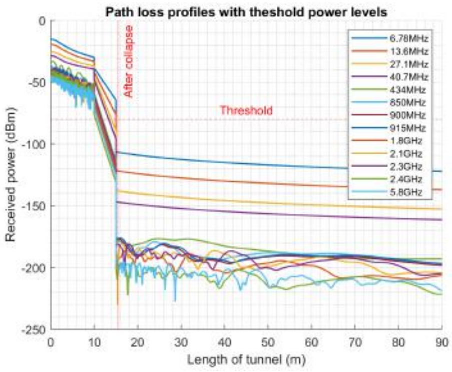


D = 10m, C = 5m.

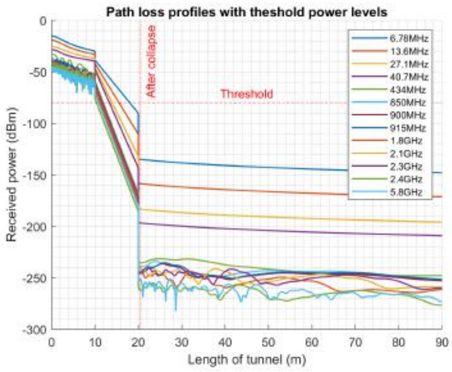


D = 10m, C = 10m.

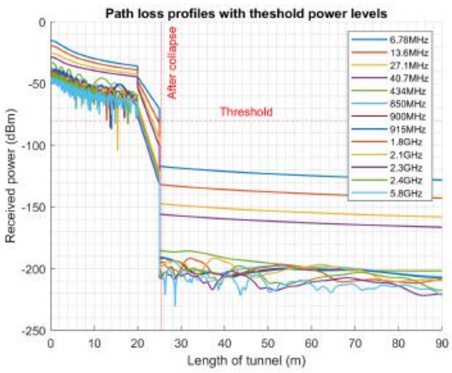


D = 20m, C = 5m.

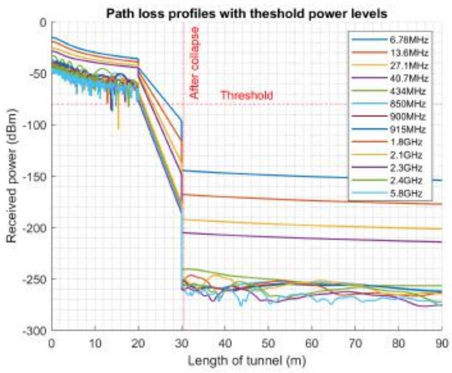


D = 20m, C = 10m.

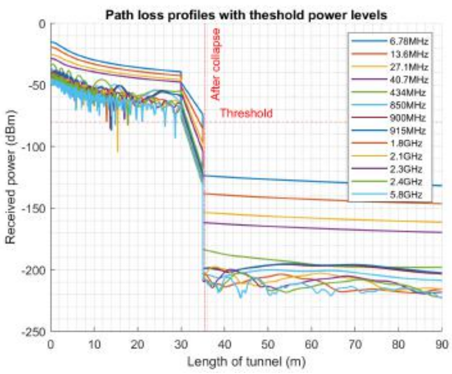


D = 30m, C = 5m.

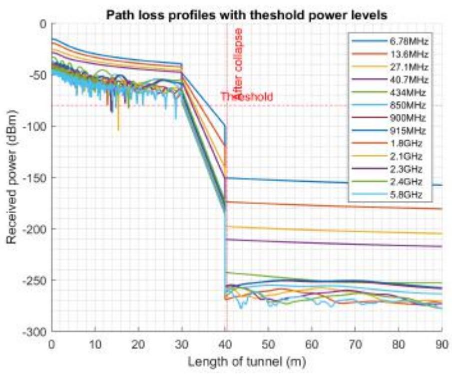


D = 30m, C = 10m.

Figure A.1: P = 1mW and an antenna gain of 1.

### A.1.2 Gain = 4

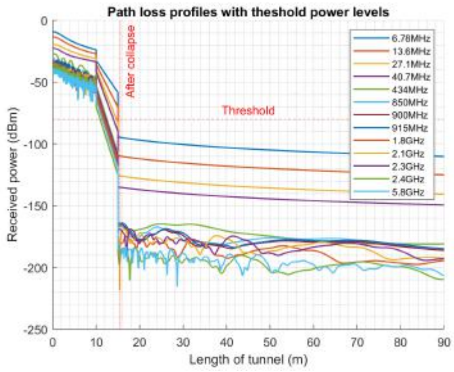


D = 10m, C = 5m.

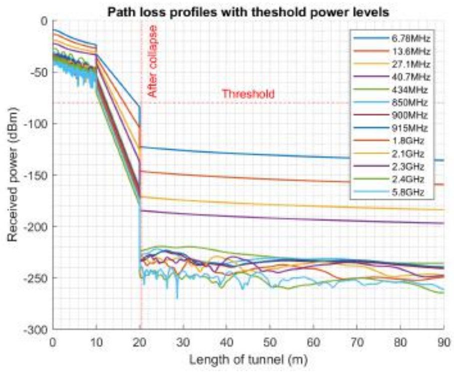


D = 10m, C = 10m.

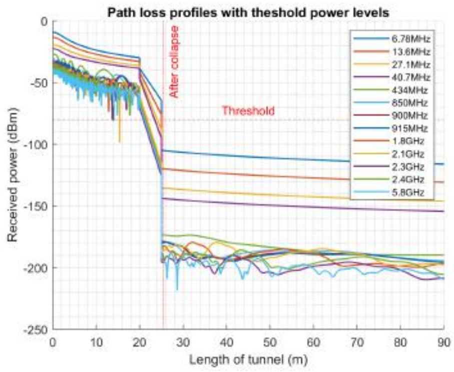


D = 20m, C = 5m.

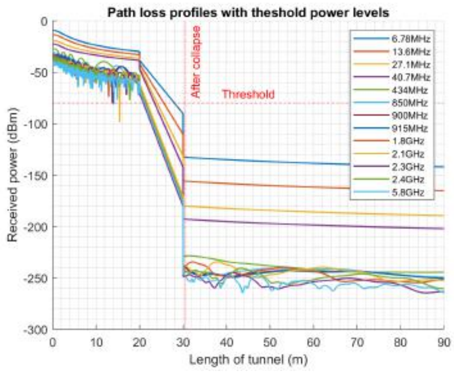


D = 20m, C = 10m.

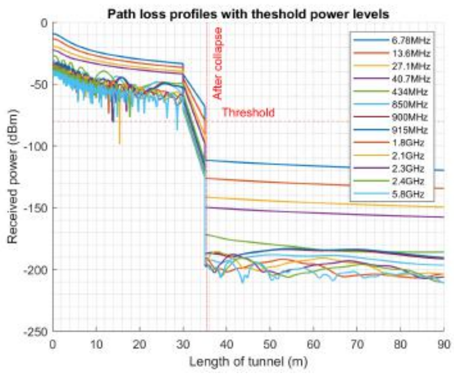


D = 30m, C = 5m.

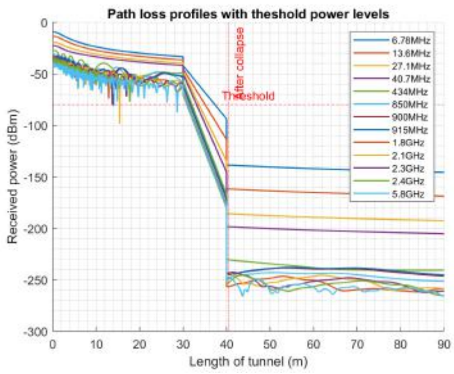


D = 30m, C = 10m.

Figure A.2: P = 1mW and an antenna gain of 4.

## A.2 10 mW Transmission power

### A.2.1 Gain = 1

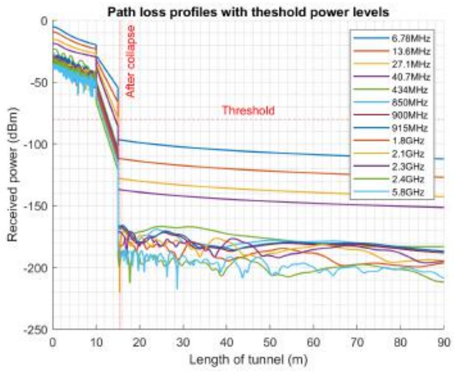


D = 10m, C = 5m.

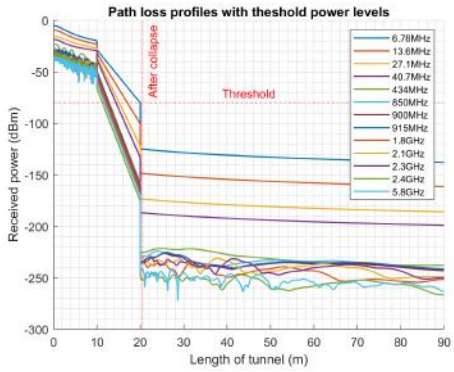


D = 10m, C = 10m.

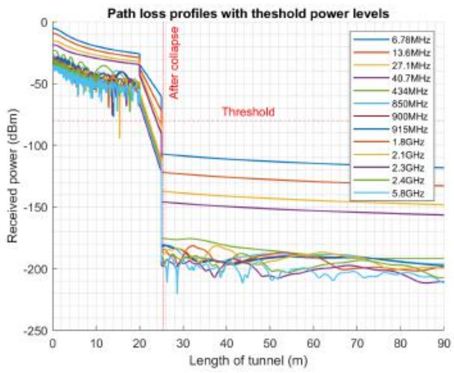


D = 20m, C = 5m.

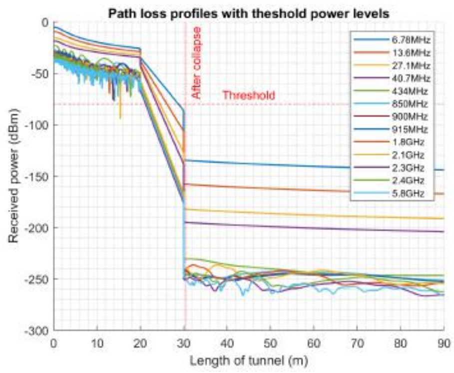


D = 20m, C = 10m.

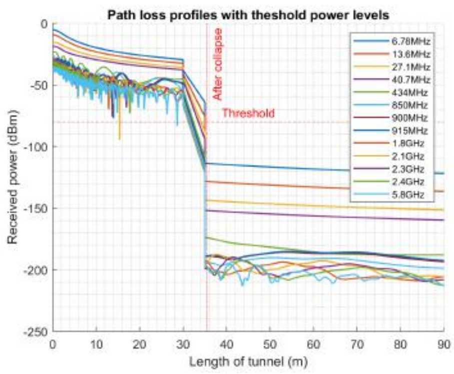


D = 30m, C = 5m.

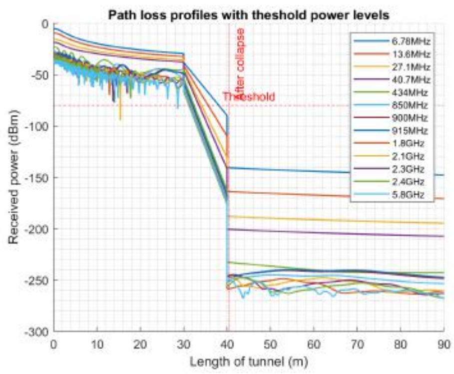


D = 30m, C = 10m.

Figure A.3: P = 10mW and an antenna gain of 1.

### A.2.2 Gain = 4

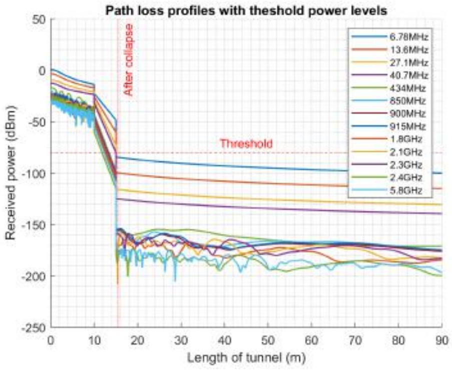


D = 10m, C = 5m.

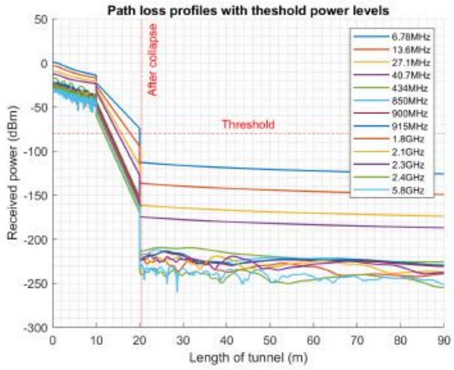


D = 10m, C = 10m.

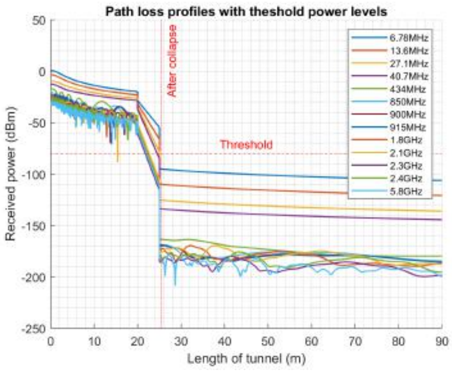


D = 20m, C = 5m.

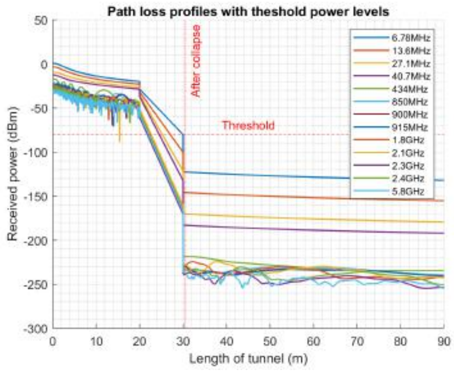


D = 20m, C = 10m.

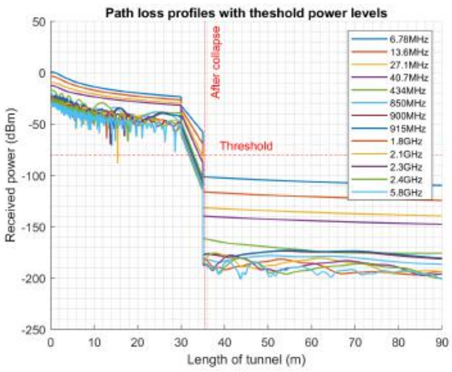


D = 30m, C = 5m.

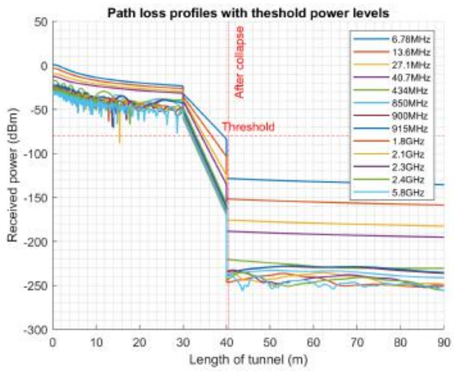


D = 30m, C = 10m.

Figure A.4: P = 10mW and an antenna gain of 4.

## A.3 100 mW Transmission power

### A.3.1 Gain = 1

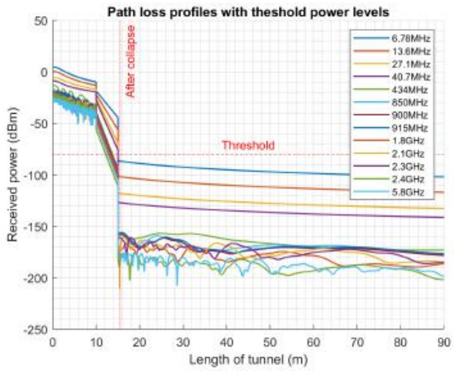


D = 10m, C = 5m.

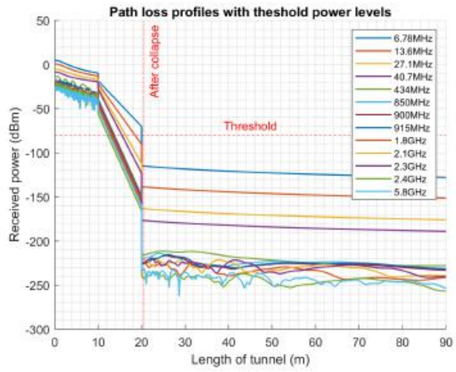


D = 10m, C = 10m.

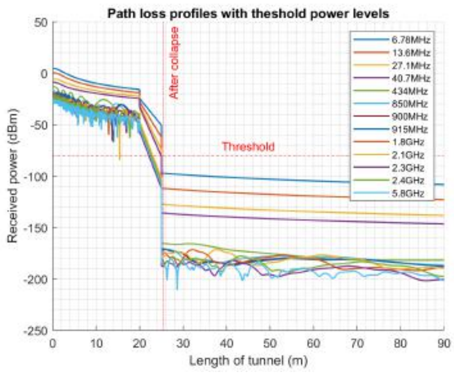


D = 20m, C = 5m.

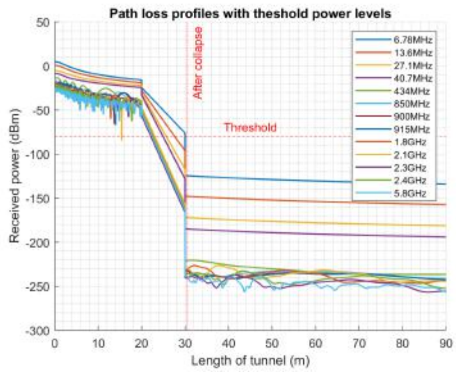


D = 20m, C = 10m.

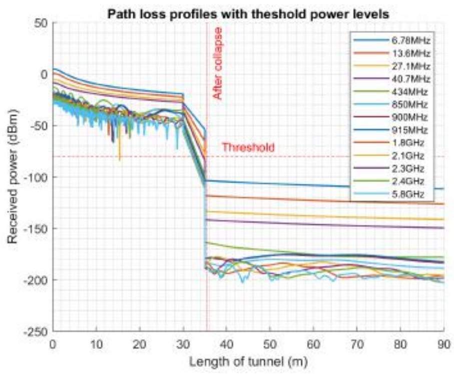


D = 30m, C = 5m.

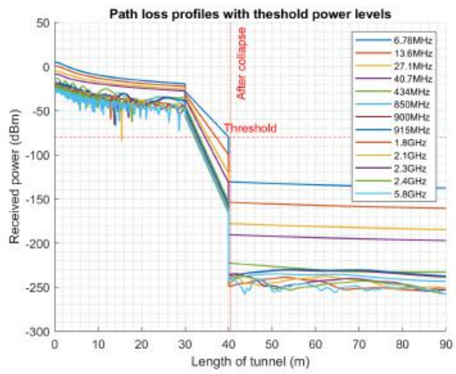


D = 30m, C = 10m.

Figure A.5: P = 100mW and an antenna gain of 1.

### A.3.2 Gain = 4

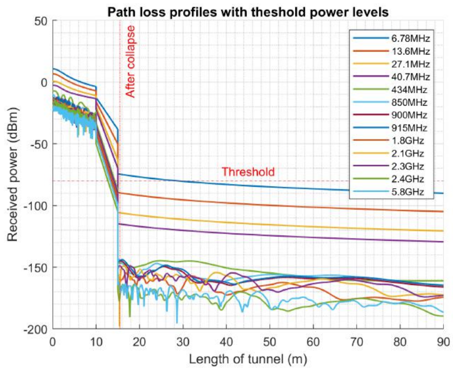


D = 10m, C = 5m.

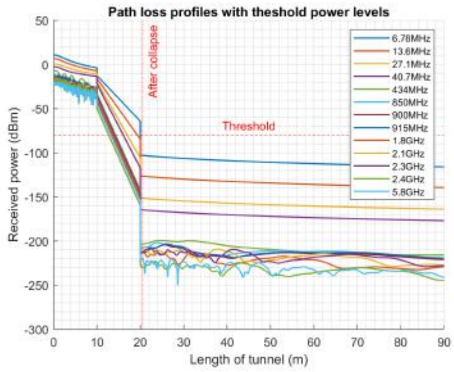


D = 10m, C = 10m.

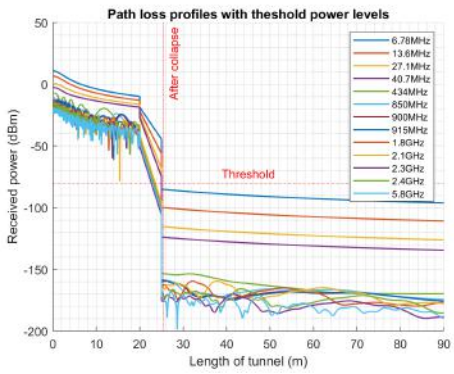


D = 20m, C = 5m.

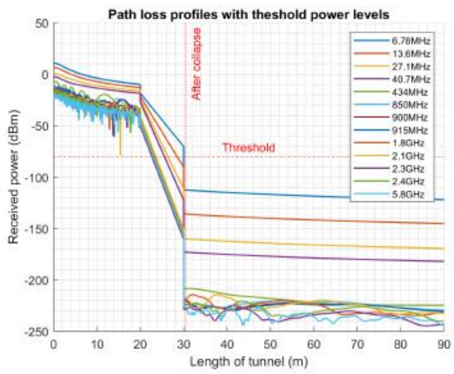


D = 20m, C = 10m.

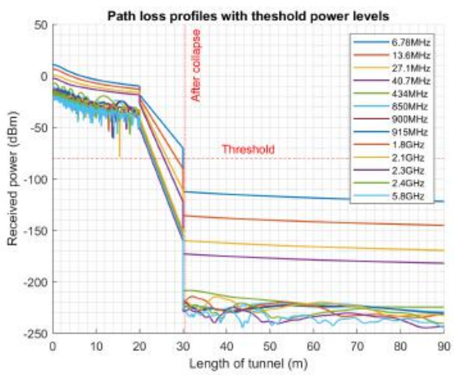


D = 30m, C = 5m.

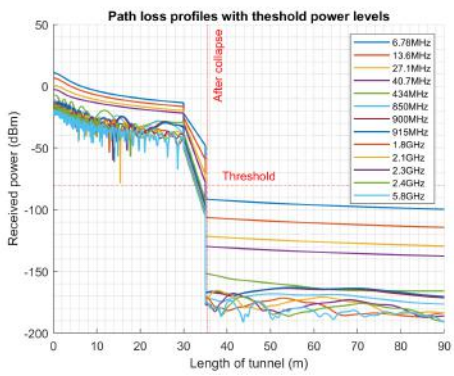


D = 30m, C = 10m.

Figure A.6: P = 100mW and an antenna gain of 4.

## A.4 1000 mW Transmission power

### A.4.1 Gain = 1

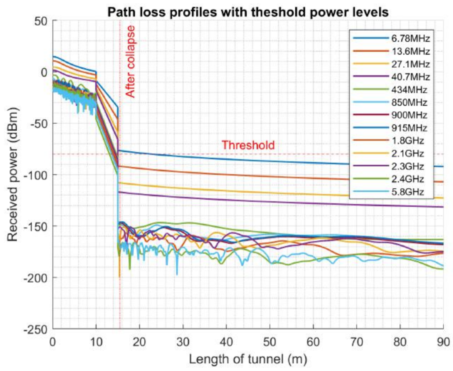


D = 10m, C = 5m.

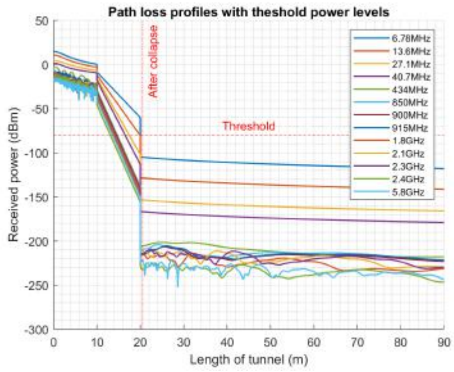


D = 10m, C = 10m.

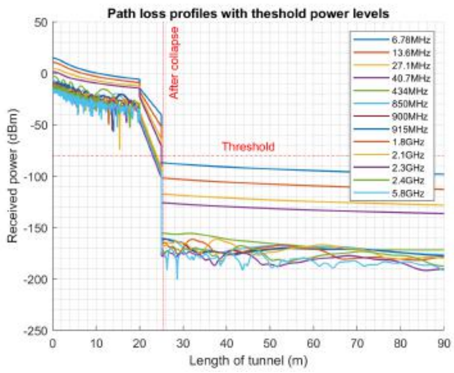


D = 20m, C = 5m.

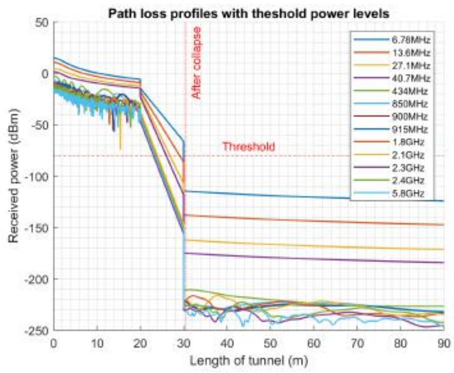


D = 20m, C = 10m.

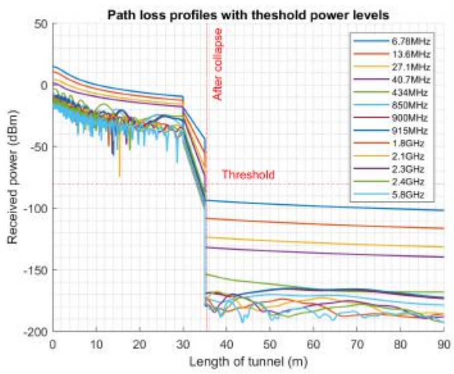


D = 30m, C = 5m.

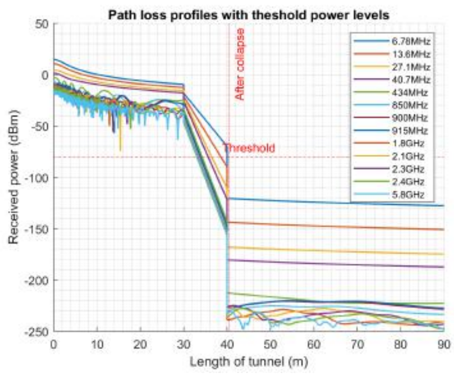


D = 30m, C = 10m.

Figure A.7: P = 1000mW and an antenna gain of 1.

### A.4.2 Gain = 4

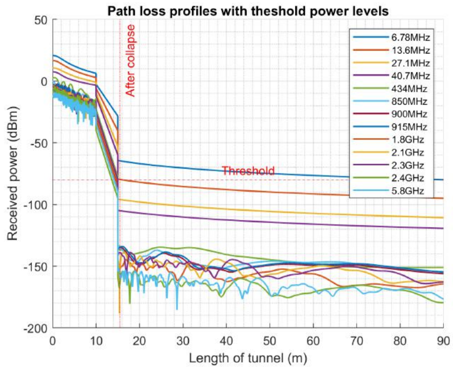


D = 10m, C = 5m.

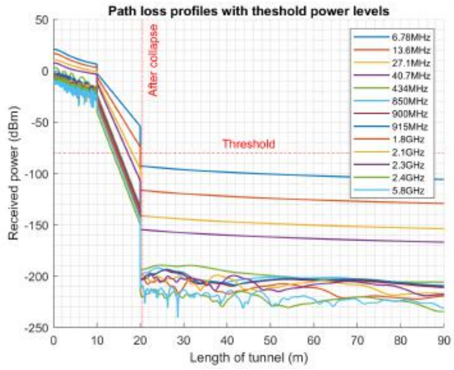


D = 10m, C = 10m.

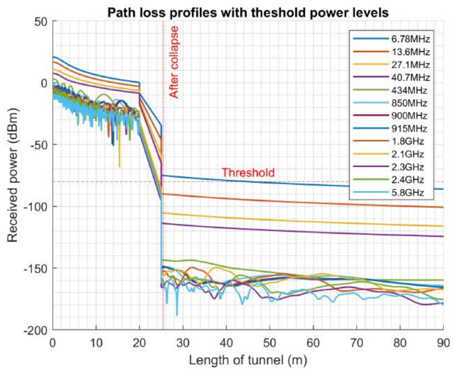


D = 20m, C = 5m.

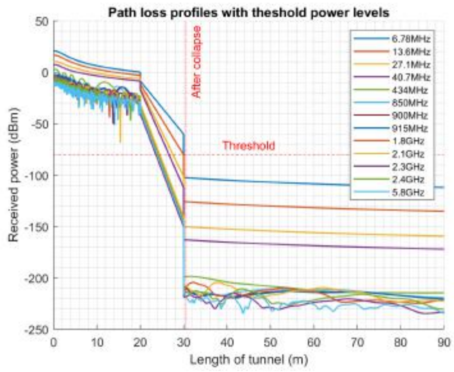


D = 20m, C = 10m.

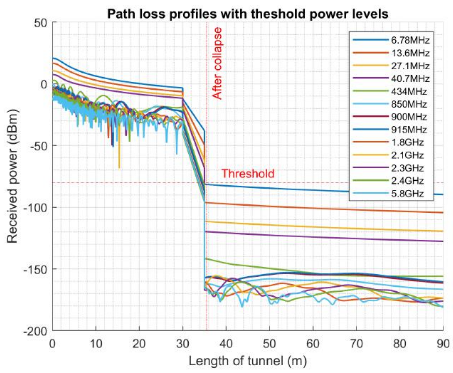


D = 30m, C = 5m.

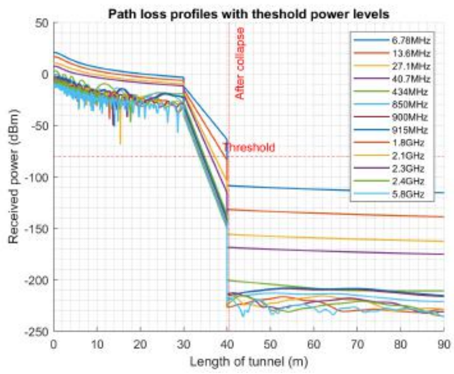


D = 30m, C = 10m.

Figure A.8: P = 1000mW and an antenna gain of 4.

## A.5 Node deployments

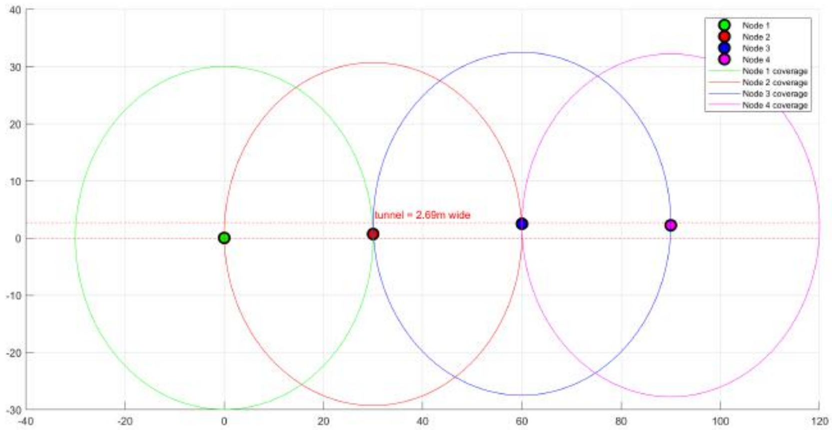


Figure A.9: Random node deployment 1

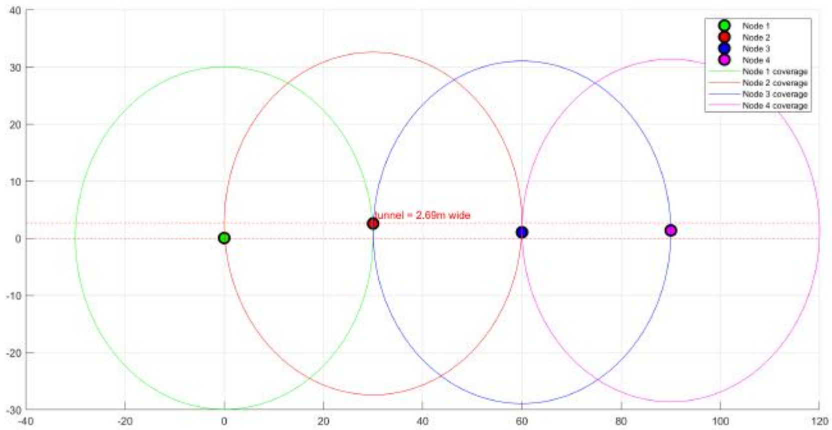


Figure A.10: Random node deployment 2

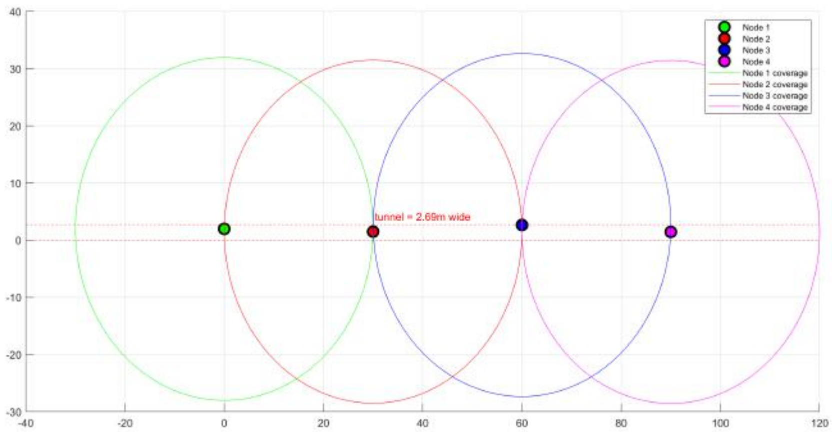


Figure A.11: Random node deployment 3

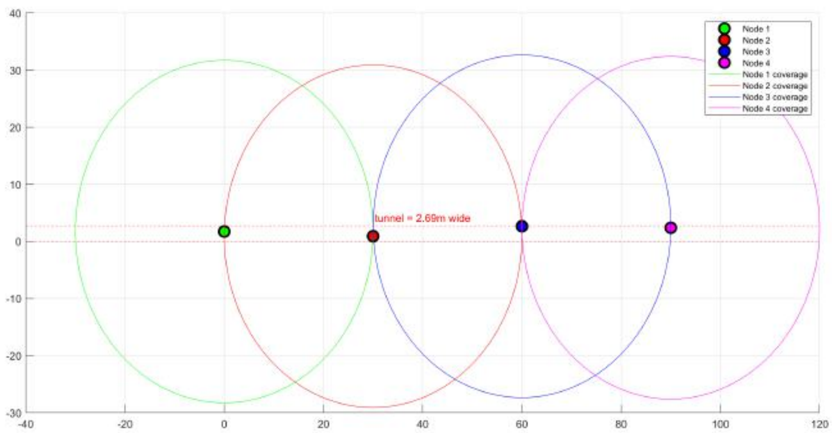


Figure A.12: Random node deployment 4

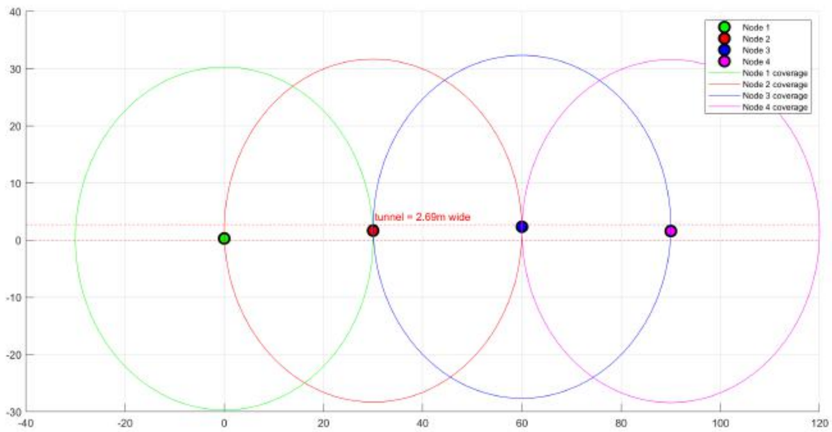


Figure A.13: Random node deployment 5

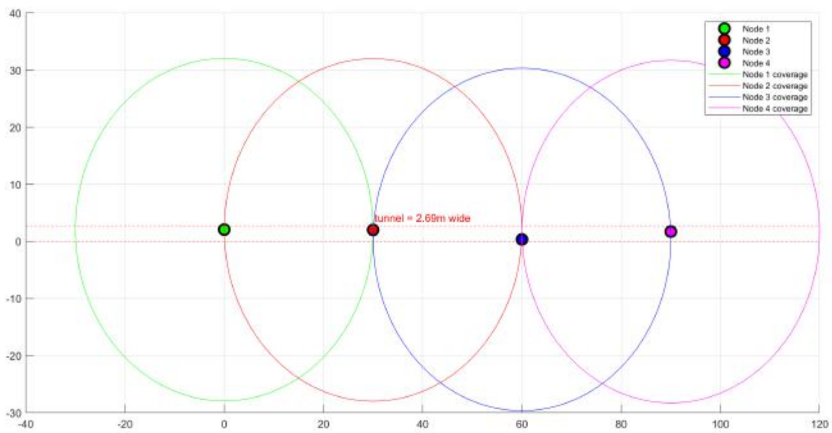


Figure A.14: Random node deployment 6

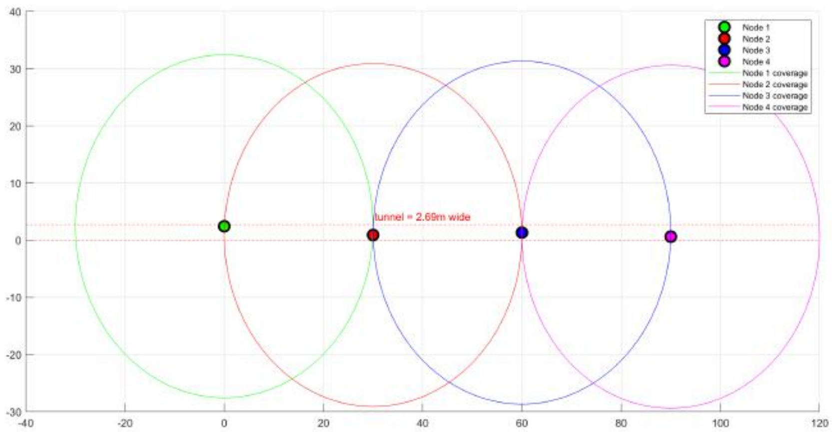


Figure A.15: Random node deployment 7

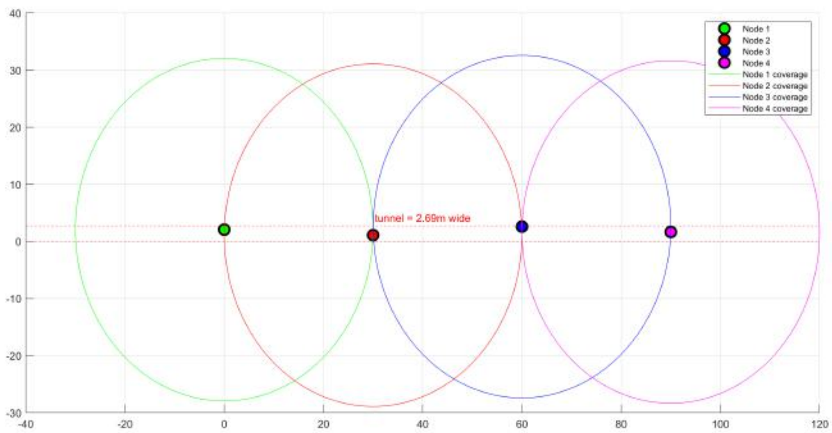


Figure A.16: Random node deployment 8

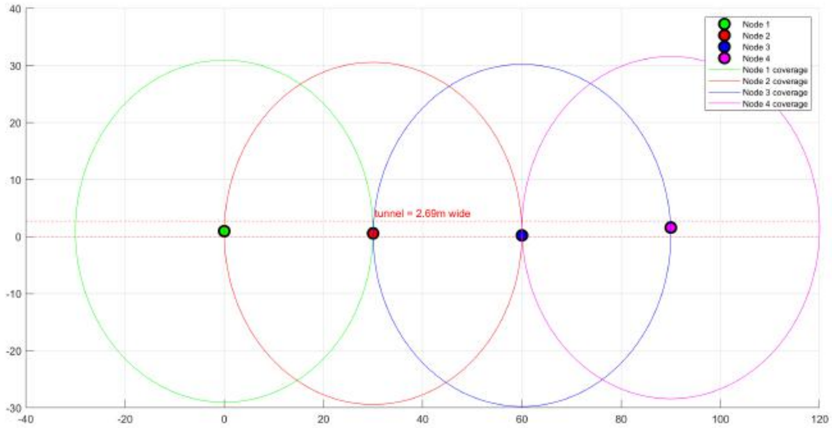


Figure A.17: Random node deployment 9

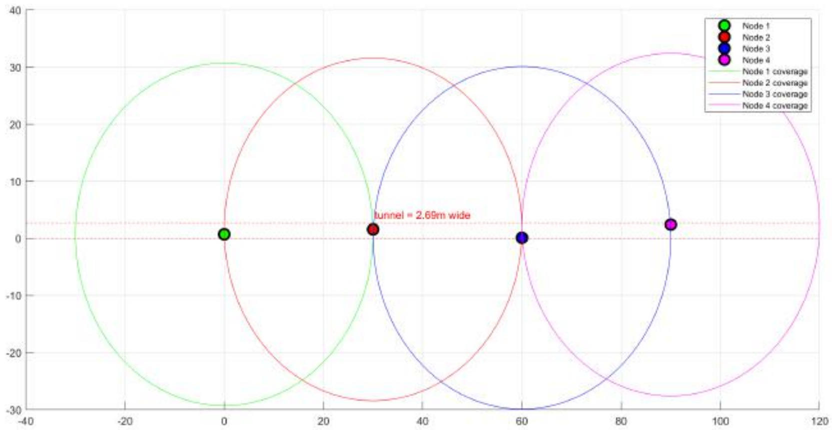


Figure A.18: Random node deployment 10

# References


[1] University of the Witwatersrand, *The wits 21st century research institutes: wits mining research institute*, Information Brochure.

[2] Chamber of Mines of South Africa, *Gold & gold mining in south africa*, http://www.chamberofmines.org.za/sa-mining/gold, Last accessed on 07 Nov 2017.

[3] Moneyweb, *Deeper gets deadly for workers in aging south africa gold mines*, https://www.moneyweb.co.za/news/industry/deeper-gets-deadly-for-workers-in-aging-south-africa-gold-mines/, Last accessed on 06 Nov 2017.

[4] J. D. Plessis, D. Hoffman, W. Marx, and R. Westhuizen, *Optimising ventilation and cooling systems for an operating mine using network simulation models*, https://www.ammsa.org.za/knowledge-hub/presentation-archive/2014/summary/2-technical-papers/512-optimising-ventilation-and-cooling-systems-for-an-operating-mine-using-network-simulation-models, 2013.

[5] M. Biffi and D. Stanton, "Meeting the reduced availability and rising costs of electrical power: anglo platinum ventilation and cooling strategies", in *The 4th International Platinum Conference, Platinum in transition 'Boom or Bust'*, The Southern African Institute of Mining and Metallurgy, 2010, pp. 293–302.

[6] Nelmia Robotics Insight, *Robotization of the mining industry*, http://nelmia.com/content/robotization-mining-industry, Last accessed on 06 Nov 2017.

[7] T. Simonite, *Mining 24 hours a day with robots*, https://www.technologyreview.com/s/603170/mining-24-hours-a-day-with-robots/, Last accessed on 06 Nov 2017.

[8] A. Lane and J. Beier, *The future of mining in south africa, innovation imperative*, Deloitte Report, 2014.

[9] Prof. F. Cawood, Personal Communication: Briefing on Research Objectives, 2017.

[10] The New York Times, *Chile mining accident (2010)*, https://www.nytimes.com/topic/subject/chile-mining-accident-2010, Last accessed on 24 Mar 2019.

[11] Eyewitness News, *Lily mine collapse*, https://ewn.co.za/Topic/Lily-Mine-collapse, Last accessed on 24 Mar 2019.

[12] NK News, *Six miners dead, one rescued 10 days after mine collapse in north korea*, https://www.nknews.org/2017/03/six-miners-dead-one-rescued-ten-days-after-mine-collapse-in-north-korea/, Last accessed on 27 May 2017.

[13] Nigerian Echo, *25 deadincentralafricangoldminecollapse*, http://nigerianecho.com/25-dead-in-central-african-gold-mine-collapse/, Last accessed on 27 May 2017.

[14] S. Yarkan, S. Guzelgoz, H. Arslan, and R. R. Murphy, "Underground mine communications: a survey", in *IEEE Communications Surveys & Tutorials*, vol. 11, 2009, pp. 125–142.

[15] G. Einicke, D. Dekker, and D. Hainsworth, "A review of underground communications systems", in *Technology Exchange Workshop in Coal Mine Productivity: Underground Mining Methods and Communications Systems*, The Commonwealth Scientific and Industrial Research Organisation, 1997, pp. 1–9.

[16] R. S. Nutter and M. D. Aldridge, "Status of mine monitoring and communications", in *IEEE Transactions on Industry Applications*, vol. 24, IEEE, 1988, pp. 820–826.

[17] Shauenburg Systems, *Mimacs: mine wide integrated monitoring and control system*, http://schauenburg.co.za/products/mimacs/, Last accessed on 03 Nov 2017.

[18] Minetec, *Solutions - trax, smarts and safedirect*, http://minetec.com.au/, Last accessed on 03 Nov 2017.

[19] GeoSonics Vibra-Tech, *Seismographs*, http://www.geosonicsvibratech.com/products/seismographs/, Last accessed on 03 Nov 2017.

[20] M. R. Yenchek, G. T. Homce, N. W. Damiano, and J. R. Srednicki, "Niosh-sponsored research in through-the-earth communications for mines: a status report", *IEEE Transactions on Industry Applications*, vol. 48, pp. 1700–1707, 5 Sep. 2012.

[21] V. Kononov, *Develop a Trapped Miner Location System and an Adequate Rescue Strategy and Associated Technologies*. CSIR Division of Mining Technology, SA. Tech Report, 1998, pp. 1–36.

[22] J. P. Carreno, L. S. e Silva, S. O. de Almeida Neves, A. J. B. Leonardo Aguayo, A. N. Barreto, and L. G. U. Garcia, "Through-the-earth (tte) communications for underground mines", *Journal of Communications and Information Systems*, vol. 31, pp. 164–176, 1 2016.

[23] L. G. Stolarczyk, "Emergency and operational low and medium frequency band radio communications system for underground mines", *IEEE TRANSACTIONS ON INDUSTRY APPLICATIONS*, vol. 27, pp. 780–790, 4 Jul. 1991.

[24] MineArc Systems, *Rescue Dog Communication System*. Product Brochure.

[25] National Instruments, *What is a wireless sensor network*, `http://www.ni.com/white-paper/7142/en/`, Last accessed on 07 Nov 2017.

[26] A. M. Abu-Mahfouz, S. J. Isaac, C. P. Kruger, N. Aakvaag, and B. Fismen, "Wireless gas sensing in south african underground platinum mines", *WCNC (Services, Applications, and Business)*, vol. 1, pp. 3432–3437, 2014.

[27] M. Deng and Q. Chen, "Coal and gas outburst monitoring system based on wsn", *Symposium on Security Detection and Information Processing*, pp. 387–391, 2010.

[28] S. Molina, I. Soto, and R. Carrasco, "Detection of gases and collapses in underground mines using wsn", pp. 219–225, 2011.

[29] Y. S. Dohare, T. Maity, P. S. Paul, and P. S. Das, "Design of surveillance and safety system for underground coal mines based on low power wsn", *International Conference on Signal Propagation and Computer Technology*, vol. 8, pp. 116–119, 2014.

[30] U. I. Minhas, I. H. Naqvi, S. Qaisar, K. Ali, S. Shalid, and M. A. Aslam, "A wsn for monitoring and event reporting in underground mine environments", *IEEE Systems Journal*, pp. 1–12,

[31] P. Chen and C. Zhao, "Area wireless sensor networks for personnel location under coalmine", *Second IEEE Conference on Industrial Electronics and Applications*, pp. 2882–2885, 2007.

[32] Z. Liu, C. Li, Q. Ding, and D. Wu, "A coal mine personnel global positioning system based on wireless sensor networks", in *Proceedings of the 8th World Congress on Intelligent Control and Automation*, IEEE, Jul. 2010, pp. 7026–7031.

[33] K. Sohraby, D. Minoli, and T. Znati, *Wireless Sensor Networks: Technology, Protocols, and Applications*. John Wiley & Sons Inc., Hoboken, New Jersey, 2007, ch. 2–3, pp. 75–91.

[34] R. Jain, *Channel Models A Tutorial*. Tech Report, 2007.

[35] A. E. Forooshani, S. Bashir, and D. G. Michelson, “A survey of wireless communications and propagation modeling in underground mines”, in *IEEE Communications Survey & Tutorials*, vol. 15, 2013, pp. 1524–1545.

[36] Z. Sun and I. F. Akyildiz, “Channel modeling and analysis for wireless networks in underground mines and road tunnels”, in *IEEE Transactions on Communications*, vol. 58, Jun. 2010, pp. 1758–1768.

[37] M. Ndoh and G. Y. Delisle, *Underground Mines Wireless Propagation Modeling*. IEEE, 2004, pp. 1–5.

[38] A. Goldsmith, *Wireless Communications*. Cambridge University Press, 2005, ch. 2–3, pp. 24–84.

[39] A. F. Molisch, *Wireless Communications*. John Wiley and Sons, Ltd, 2011, ch. 2–4, pp. 27–67.

[40] T. S. Rappaport, *Wireless Communications: Principles and Practice*. Prentice Hall, 2002, pp. 160–180.

[41] B. Austin, “Radio communication in mines”, MSc Dissertation, Faculty of Engineering, University of the Witwatersrand, Johannesburg, 1977.

[42] A. G. Emslie, R. L. Lagage, and P. F. Strong, “Theory of the propagation of uhf radio waves in coal mine tunnels”, in *IEEE Transactions on Antennas and Propagation*, vol. 23, Mar. 1975, pp. 192–205.

[43] A. Hrovat, G. Kandus, and T. Javornik, “A survey of radio propagation modeling for tunnels”, in *IEEE Communications Survey & Tutorials*, vol. 16, 2014, pp. 658–669.

[44] C. Gentile, F. Valoit, and N. Moayeri, “A raytracing model for wireless propagation in tunnels with varying cross section”, in *Globecom 2012 - Wireless Communications Symposium*, 2012.

[45] J. Poutanen, *Geometry-based radio channel modeling: propagation analysis and concept development*, PhD Thesis, 2011.

[46] L. Robins, *Wireless Propagation Modeling Techniques for Underground Mine Tunnels*. School of Electrical and Information Engineering, University of the Witwatersrand, 2016, pp. 1–41.

[47] I. Hussain, "Channel modeling and analysis of wits mock-mine with different antenna parameters", MSc Research Report, University of the Witwatersrand, Johannesburg, Nov. 2016.

[48] M. Boutin, A. Benzakour, C. L. Despins, and S. Affes, "Radio wave characterization and modeling in underground mine tunnels", in *IEEE Transactions on Antennas and Propagation*, vol. 56, IEEE, 2008, pp. 540–549.

[49] S. Boutin, M. Affes, C. Despins, and T. Denidni, "Statistical modeling of a radio propagation channel in an underground mine at 2.4 and 5.8 ghz", in *IEEE VTC*, vol. 1, IEEE, 2005, pp. 78–81.

[50] Y. Rissafi, L. Talbi, and M. Ghaddar, "Experimental characterization of an uwb propagation channel in underground mines", in *IEEE Transactions on Antennas and Propagation*, vol. 60, Jan. 2012, pp. 240–246.

[51] M. Lienard and P. Degauque, "Natural wave propagation in mine environments", in *IEEE Transactions on Antennas and Propagation*, vol. 48, Sep. 2000, pp. 1326–1339.

[52] C. Nerguizian, C. L. Despins, S. Affes, and M. Djadel, "Radio-channel characterization of an underground mine at 2.4 ghz", in *IEEE Transactions on Wireless Communications*, vol. 4, Sep. 2005, pp. 2441–2453.

[53] K. A. Qaraqe, S. Yarkan, S. Guzelgoz, and H. Arslan, "Statistical wireless channel propagation characteristics in underground mines at 900 mhz: a comparative analysis with indoor channels", *Ad Hoc Networks, Elsevier*, pp. 1–2, 2011.

[54] Z. Sun and I. F. Akyildiz, *Channel Modeling of Wireless Networks in Tunnels*. School of Electrical and Computer Engineering, Georgia Institute of Technology, Tech Report, pp. 1–5.

[55] S. Dey, *Five performance metrics for wireless device networking*, `https://www.ecnmag.com/article/2011/09/five-performance-metrics-wireless-device-networking`, Last accessed on 07 Nov 2017.

[56] K. Benkic, M. Malajner, P. Planinsic, and Z. Cucej, "Using rssi value for distance estimation in wireless sensor networks based on zigbee", SPaRC Laboratory, UM-FERI MAribor, Slovenia, Tech. Rep.

[57] M. Sheffena, "Industrial wireless sensor networks: channel modeling and performance evaluation", *EURASIP Journal on Wireless Communications and Networking*, pp. 297–304, 2012.

[58] D. Sexton, M. Mahony, and M. Lapinski, "Radio channel quality in industrial wireless sensor networks", in *5th Sensors for Industry Conference*, Houston, Texas, USA, 2005.

[59] M. Sepulcre, J. A. Palazon, and J. Gozalvez, "Wireless connectivity for mobile sensing applications in industrial environments", Ubiquitous Wireless Communications Research Laboratory, University Miguel Hernández of Elche, Spain and INDRA Sistemas S.A., 28108 Alcobendas, Madrid, Spain, Tech. Rep., 2011.

[60] K. A. Agha and S. Martin, "Routing in mobile ad hoc networks", in *Wireless Network Design*, J. Kennington, E. Olinick, and D. Rajan, Eds., New York, Dordrecht, Heidelberg, London: Springer, 2011, ch. 9, pp. 199–216.

[61] Altair Hyperworks, *Winprop - tunnel and underground*, `https://altairhyperworks.com/product/FEKO/WinProp---Tunnel-and-Underground`, Last accessed on 25 Mar 2019.

[62] Zolertia, *Zolertia re-mote platform*, `https://github.com/Zolertia/Resources/wiki/RE-Mote`, Last accessed on 24 June 2019.

[63] I. Dove, "Analysis of radio propagation inside the human body for in-body localization purposes", Master's thesis, University of Twente, 2014.

[64] LowPowerLab, *Example node*, `https://github.com/LowPowerLab/RFM69/blob/master/Examples/Node/Node.ino`, Last accessed on 24 June 2019.